Title
Regulation and Mechanisms of Cohesin Function and Higher Order Chromosome Structure

Author
Eng, Thomas Tong

Publication Date
2015

Peer reviewed|Thesis/dissertation

Regulation and Mechanisms of Cohesin Function and Higher Order Chromosome Structure

By

Thomas Tong Eng

A dissertation submitted in partial satisfaction of the

requirements for the degree of

Doctor of Philosophy

in

Molecular and Cell Biology

in the

Graduate Division

of the

University of California, Berkeley

Committee in charge:

Professor Douglas E. Koshland, Chair
Professor Barbara J. Meyer
Professor Georjana Barnes
Professor Daniel Zilberman

Spring 2015

Abstract

Regulation and Mechanisms of Cohesin Function and Higher Order Chromosome Structure

by

Thomas Tong Eng

Doctor of Philosophy in Molecular and Cell Biology

University of California, Berkeley

Professor Douglas Koshland, Chair

Cohesin is an essential protein complex required for chromosome dynamics and architecture. Its activities are required to promote sister chromatid cohesion, chromosome compaction, transcriptional regulation, as well as efficient DNA repair. Cohesin activity is regulated by several well-characterized protein accessory factors, but the molecular mechanism by which cohesin acts upon its substrate, DNA, remains elusive. In the absence of structural information elucidating how cohesin can interact with DNA to tether sister chromatids or mediate chromosome compaction, many models have been proposed. The simplest of these models postulates that cohesin forms a ring-like structure, and the topological entrapment of a sister chromatid is necessary and sufficient to mediate sister chromatid cohesion as well as condensation. Other models reject the notion that topological entrapment of DNA by cohesin is sufficient for sister chromatid cohesion or condensation, and propose that a second step after DNA binding is required for function.

In this dissertation, I utilized genetic and biochemical analyses to characterize how cohesin could tether DNA. Through mutagenesis of cohesin's regulatory subunit, Mcd1p, I characterized a new domain in this key subunit that was required for viability, cohesion, and condensation. We utilized a new system for generating conditional null alleles in cohesin subunits, allowing for rapid analysis and characterization of these alleles in the absence of wild-type cohesin complexes. We expanded the conserved domain to a conserved ten amino acid domain in Mcd1p through the use of another directed mutagenesis screen in *MCD1,* and called this domain the Regulator of Cohesion and Condensation (*ROCC*). Importantly, mutant alleles in the *ROCC* box disrupted sister chromatid cohesion as well as chromosome condensation without perturbing cohesin's stable binding to chromosomes. This observation was incompatible with the prevailing model in the field, where cohesin binding to DNA dictates its ability to generate cohesion.

While we had evidence that cohesin could stably bind DNA but was unable to generate cohesion, my dissertation also uncovered an orthogonal line of evidence that further supported the possibility for higher order cohesin interactions. I previously characterized

ROCC mutants as inviable in the absence of a wild-type *MCD1* allele. However, when placed in *trans* with a second recessive inviable allele, this strain showed restoration of cohesin function, when none was expected. This inter-allelic complementation is consistent with a functional interaction between cohesin complexes, as evidenced by sister chromatid cohesion, chromosome condensation, and viability being restored. Cohesin's stable binding to chromosomes is restored in the *trans* configuration.

In sum, this dissertation furthers our understanding of how cohesin is able to tether sister chromatids on chromosomes. We show that cohesin can be stably bound to chromosomes, but unable to tether sisters, which contradicts the most common assumptions held in the field. Furthermore, our evidence for interallelic complementation provides strong evidence for a physical communication between cohesin complexes.

This dissertation is dedicated to my niece, Alice Chen,
who was born on March 8, 2015.

Table of Contents

CHAPTER ONE: INTRODUCTION TO COHESIN

Cohesin: A Protein Complex Required for Chromosome Segregation

What factors govern chromosome architecture? What gives chromosomes their distinctive shape, and is this distinctive chromosome shape necessary for function? Since the time of Walther Fleming, nearly one hundred and forty years ago, researchers have sought to understand the underlying molecular determinants governing chromosome structure. We now know that in order to ensure faithful segregation of genetic material, these physical stands of hereditary material needed to be properly duplicated and segregated from mother to daughter cell. Early work from *Drosophila melanogaster* identified a genetic locus that was required to maintain chromosome shape, while other investigators reported factors required for sister chromatid cohesion in meiosis, specific to centromeres (Perrimon *et al.*, 1985; Miyazaki and Orr-Weaver, 1992). However, identification of the protein complex itself that provided the physical linkages— termed cohesin — came from the budding yeast *Saccharomyces cerevisiae*.

Initially characterized for its essential role in plasmid segregation, cohesin is now appreciated for its varied functions in chromosome dynamics (Strunnikov *et al.*, 1993; Guacci *et al.*, 1997). Comprised of four core subunits (Smc1p, Smc3p, Mcd1p, and Scc3p) (Figure 1), cohesin is best known for its role in mediating sister chromatid cohesion, as it ensures bipolar attachment of chromosomes to the spindle through kinetochore attachments. Cohesin helps orient the kinetochores to bind opposite poles through steric constraints and a tension based mechanism (Tanaka *et al.*, 2000; Dewar *et al.*, 2004). However, cohesin's binding to chromosomes is not just at centromeres, but at regular intervals on chromosome arms (termed cohesin associated regions, or CARs) which may explain its other essential roles in transcriptional regulation, DNA repair, as well as chromosome condensation (Blat and Kleckner, 1999; Laloraya *et al.*, 2000; Lengronne *et al.*, 2004; Kogut *et al.*, 2009).

A number of reports using genetic and biochemical methods have teased out many of the regulatory mechanisms that govern cohesin function, mainly though the identification of cohesin cofactors which form separate essential complexes, as diagrammed in Figure 2. First, the cohesin loading complex, composed of Scc2p and Scc4p, is required for cohesin's binding to DNA (Ciosk *et al.*, 2000). Next, a second complex, a homodimer of Eco1p (also known as Ctf7p), promotes cohesion establishment during S phase (Skibbens *et al.*, 1999; Tóth *et al.*, 1999; Onn *et al.*, 2009). It is thought that cohesin is acetylated in order to establish cohesion (Rolef Ben-Shahar *et al.*, 2008; Unal *et al.*, 2008; Zhang *et al.*, 2008).

Once established, however, sister chromatid cohesion must be actively maintained until anaphase onset. Cells defective for Pds5p function are able to establish cohesion, but fail to maintain cohesion in M phase arrested cells (Hartman *et al.*, 2000). It is thought that Pds5p acts as a substoichiometric binding partner of the core cohesin complex, as well as in a separate complex containing two other cohesin accessory proteins, Scc3p and Wpl1p (Kueng *et al.*, 2006). If Pds5 is not bound to every cohesin complex, it is possible that in wild-type cells, some chromosomal loci fail to maintain cohesion, or that a single Pds5p molecule can allow multiple cohesin complexes to maintain sister chromatid cohesion, especially if cohesin complexes could interact.

Once all chromosomes are properly attached to the mitotic spindle, the spindle assembly checkpoint is inactivated, and thus cells proceed through anaphase. The sister chromatids are finally allowed to segregate by dissolving cohesion through the proteolytic degradation of the cohesin complex by the protease Esp1p (Ciosk *et al.*, 1998; Uhlmann *et al.*, 1999). As both mother and daughter cell now contain a complete copy of the genetic material, both are competent to reenter the cell cycle and undergo mitotic division once again.

The Remarkable Structure of the Cohesin Complex

In order to understand how cohesin might function on chromosomes, many researchers have taken a biochemical approach in the hope that cohesin's structure could shed insights into its varied chromatin-bound metabolisms. Highly conserved throughout eukaryotes, it is speculated that the SMC (Structural Maintenance of Chromosomes) family proteins provide the bulk of function. Smc1p, the founding member of this family, contains two conserved globular domains at the amino and carboxyl termini, separated by a long coiled coil domain (Strunnikov *et al.*, 1993; Haering *et al.*, 2002). While the coiled-coils show little to no sequence conservation from yeast to human, the domain is bisected by a conserved "hinge" domain by which the Smc protein folds back on itself (Kurze *et al.*, 2011). As diagrammed in Figure 1, the anti-parallel fold unites the N and C globular regions forming a head domain, which each supply one half of two different ATPases (Löwe *et al.*, 2001; Arumugam *et al.*, 2006).

The addition of the second Smc protein allows formation of a heterodimer (Smc1p and Smc3p) with a number of important interactions. The Smc1p and Smc3p head domains together form two functional ATPase domains (Melby *et al.*, 1998; Hirano, 2001). Second, the heterodimerized hinge domain forms a "toroid" structure, which is required for cohesin function on chromosomes (Kurze *et al.*, 2011). These ATPase domains are highly conserved throughout all eukaryotes.

What is the role of the coiled-coil in Smc1p and Smc3p? Mammalian Smc1p and Smc3p coiled-coils are strongly conserved, but much less so when compared to invertebrates or eukaryotes as a whole (White and Erickson, 2006; 2009). Insertion mutants in the coiled-coils of budding yeast Smc1 can be lethal, as the mutant alleles disrupted cohesin's binding to DNA failed to establish sister chromatid cohesion (Milutinovich *et al.*, 2007). The coiled-coils, as such, could serve as interaction platforms for intra-molecule or inter-molecule interactions. Evidence to support this comes form the coiled-coils of Rad50p, but the biological relevance of such an interaction is not understood (Lammens *et al.*, 2004; 2011; Huis In 't Veld *et al.*, 2014; Rojowska *et al.*, 2014).

The third member of the cohesin complex, Mcd1p, is thought to be cohesin's key regulatory component. Mcd1p has no known enzymatic activity. Mcd1p interacts with both Smc1p and Smc3p, but not in a symmetrical manner (Haering *et al.*, 2004a; Gligoris *et al.*, 2014a). The N terminal of Mcd1 shows a number of intimate contacts with both the base of the coiled-coil as well as the head domain of Smc3p, while the C terminal domain interacts exclusively with the head domain of Smc1p (Haering *et al.*, 2004a; Gligoris *et al.*, 2014a). Due to its spatial proximity to the ATPase domains of Smc1p and Smc3p, Mcd1p is likely to be a key regulator of cohesin function on chromosomes, as it is the only cohesin subunit directly targeted for proteosomal degradation at the anaphase transition (Guacci *et al.*, 1997; Uhlmann *et al.*, 1999; Haering *et al.*, 2004b).

The final member of the core cohesin complex, Scc3p, interacts exclusively with Mcd1p and is not thought to interact with either Smc1p or Smc3p (Tóth *et al.*, 1999; Hara *et al.*, 2014; Roig *et al.*, 2014b). Like Mcd1p, Scc3p has no known enzymatic activity. Recent analysis of mutants in Scc3 suggest that it may play a role in interacting with the cohesin loader to regulate cohesin binding to chromosomes (Orgil *et al.*, 2015). While Scc3p is part of the core cohesin complex, as it is found in equal stoichiometry with Smc1p, Smc3p, and Mcd1p, over-expression of wild-type Scc3p can restore cohesion after inactivation of scc3-1p in M phase arrested cells (Losada *et al.*, 2000; Roig *et al.*, 2014a). This is intriguing as it has been thought that cohesion cannot be generated outside of S phase except in response to DNA damage (Unal *et al.*, 2007). This has been interpreted as consistent with Scc3p capable of subunit exchange on stably bound cohesin complexes, but would also be consistent with Scc3p providing the DNA tethering activity after cohesin binding. It would be interesting to determine if this restoration of damage-independent, S phase independent cohesion could be observed using overexpression of Pds5p in *pds5-1* strains.

While the protein-protein interactions between the core cohesin subunits is well characterized, it remains a mystery if enzymatic functions remain to be revealed.

Is there a relationship between cohesin acetylation and activation of the Smc1/Smc3 ATPase? The mechanistic relationship between ATPase activation and how cohesion is generated remains a topic of intense fascination (Arumugam *et al.*, 2006; Heidinger-Pauli *et al.*, 2010; Ladurner *et al.*, 2014; Murayama and Uhlmann, 2014). It is possible that the other subunits exclusively contain structural or regulatory domains and no additional enzymatic activities. Part of the mystery is the lack of discernible protein motifs in these cohesin related proteins. Much of Scc3p, Pds5p, and Scc2p is composed of HEAT repeats, which are loosely defined as protein-protein interaction domains (Hartman *et al.*, 2000; Neuwald and Hirano, 2000; Panizza *et al.*, 2000; Tonkin *et al.*, 2004).

As might be expected for a ~800kDa protein with a large, disordered domain, no crystal structure of the cohesin holocomplex has been published, to date. Soluble, chromatin-free cohesin complexes have been examined by electron microscopy. When purified, Smc1p, Smc3p heterodimers are visualized, they form appear as V shaped dimers or floppy, circular rings with the hinge at the apex of the V and the heads disassociated (Anderson, 2002; Haering *et al.*, 2002; Huis In 't Veld *et al.*, 2014). The addition of Mcd1p to these purified complexes (again in the absence of DNA) show similar structures for Smc1p and Smc3p, but Mcd1p is now bound near the head domains of the dimer (Anderson, 2002; Haering *et al.*, 2002; Huis In 't Veld *et al.*, 2014). It is from these images that researchers speculated that Mcd1p could regulate cohesin function on DNA by holding the Smc1p and Smc3p heads together.

While the soluble pool of Smc1p and Smc3p is competent to undergo dimerization, it is not sufficient to bind to chromosomes. By examining chromatin extracts from *Xenopus laevis*, Losada and colleagues observed that the cohesin bound to frog chromosomes contained Smc1p, Smc3p, Mcd1p, and Scc3p (Losada *et al.*, 1998). Tóth *et al* showed inactivating any single cohesin subunit with a temperature sensitive allele destabilized cohesin's association with chromatin (1999). This evidence implied that the Smc1p, Smc3p heterodimer was not sufficient to bind chromosomes, but instead required the complete complex composed of Smc1p, Smc3p, Mcd1p, and Scc3p (Tóth *et al.*, 1999).

Evaluation of Cohesin Function: Chromosome Spreads and Sister Chromatid Cohesion

How were the first defects in sister chromatid cohesion identified? Other model organisms, in contrast to budding yeast, have cytologically distinguishable chromosomes using simple cytological stains to visualize the sister chromatids. In fact, the earliest described cohesion defects in the literature were described in

Drosophila, with the identification of *PASC (*Parallel Sister Chromatids) (Perrimon *et al.*, 1985). The rare "escaper" larvae that were homozygous for *pasc* mutants exhibited a "drastic effect" on the condensation and "morphology of anaphase chromosomes" (Perrimon *et al.*, 1985). A more careful analysis of larval neuroblasts showed that these rare, third instar larvae had fully separated sister chromatids, with no cohesion at the arms or between centromeres (Vernì *et al.*, 2000). The next cohesion defects to be described were mutant alleles in Ord and Mei-S332, and was characterized as having a meiotic specific, centromere specific cohesion defect (Miyazaki and Orr-Weaver, 1992; Kerrebrock *et al.*, 1995). The complexity of working with multiceullar organisms precluded using this simple cytological assay to isolate many cohesion defective mutants, including those that impacted the core cohesin complex.

While *SMC1* had been cloned in budding yeast, it was harder to make claims more specific than its general role in chromosome segregation, as inferred from its increased plasmid loss phenotype (Larionov *et al.*, 1985; Strunnikov *et al.*, 1993). Individual yeast chromosomes could not be monitored with cytological stains, as in larger organisms. This roadblock in directly tracking a chromatid for cohesion was removed by the advent of fluorescent in situ hybridization (FISH) (Guacci *et al.*, 1994). Using FISH, the PDS screen (*p*recocious *d*issociation of *s*isters) identified temperature sensitive mutants that were specifically defective for cohesion in M phase arrest. This screen identified three key regulators of cohesion in one fell swoop. Pds1p was required to prevent cohesion dissolution before anaphase onset, as it physically prevented activation of Esp1p (Separase) (Yamamoto *et al.*, 1996a; 1996b; Ciosk *et al.*, 1998). Mcd1p (also known as Pds3p) is the key regulatory protein of the cohesin complex (Guacci *et al.*, 1997; Michaelis *et al.*, 1997). Pds5p was not part of the core complex or the anaphase cohesion dissolution pathway, but was part of another molecular mechanism required to maintain sister chromatid cohesion (Hartman *et al.*, 2000; Noble *et al.*, 2006). Concurrent identification of SMC family members were identified in budding yeast, *Caenorhabditis elegans* as well as *Xenopus laevis* in the same timeframe (Chuang *et al.*, 1994; Hirano and Mitchison, 1994; Michaelis *et al.*, 1997).

To date, there are three assays in budding yeast for assessing sister chromatid cohesion. The first measures the proximity of sister chromatids *in vivo*. Representative images from all assays discussed are described in Figure 2. The second is a functional assay, by which cells are asked to segregate chromosomes through anaphase. The final assay uses a sucrose gradient to fractionate plasmids from crude yeast extract, and the cohesive state of that plasmid is inferred from its migration in an agarose gel. We will discuss all three methods below.

Investigators have devised two approaches to measure sister chromatid proximity. The most commonly used of these assays was devised by Andrew Belmonte and Andy Murray, and utilized direct visualization of sister chromatids with GFP fusion proteins (Straight *et al.*, 1996). Tandem, ~256 copy arrays of LacO repeats are integrated at a single locus in the genome. LacI-GFP is expressed in the same cell. LacI-GFP is brought to the nucleus, where it binds to LacO. In wild-type cells, replicated sister chromatids are held in close proximity such that GFP is resolved as a single focus. If sister chromatid cohesion is defective, sisters diffuse apart such that GFP is now resolved as two foci. This standard for directly measuring sister chromatid cohesion, and is usable in both live and fixed cells. This method allows rapid processing of samples such that a kinetic time-course assay of cohesion dissolution can be characterized. The tandem LacO repeats are not necessarily representative of sister chromatid cohesion at single copy loci, and may reflect the cohesion-state more akin to heterochromatic domains or the rDNA loop, which is composed of ~140 tandem repeats of rDNA associated genes.

The other method for DNA proximity measurement is DNA FISH, as described in the PDS screen above (Guacci *et al.*, 1994). A fluorescent DNA probe can be generated for any genetic locus. This allows direct assessment of cohesion at single copy, non-repetitive genetic loci, but the cells must be fixed and the protocol is technically challenging (Guacci *et al.*, 1994). In principle any locus can be examined by chromosome FISH, but it cannot be used for live cells. These two methods provide complementary approaches to assaying cohesion in different mutants and provide the necessary tools for distinguishing global versus local cohesion defects.

The second assay for measuring sister chromatid cohesion is a functional segregation assay, by which cells containing LacO arrays integrated near centromeric regions are arrested in nocodazole to disrupt the spindle, which is assembled in S phase. Sister chromatids must utilize cohesin in order to remain tethered during this time. After all cells have arrested at the spindle assembly checkpoint, nocodazole is removed and the spindle is allowed to reform. If sister chromatid cohesion is functional, close to 95% of cells will show wild-type segregation of replicated sister chromatids. If cohesion is disrupted, segregation will be random, and as such only 50% of cells will show proper segregation of replicated sister chromatids between the mother and daughter cell.

The third method, as mentioned above, measures the sedimentation and migration of a plasmid harvested from yeast lysates (Ivanov and Nasmyth, 2007). The yeast lysate is fractionated by sucrose gradient centrifugation, and each fraction is resolved on an agarose gel. The plasmid is then identified from the crude lysate by southern blot analysis across ~75 fractions. In wild-type cells

arrested in nocodazole, the plasmid migrates as two bands (Ivanov and Nasmyth, 2007). This pattern is somewhat different from plasmids isolated from the crude extract from G1 staged or asynchronous cells, and the overall percentage of plasmids interpreted to be “cohesed” is very small. However, if cohesin is topogically crosslinked and plasmids are extracted and chemically crosslinked *in vitro*, a small population of plasmid DNA retains the slower mobility, and other rare plasmid species are detected (Haering *et al.*, 2008). While Ivanov and colleagues argue that the migration patterns are different due to the presence or absence of cohesion, plasmid concatenation or compaction could easily have large impacts on migration patterns observed in agarose gels. Due to the tedious nature of the assay, it is also technically difficult (if not impossible) to conduct the same cohesion kinetics assay used to distinguish between cohesion establishment or cohesion maintenance defects as with LacO arrays, limiting the analysis to simple end-point readouts. Not surprisingly, this assay has not been adopted by any other labs in the field, and its biological relevance remains controversial.

Models for Cohesin Binding to DNA

The seminal images from rotary shadow electron microscopy that show cohesin forming V shaped or ring-like structures has influenced how we think about cohesin function on chromosomes (Anderson, 2002). The simplest of these models posits that the electron microscopy images are exactly correct, and that the ring-like topology is indicative of cohesin function. As diagrammed in Figure 4, the core cohesin complex binds to a pre-replicated chromosome such that the sister chromatid is held within a large ring, as proteolytic cleavage of the cohesin complex disrupted its binding to DNA (Gruber *et al.*, 2003; Ivanov and Nasmyth, 2005). This simple model ties cohesin’s stable binding to DNA to cohesion generation, as the mere presence of cohesin on chromosomes prior to their replication allows for the correct pair of sisters to be tethered concurrent with replication. However, showing that a protein’s stable binding to DNA is disrupted by proteolytic cleavage does not imply that the protein forms a ring; merely, one has instead shown that the protein’s DNA binding is disrupted by cleavage. More convincing data in support of cohesin’s toplogy came from chemically-crosslinked cohesin rings in the topologically closed configuration. Using an *in vitro* assay, Haering and colleagues examined if this crosslinked cohesin was competent to support comigration of denatured plasmids through an agarose gel (Haering *et al.*, 2008). The authors reported that upon chemical crosslinking, approximately 5% of recoverable crosslinked plasmids showed a migration pattern consistent topological entrapment by cohesin (Haering *et al.*, 2008). A mathematical model of their crosslinking efficiency was consistent with a single cohesin ring mediating function rather than any other form (Haering *et al.*, 2008). Interestingly, the

authors did not cross-link wild-type cohesin, but a fusion protein in which the Smc1p and Mcd1 were connected at the incorrect domain by a flexible linker (Haering *et al.*, 2008; Gligoris *et al.*, 2014b).

While the *in vitro* evidence clearly demonstrates that cohesin can topologically interact with an small fraction of plasmid DNA resulting in a mobility shift in an agarose gel, it is less clear if the same interactions occur in the context of linear chromosomes mediating global chromosome architecture. As diagrammed in Figure 4, there are other models for cohesin function; while the simple cohesin ring might be necessary for cohesin's varied activities on DNA, it is not sufficient. Instead, these models posit that higher order cohesin structures could form on chromosomes, and these cohesin-cohesin interactions would be required to generate cohesion, condensation, or DNA repair. We will refer to these interactions in the future as cohesin oligomers. If these cohesin-cohesin interactions are required for function, one would then predict that a homodimeric interaction (such as between Smc1p and another Smc1p) should be detectable in the soluble lysate, which has not been reported in the literature to date (Haering *et al.*, 2002).

While the biochemical data in support of cohesin oligomers has not yet been reported, a number of unresolved inconsistencies against the embrace model exist in the literature. For the embrace model to be correct, cohesin's stable binding to chromosomes would be both necessary and sufficient to tether sister chromatids on a global level. The first inconsistency is that cohesin at the centromere does not provide cohesion, but instead acts to form intra-stand loops to generate a centromere barrel (Yeh *et al.*, 2008). Secondly, cohesin at the silent mating loci (*HML* and *HMR*) are stably bound to DNA and function as boundary elements to limit Sir2p mediated gene silencing (Donze *et al.*, 1999). If the silent mating locus is excised from the genome and circularized via LoxP recombination, cohesin fails to maintain sister chromatid cohesion between these newly circularized regions (Chang *et al.*, 2005). Similar roles for cohesin in the formation of intra-strand loops in regulating transcription have been reported in flies and human (Rollins *et al.*, 1999; Misulovin *et al.*, 2008; Wendt *et al.*, 2008).These data imply that at topologically unique loci, cohesin might exist in alternative configurations that allow cohesin to play extraordinary roles distinct from cohesion or condensation.

The previous results do not rule out the possibility that the majority of time, cohesin's stable binding to DNA is necessary and sufficient to generate cohesion, which is required genome-wide. However, *eco1Δ wpl1Δ* strains show stable cohesin binding and viability, due to restoration of chromosome compaction (Rolef Ben-Shahar *et al.*, 2008; Sutani *et al.*, 2009; Guacci and Koshland, 2012). Cohesin was still unable to restore global sister chromatid cohesion, as

measured by chromosome segregation efficiency after *de novo* assembly of the spindle after nocodazole treatment (Guacci and Koshland, 2012). These results suggested that cohesin's competence to generate cohesion was not dictated by its stable binding to chromosomes, as measured by florescence recovery after photobleaching (FRAP). Taken together these results suggest that the embrace model is at best, in need of revision, or at worst, abandoned entirely.

Cohesin Binds Chromosomes at Discrete Chromosome Addresses

Cohesin is not constitutively bound to chromosomes; cohesin is loaded onto chromosomes by the Scc2p/Scc4p loader complex, and removed during anaphase to allow chromosome segregation (Yamamoto *et al.*, 1996b; Uhlmann *et al.*, 1999; Ciosk *et al.*, 2000). In budding yeast, cohesin is reloaded at the G1/S transition. Vertebrates, in contrast, allow cohesin to rebind chromosomes in telophase of the preceding cell cycle (Losada *et al.*, 1998; Darwiche *et al.*, 1999; Sumara *et al.*, 2000).

Where does cohesin bind to chromosomes? Using indirect immunofluorescence against cohesin proteins against chromosomes spread on glass slides, cohesin appeared to bind chromosomes globally without specific enrichment at distinct foci (Guacci *et al.*, 1997; Michaelis *et al.*, 1997). Higher resolution chromosome spread techniques ("super spreads"), again in budding yeast, suggested that approximately 100 distinct cohesin foci were present in a single yeast mass (Ciosk *et al.*, 2000). However, high resolution mapping of cohesin binding sites by chromatin immunoprecipitation followed by either PCR or microarray analysis suggested that in a population of synchronously arrested yeast cells, up to ~1,000 sites could be identified (Blat and Kleckner, 1999; Tanaka *et al.*, 1999; Laloraya *et al.*, 2000).

This high resolution mapping demonstrated that cohesin was enriched in a broad, peri-centromeric domain flanking each centromere, and at a lower density at regularly spaced intervals at chromosomal arm loci. These regions were roughly spaced every ~10kb and termed cohesin associated regions (CARs) (Laloraya *et al.*, 2000). In budding yeast, CARs tended to be AT rich in DNA basepair composition and enriched between convergently transcribed genes (Laloraya *et al.*, 2000; Lengronne *et al.*, 2004). While the regular spacing is also observed in metazoans, these cohesin associated regions tend to be enriched instead at transcription start sites as well as gene bodies, as opposed to intergenic regions between two convergent promoters (Lengronne *et al.*, 2004; Parelho *et al.*, 2008; Kagey *et al.*, 2010). To date, no sequence determinant for cohesin binding has been identified. Additionally, the CAR itself is a 1kb region of enrichment, which may reflect a number of possible scenarios of cohesin interaction with DNA

(Laloraya *et al.*, 2000). As ChIP data reflects the percentage of a given DNA amplicon that contains a crosslinked protein in a population of cells, it cannot determine the number of cohesin molecules present on any single sequence in a specific cell. Formally, it is possible that at any given CAR, a single cohesin molecule is always present but at a variable position within a 1kb domain. It may also reflect a large number of cohesin molecules present at a single CAR, which is only occupied in a subset of cells. If we try to reconcile the global distribution of the cohesin complex by ChIP with what we observe by chromosome spreads, it is formally possible that of the 1,000 CARs detected, only ~100 are utilized in any given cell.

As there is no known DNA binding motif indicative of cohesin's residence on DNA, which amino acids in cohesin make contact with DNA? As mentioned earlier, only the intact cohesin complex is competent to bind DNA; abrogation of any single subunit impairs cohesin loading (Michaelis *et al.*, 1997; Tóth *et al.*, 1999). Artificial cleavage of either Smc3p or Mcd1p by use of an engineered TEV-protease cleavage domain in either subunit can also disrupt chromosomal binding (Hornig and Uhlmann, 2004; Ivanov and Nasmyth, 2005). This strongly implies that any mutation that disrupts formation of the core complex will disrupt binding to DNA. Additionally, mutants that are compromised for Smc3p ATPase function are unable to bind DNA, suggesting that ATP binding and hydrolysis are involved in binding DNA (Arumugam *et al.*, 2003; Heidinger-Pauli *et al.*, 2010; Ladurner *et al.*, 2014). Additionally, mutations in the SCD domain of Scc3 block cohesin from interacting with the cohesin loader Scc2p, implying that a domain in Scc3p is required to load the core complex onto DNA (Orgil *et al.*, 2015). We must conclude there are no known regions or single amino acids that allows cohesin to physically contact DNA. Instead, these results are consistent with a number of domains in cohesin either required for interacting with the loader Scc2p, or that cohesin does not make a specific contact with DNA and instead traps the substrate by a topological manner.

Post Translational Modifications Regulate Cohesin Function After DNA Binding

After binding DNA, what coordinates activation of cohesin activity? A number of post-translational modifications, such as phosphorylation, acetylation, and SUMOlyation, are known to occur on cohesin complexes, and are thought to be restricted to cohesin's DNA-bound state.

Phosphorylation

Historically, it was evident that cohesin was phosphorylated in a cell cycle

dependent manner by Cdc5 (Polo kinase), but the relevance of this phosphorylation remained enigmatic (Alexandru *et al.*, 2001). Cells depleted for Cdc5p by inhibiting *GAL1* mediated transcription were inviable on YPD plates. However, these cells showed only a modest delay through a single cell cycle and no cohesion defect, although Cdc5 protein levels were never directly assayed by western blot (Alexandru *et al.*, 2001). Strains in which 2 (out of ~20) possible serines were mutated to alanine in order to block phosphorylation also failed to show a cohesion defect, but it was formally possible that Alexandru and colleagues had not mutated the correct residues required for cohesion. Ultimately the authors were not successful in linking the inviable phenotype from *GAL1* inactivation of *CDC5* with the phosphorylation of Mcd1p and therefore, cohesin.

Part of the mystery was eventually resolved with the identification of cohesin's prophase removal pathway in higher eukaryotes. In higher eukaryotes, phosphorylation of Mcd1p by Polo kinase protects cohesin at the centromere from removal, while cohesin at chromosome arm sites is removed in order to generate chromosome resolution (Sumara *et al.*, 2002). Mcd1p is not the only subunit known to be phosphorylated for removal; Scc3 shows a similar pattern (Losada *et al.*, 2000). Inactivation of Polo kinase results in under condensed, poorly resolved chromosomes in metaphase, and the appearance of anaphase bridges upon segregation. This result suggests that in higher eukaryotes, Cdc5/ Polo kinase is required for chromosome condensation or chromosome resolution.

Since Cdc5p and cohesin phosphorylation are thought to be highly conserved, it is inconsistent that a similar role for cohesin removal is not readily apparent in budding yeast. Part of the answer may be due to the incomplete penetrance of a *GAL1* inactivation in yeast mitosis, as meiotic yeast cells lacking Cdc5p stall in metaphase I with a cohesion defect (Lee and Amon, 2003). If yeast Cdc5p is highly produrant, transient inactivation may not allow enough time for protein turnover. In contrast, yeast meiosis is measured in hours, not minutes, and as such, could account for the difference in cohesion competency between the two cell cycles.

Acetylation

In addition to phosphorylation, cohesin acetylation was also identified as a key regulator of cohesion generation. Using a bioinformatics approach, Ivanov and colleagues identified Eco1p/Ctf7p as a possible acetyltransferase, and then demonstrated it had the capability to acetylate cohesin proteins *in vitro* (Ivanov *et al.*, 2002). Eco1p activity was dispensable for cohesin binding to all DNA loci, but was required to establish cohesion in all cases assessed (Skibbens *et al.*, 1999; Tóth *et al.*, 1999). In addition, it was also demonstrated that Eco1p could

generate global sister chromatid cohesion in response to a single double strand break after replication, decoupling cohesion generation from S phase (Sjögren and Nasmyth, 2001; Ström *et al.*, 2004; Unal *et al.*, 2004; 2007).

Was Eco1p modulating cohesin activity through its acetyltransferase activity? A number of investigators demonstrated that two highly conserved lysines in Smc3p were required for cohesion generation (Rolef Ben-Shahar *et al.*, 2008; Unal *et al.*, 2008; Zhang *et al.*, 2008). Like a cell compromised for Eco1p activity, mutating these two lysines (K112 and K113) to asparagines blocked the establishment of sister chromatid cohesion (Rolef Ben-Shahar *et al.*, 2008; Unal *et al.*, 2008). Additionally, an Smc3p acetyl-mimic could partially restore cohesion in an *eco1-1* temperature sensitive strain (Unal *et al.*, 2008). These data in sum corroborated a role for Smc3p acetylation and generation of a cohesion-competent state.

Cohesin acetylation, however, is not the simple molecular cue responsible for sister chromatid cohesion. To reiterate, the restoration of cohesion in the Smc3 acetyl-mimic to bypass a *eco1-1* strain was still partial; Smc3 acetyl-mimics are sick but viable, and in contrast display pronounced cohesion defects (Unal *et al.*, 2008; Guacci and Koshland, 2012). As the acetyl-mimics prevent the modulation of acetylation state at either lysine, there are two possible interpretations for the strong cohesion defects. First, it is formally possible that the dosage of acetylated vs. unacetylated cohesin is important for regulating cohesion establishment. Secondly, if the transition from acetylated to non-acetylated cohesin is important, an acetyl-mimic or acetyl-null allele trapped in a single state would be refractory to any sort of conformational change necessary to generate wild-type cohesion. As such, we must consider cohesin acetylation as necessary, but not sufficient for the establishment of sister chromatid cohesion.

SUMOlyation

Cohesin's third and final post-translational modification is SUMOlyation, a small ubiquitin-like modification that also occurs on lysine residues. In budding yeast, this post-translationally conjugated moiety is encoded by the *SMT3* locus, first identified in a screen for high copy suppressors of *mif2* defective strains (Meluh and Koshland, 1995; Takahashi *et al.*, 1999; 2006) . SUMO moieties are conjugated in a stepwise manner by a cascade of enzymes (the E2 ligase Ubc9p and the E3 ligases Mms21p, Siz1p and Siz2p). SUMO moieties are removed by SUMO isopeptidase, Ulp1p and Ulp2p/Smt4p. Using a 2μM over-expression library, Noble and colleagues observed that overexpression of *ULP2*/*SMT4* was able to rescue the temperature sensitivity of *pds5-1* strains (2003). *ULP1* over-expression was also able to rescue the temperature sensitivity of *pds5-1* strains, albeit not to the same degree (Noble *et al.*, 2006). This is consistent with a report

from D'Ambrosio and colleagues, who reported that Mcd1p is hyper-SUMOlyated in *pds5-1* strains, but not *smc3-42* strains (2014). While Noble and colleagues reported good rescue of viability in *pGAL-ULP2 pds5-2* strains, cohesion was only weakly restored. This suggests that SUMOlyation is promoting cohesin's role in chromosome condensation, and to a much lesser role, sister chromatid cohesion.

As a subset of SUMOlyated proteins are polysumolyated as a marker for proteasomal degradation, D'Ambrosio and colleagues extended their analysis of SUMO mutants to utilize SUMO moieties that were defective for branched-chain formation, limiting SUMOlyation to mono-SUMO species (2014). Surprisingly, *pds5-1 smt3-3R* strains, which could not generate poly-sumolyated chains, show robust viability and cohesion at 35˚C, when the parental *pds5-1* strain was inviable and cohesion defective (D'Ambrosio and Lavoie, 2014). Treatment of *pds5-1* strains with the proteasome inhibitor MG132 phenocopied *pds5-1 smt3-3R* strains, demonstrating that the polysumolyated species were indeed targeted for degradation (D'Ambrosio and Lavoie, 2014). These data implies that Pds5p promotes cohesion maintenance by regulating cohesin SUMOlyation, and enrichment of poly-sumolyated cohesin species leads to defects in maintaining sister chromatid cohesion. It is interesting that the suppression of *pds5* mutants is so different by fairly similar components of the SUMO ligase pathway; over-expression of Ulp2p should, in principle, prevent buildup of SUMOlyated cohesin. However, it is possible that many different classes of SUMO species are found on cohesin, and Ulp2p is not as efficient as removing branched species, leading to an enrichment of these toxic cohesin species.

Is SUMOlyation dispensable for cohesion establishment, but required for maintenance? The previous data is consistent with a role for SUMOlyation correlating with Pds5p function. Bachant and colleagues reported that *ulp2-Δ* strains were defective for cohesion at the centromere-proximal loci, up to 23 kb away *CEN3* (Bachant *et al.*, 2002). The locus specific loss of cohesion maintenance could reflect a different chromatin configuration at the centromere, such as the cohesin barrel (described below).

Chromosome Architecture: Cohesin Forms a Centromere Barrel

Does cohesin contribute to chromosome architecture at unique chromosomal loci? It has been well established that cohesin promotes the poleward migration of sister chromatids by allowing assembly of bioriented kinetochores on the metaphase spindle. One would then predict that sister chromatids immediately adjacent to centromeres (which must be tethered) would rarely appear separated. However, direct observations of centromeric cohesion by LacO arrays

near centromeres suggested that while cohesin binding to DNA was highly enriched, the locus itself showed showed a cohesion defect (Yeh *et al.*, 2008).

High resolution microscopy of fluorescently labeled cohesin resolved this inconsistency, as cohesin at the centromere contributed to the formation of a cohesin axis. Yeh and colleagues postulated that this cohesin was not utilized for tethering sister chromatids, but rather acted to form intrastrand chromatin loops (2008). These loops (on the same sister chromatid) would position the centromeric nucleosome variant, CENP-A, in such a way that it would promote assembly of the kinetochore. The cohesin barrel (and kinetochore assembly) was disrupted in *mcd1-1* strains, providing further evidence that the unusual centromere structure was important for chromosome segregation (Yeh *et al.*, 2008). It is interesting to emphasize that cohesin immediately over centromeres is stably bound, but not used to generate cohesion (Yeh *et al.*, 2008).

The Research Aims of this Dissertation

In order to address some of the important gaps in our understanding of cohesin's ability to tether sisters, I took a genetics and biochemical approach to find mutants in cohesin's regulatory subunit that were inviable in the absence of wild-type. We focused on cohesin's regulatory subunit, Mcd1p, as we reasoned it was the most likely to give the most penetrant phenotype. Mutants that blocked the formation of the core cohesin complex would be the least interesting, as we were interested in mutants that were compromised downstream of DNA binding. As an orthogonal approach to characterizing our mutants in the presence of a temperature sensitive allele, we also utilized the auxin degron to generate auxin sensitive conditional-null alleles of all the cohesin subunits as well as several of its regulatory factors. These alleles allowed an unparalleled ability to characterize cohesin alleles without the presence of wild-type. With these tools, we are able to make several key findings. First, we demonstrate that cohesin can be stably bound to chromosomes, but unable to tether. Second, we find genetic evidence for communication between cohesin complexes with the observation of interallelic complementation. Using an auxin sensitive allele of Cdc5p, we also show that Cdc5p is required for the maintenance of sister chromatid cohesion, resolving a longstanding inconsistency between metazoan Cdc5p and budding yeast. Finally, an auxin sensitive allele of Wpl1p demonstrates that Wpl1 is essential in budding yeast, but only upon an extended auxin treatment in stationary cells. This surprising result is consistent with a report from Tedeschi and colleagues describing a role for Wapal in maintaining interphase chromosome structure in starved mammalian cell culture (2013).

References

Alexandru, G., Uhlmann, F., Mechtler, K., Poupart, M. A., and Nasmyth, K. (2001). Phosphorylation of the cohesin subunit Scc1 by Polo/Cdc5 kinase regulates sister chromatid separation in yeast. Cell *105*, 459–472.

Anderson, D. E. (2002). Condensin and cohesin display different arm conformations with characteristic hinge angles. The Journal of Cell Biology *156*, 419–424.

Arumugam, P., Gruber, S., Tanaka, K., Haering, C. H., Mechtler, K., and Nasmyth, K. (2003). ATP hydrolysis is required for cohesin's association with chromosomes. Curr Biol *13*, 1941–1953.

Arumugam, P., Nishino, T., Haering, C. H., Gruber, S., and Nasmyth, K. (2006). Cohesin's ATPase activity is stimulated by the C-terminal Winged-Helix domain of its kleisin subunit. Curr Biol *16*, 1998–2008.

Bachant, J., Alcasabas, A., Blat, Y., Kleckner, N., and Elledge, S. J. (2002). The SUMO-1 isopeptidase Smt4 is linked to centromeric cohesion through SUMO-1 modification of DNA topoisomerase II. Mol Cell *9*, 1169–1182.

Blat, Y., and Kleckner, N. (1999). Cohesins bind to preferential sites along yeast chromosome III, with differential regulation along arms versus the centric region. Cell *98*, 249–259.

Chang, C.-R., Wu, C.-S., Hom, Y., and Gartenberg, M. R. (2005). Targeting of cohesin by transcriptionally silent chromatin. *19*, 3031–3042.

Chuang, P. T., Albertson, D. G., and Meyer, B. J. (1994). DPY-27:a chromosome condensation protein homolog that regulates C. elegans dosage compensation through association with the X chromosome. Cell *79*, 459–474.

Ciosk, R., Shirayama, M., Shevchenko, A., Tanaka, T., Tóth, A., and Nasmyth, K. (2000). Cohesin's binding to chromosomes depends on a separate complex consisting of Scc2 and Scc4 proteins. Mol Cell *5*, 243–254.

Ciosk, R., Zachariae, W., Michaelis, C., Shevchenko, A., Mann, M., and Nasmyth, K. (1998). An ESP1/PDS1 complex regulates loss of sister chromatid cohesion at the metaphase to anaphase transition in yeast. Cell *93*, 1067–1076.

D'Ambrosio, L. M., and Lavoie, B. D. (2014). Pds5 Prevents the PolySUMO-Dependent Separation of Sister Chromatids. Curr Biol *24*, 361–371.

Darwiche, N., Freeman, L. A., and Strunnikov, A. (1999). Characterization of the components of the putative mammalian sister chromatid cohesion complex. Gene *233*, 39–47.

Dewar, H., Tanaka, K., Nasmyth, K., and Tanaka, T. U. (2004). Tension between two kinetochores suffices for their bi-orientation on the mitotic spindle. Nature *428*, 93–97.

Donze, D., Adams, C. R., Rine, J., and Kamakaka, R. T. (1999). The boundaries of the silenced HMR domain in Saccharomyces cerevisiae. *13*, 698–708.

Gligoris, T. G., Scheinost, J. C., Bürmann, F., Petela, N., Chan, K.-L., Uluocak, P., Beckouët, F., Gruber, S., Nasmyth, K., and Löwe, J. (2014a). Closing the cohesin ring: structure and function of its Smc3-kleisin interface. Science *346*, 963–967.

Gligoris, T. G., Scheinost, J. C., Bürmann, F., Petela, N., Chan, K.-L., Uluocak, P., Beckouët, F., Gruber, S., Nasmyth, K., and Löwe, J. (2014b). Closing the cohesin ring: structure and function of its Smc3-kleisin interface. Science *346*, 963–967.

Gruber, S., Haering, C. H., and Nasmyth, K. (2003). Chromosomal cohesin forms a ring. Cell *112*, 765–777.

Guacci, V., and Koshland, D. (2012). Cohesin-independent segregation of sister chromatids in budding yeast. Mol Biol Cell *23*, 729–739.

Guacci, V., Hogan, E., and Koshland, D. (1994). Chromosome condensation and sister chromatid pairing in budding yeast. The Journal of Cell Biology *125*, 517–530.

Guacci, V., Koshland, D., and Strunnikov, A. (1997). A direct link between sister chromatid cohesion and chromosome condensation revealed through the analysis of MCD1 in S. cerevisiae. Cell *91*, 47–57.

Haering, C. H., Farcas, A.-M., Arumugam, P., Metson, J., and Nasmyth, K. (2008). The cohesin ring concatenates sister DNA molecules. Nature *454*, 297–301.

Haering, C. H., Löwe, J., Hochwagen, A., and Nasmyth, K. (2002). Molecular architecture of SMC proteins and the yeast cohesin complex. Mol Cell *9*, 773–788.

Haering, C. H., Schoffnegger, D., Nishino, T., Helmhart, W., Nasmyth, K., and

Löwe, J. (2004a). Structure and stability of cohesin's Smc1-kleisin interaction. Mol Cell *15*, 951–964.

Haering, C. H., Schoffnegger, D., Nishino, T., Helmhart, W., Nasmyth, K., and Löwe, J. (2004b). Structure and stability of cohesin's Smc1-kleisin interaction. Mol Cell *15*, 951–964.

Hara, K., Zheng, G., Qu, Q., Liu, H., Ouyang, Z., Chen, Z., Tomchick, D. R., and Yu, H. (2014). Structure of cohesin subcomplex pinpoints direct shugoshin-Wapl antagonism in centromeric cohesion. Nat. Struct. Mol. Biol. *21*, 864–870.

Hartman, T., Stead, K., Koshland, D., and Guacci, V. (2000). Pds5p is an essential chromosomal protein required for both sister chromatid cohesion and condensation in Saccharomyces cerevisiae. The Journal of Cell Biology *151*, 613–626.

Heidinger-Pauli, J. M., Onn, I., and Koshland, D. (2010). Genetic evidence that the acetylation of the Smc3p subunit of cohesin modulates its ATP-bound state to promote cohesion establishment in Saccharomyces cerevisiae. Genetics *185*, 1249–1256.

Hirano, M. (2001). Bimodal activation of SMC ATPase by intra- and inter-molecular interactions. Embo J *20*, 3238–3250.

Hirano, T., and Mitchison, T. J. (1994). A heterodimeric coiled-coil protein required for mitotic chromosome condensation in vitro. Cell *79*, 449–458.

Hornig, N. C. D., and Uhlmann, F. (2004). Preferential cleavage of chromatin-bound cohesin after targeted phosphorylation by Polo-like kinase. Embo J *23*, 3144–3153.

Huis In 't Veld, P. J., Herzog, F., Ladurner, R., Davidson, I. F., Piric, S., Kreidl, E., Bhaskara, V., Aebersold, R., and Peters, J.-M. (2014). Characterization of a DNA exit gate in the human cohesin ring. Science *346*, 968–972.

Ivanov, D., and Nasmyth, K. (2005). A topological interaction between cohesin rings and a circular minichromosome. Cell *122*, 849–860.

Ivanov, D., and Nasmyth, K. (2007). A physical assay for sister chromatid cohesion in vitro. Mol Cell *27*, 300–310.

Ivanov, D., Schleiffer, A., Eisenhaber, F., Mechtler, K., Haering, C. H., and Nasmyth, K. (2002). Eco1 is a novel acetyltransferase that can acetylate proteins involved in cohesion. Current Biology *12*, 323–328.

Kagey, M. H. *et al.* (2010). Mediator and cohesin connect gene expression and chromatin architecture. Nature *467*, 430–435.

Kerrebrock, A. W., Moore, D. P., Wu, J. S., and Orr-Weaver, T. L. (1995). Mei-S332, a Drosophila protein required for sister-chromatid cohesion, can localize to meiotic centromere regions. Cell *83*, 247–256.

Kogut, I., Wang, J., Guacci, V., Mistry, R. K., and Megee, P. C. (2009). The Scc2/Scc4 cohesin loader determines the distribution of cohesin on budding yeast chromosomes. Genes Dev. *23*, 2345–2357.

Kueng, S., Hegemann, B., Peters, B. H., Lipp, J. J., Schleiffer, A., Mechtler, K., and Peters, J.-M. (2006). Wapl Controls the Dynamic Association of Cohesin with Chromatin. Cell *127*, 955–967.

Kurze, A. *et al.* (2011). A positively charged channel within the Smc1/Smc3 hinge required for sister chromatid cohesion. Embo J *30*, 364–378.

Ladurner, R., Bhaskara, V., Huis In 't Veld, P. J., Davidson, I. F., Kreidl, E., Petzold, G., and Peters, J.-M. (2014). Cohesin's ATPase activity couples cohesin loading onto DNA with Smc3 acetylation. Curr Biol *24*, 2228–2237.

Laloraya, S., Guacci, V., and Koshland, D. (2000). Chromosomal addresses of the cohesin component Mcd1p. The Journal of Cell Biology *151*, 1047–1056.

Lammens, A., Schele, A., and Hopfner, K.-P. (2004). Structural Biochemistry of ATP-Driven Dimerization and DNA-Stimulated Activation of SMC ATPases. Current Biology *14*, 1778–1782.

Lammens, K. *et al.* (2011). The Mre11:Rad50 Structure Shows an ATP-Dependent Molecular Clamp in DNA Double-Strand Break Repair. Cell *145*, 54–66.

Larionov, V. L., Karpova, T. S., Kouprina, N. Y., and Jouravleva, G. A. (1985). A mutant of Saccharomyces cerevisiae with impaired maintenance of centromeric plasmids. Curr. Genet. *10*, 15–20.

Lee, B. H., and Amon, A. (2003). Role of Polo-like kinase CDC5 in programming meiosis I chromosome segregation. Science *300*, 482–486.

Lengronne, A., Katou, Y., Mori, S., Yokobayashi, S., Kelly, G. P., Itoh, T., Watanabe, Y., Shirahige, K., and Uhlmann, F. (2004). Cohesin relocation from sites of chromosomal loading to places of convergent transcription. Nat Cell Biol *430*, 573–578.

Losada, A., Hirano, M., and Hirano, T. (1998). Identification of Xenopus SMC protein complexes required for sister chromatid cohesion. Genes Dev. *12*, 1986–1997.

Losada, A., Yokochi, T., Kobayashi, R., and Hirano, T. (2000). Identification and characterization of SA/Scc3p subunits in the Xenopus and human cohesin complexes. The Journal of Cell Biology *150*, 405–416.

Löwe, J., Cordell, S. C., and van den Ent, F. (2001). Crystal structure of the SMC head domain: an ABC ATPase with 900 residues antiparallel coiled-coil inserted. J. Mol. Biol. *306*, 25–35.

Melby, T. E., Ciampaglio, C. N., Briscoe, G., and Erickson, H. P. (1998). The symmetrical structure of structural maintenance of chromosomes (SMC) and MukB proteins: long, antiparallel coiled coils, folded at a flexible hinge. The Journal of Cell Biology *142*, 1595–1604.

Meluh, P. B., and Koshland, D. (1995). Evidence that the MIF2 gene of Saccharomyces cerevisiae encodes a centromere protein with homology to the mammalian centromere protein CENP-C. Mol Biol Cell *6*, 793–807.

Michaelis, C., Ciosk, R., and Nasmyth, K. (1997). Cohesins: chromosomal proteins that prevent premature separation of sister chromatids. Cell *91*, 35–45.

Milutinovich, M., Unal, E., Ward, C., Skibbens, R. V., and Koshland, D. (2007). A multi-step pathway for the establishment of sister chromatid cohesion. PLoS Genet *3*, e12.

Misulovin, Z. *et al.* (2008). Association of cohesin and Nipped-B with transcriptionally active regions of the Drosophila melanogaster genome. Chromosoma *117*, 89–102.

Miyazaki, W. Y., and Orr-Weaver, T. L. (1992). Sister-chromatid misbehavior in Drosophila ord mutants. Genetics *132*, 1047–1061.

Murayama, Y., and Uhlmann, F. (2014). Biochemical reconstitution of topological DNA binding by the cohesin ring. Nature *505*, 367–371.

Neuwald, A. F., and Hirano, T. (2000). HEAT repeats associated with condensins, cohesins, and other complexes involved in chromosome-related functions. Genome Research *10*, 1445–1452.

Noble, D., Kenna, M. A., Dix, M., Skibbens, R. V., Unal, E., and Guacci, V. (2006). Intersection between the regulators of sister chromatid cohesion

establishment and maintenance in budding yeast indicates a multi-step mechanism. Cell Cycle *5*, 2528–2536.

Onn, I., Guacci, V., and Koshland, D. E. (2009). The zinc finger of Eco1 enhances its acetyltransferase activity during sister chromatid cohesion. Nucleic Acids Research *37*, 6126–6134.

Orgil, O., Matityahu, A., Eng, T., Guacci, V., Koshland, D., and Onn, I. (2015). A conserved domain in the scc3 subunit of cohesin mediates the interaction with both mcd1 and the cohesin loader complex. PLoS Genet *11*, e1005036.

Panizza, S., Tanaka, T., Hochwagen, A., Eisenhaber, F., and Nasmyth, K. (2000). Pds5 cooperates with cohesin in maintaining sister chromatid cohesion. Curr Biol *10*, 1557–1564.

Parelho, V. *et al.* (2008). Cohesins functionally associate with CTCF on mammalian chromosome arms. Cell *132*, 422–433.

Perrimon, N., Engstrom, L., and Mahowald, A. P. (1985). Developmental genetics of the 2C-D region of the Drosophila X chromosome. Genetics *111*, 23–41.

Roig, M. B., Löwe, J., Chan, K.-L., Beckouët, F., Metson, J., and Nasmyth, K. (2014a). Structure and function of cohesin's Scc3/SA regulatory subunit. FEBS Lett. *588*, 3692–3702.

Roig, M. B., Löwe, J., Chan, K.-L., Beckouët, F., Metson, J., and Nasmyth, K. (2014b). Structure and function of cohesin’s Scc3/SA regulatory subunit. FEBS Lett. *588*, 3692–3702.

Rojowska, A., Lammens, K., Seifert, F. U., Direnberger, C., Feldmann, H., and Hopfner, K.-P. (2014). Structure of the Rad50 DNA double-strand break repair protein in complex with DNA. Embo J *33*, 2847–2859.

Rolef Ben-Shahar, T., Heeger, S., Lehane, C., East, P., Flynn, H., Skehel, M., and Uhlmann, F. (2008). Eco1-dependent cohesin acetylation during establishment of sister chromatid cohesion. Science *321*, 563–566.

Rollins, R. A., Morcillo, P., and Dorsett, D. (1999). Nipped-B, a Drosophila homologue of chromosomal adherins, participates in activation by remote enhancers in the cut and Ultrabithorax genes. Genetics *152*, 577–593.

Sjögren, C., and Nasmyth, K. (2001). Sister chromatid cohesion is required for postreplicative double-strand break repair in Saccharomyces cerevisiae. Curr Biol *11*, 991–995.

Skibbens, R. V., Corson, L. B., Koshland, D., and Hieter, P. (1999). Ctf7p is essential for sister chromatid cohesion and links mitotic chromosome structure to the DNA replication machinery. *13*, 307–319.

Straight, A. F., Belmont, A. S., Robinett, C. C., and Murray, A. W. (1996). GFP tagging of budding yeast chromosomes reveals that protein-protein interactions can mediate sister chromatid cohesion. Curr Biol *6*, 1599–1608.

Ström, L., Lindroos, H. B., Shirahige, K., and Sjögren, C. (2004). Postreplicative recruitment of cohesin to double-strand breaks is required for DNA repair. Mol Cell *16*, 1003–1015.

Strunnikov, A. V., Larionov, V. L., and Koshland, D. (1993). SMC1: an essential yeast gene encoding a putative head-rod-tail protein is required for nuclear division and defines a new ubiquitous protein family. The Journal of Cell Biology *123*, 1635–1648.

Sumara, I., Vorlaufer, E., Gieffers, C., Peters, B. H., and Peters, J. M. (2000). Characterization of vertebrate cohesin complexes and their regulation in prophase. The Journal of Cell Biology *151*, 749–762.

Sumara, I., Vorlaufer, E., Stukenberg, P. T., Kelm, O., Redemann, N., Nigg, E. A., and Peters, J.-M. (2002). The dissociation of cohesin from chromosomes in prophase is regulated by Polo-like kinase. Mol Cell *9*, 515–525.

Sutani, T., Kawaguchi, T., Kanno, R., Itoh, T., and Shirahige, K. (2009). Budding yeast Wpl1(Rad61)-Pds5 complex counteracts sister chromatid cohesion-establishing reaction. Curr Biol *19*, 492–497.

Takahashi, Y., Iwase, M., Konishi, M., Tanaka, M., Toh-e, A., and Kikuchi, Y. (1999). Smt3, a SUMO-1 homolog, is conjugated to Cdc3, a component of septin rings at the mother-bud neck in budding yeast. Biochem. Biophys. Res. Commun. *259*, 582–587.

Takahashi, Y., Yong-Gonzalez, V., Kikuchi, Y., and Strunnikov, A. (2006). SIZ1/SIZ2 control of chromosome transmission fidelity is mediated by the sumoylation of topoisomerase II. Genetics *172*, 783–794.

Tanaka, T., Cosma, M. P., Wirth, K., and Nasmyth, K. (1999). Identification of cohesin association sites at centromeres and along chromosome arms. Cell *98*, 847–858.

Tanaka, T., Fuchs, J., Loidl, J., and Nasmyth, K. (2000). Cohesin ensures bipolar attachment of microtubules to sister centromeres and resists their precocious

separation. Nat Cell Biol *2*, 492–499.

Tonkin, E. T., Wang, T.-J., Lisgo, S., Bamshad, M. J., and Strachan, T. (2004). NIPBL, encoding a homolog of fungal Scc2-type sister chromatid cohesion proteins and fly Nipped-B, is mutated in Cornelia de Lange syndrome. Nat. Genet. *36*, 636–641.

Tóth, A., Ciosk, R., Uhlmann, F., Galova, M., Schleiffer, A., and Nasmyth, K. (1999). Yeast cohesin complex requires a conserved protein, Eco1p(Ctf7), to establish cohesion between sister chromatids during DNA replication. *13*, 320–333.

Uhlmann, F., Lottspeich, F., and Nasmyth, K. (1999). Sister-chromatid separation at anaphase onset is promoted by cleavage of the cohesin subunit Scc1. Nature *400*, 37–42.

Unal, E., Arbel-Eden, A., Sattler, U., Shroff, R., Lichten, M., Haber, J. E., and Koshland, D. (2004). DNA Damage Response Pathway Uses Histone Modification to Assemble a Double-Strand Break-Specific Cohesin Domain. Mol Cell *16*, 991–1002.

Unal, E., Heidinger-Pauli, J. M., and Koshland, D. (2007). DNA Double-Strand Breaks Trigger Genome-Wide Sister-Chromatid Cohesion Through Eco1 (Ctf7). Science *317*, 245–248.

Unal, E., Heidinger-Pauli, J. M., Kim, W., Guacci, V., Onn, I., Gygi, S. P., and Koshland, D. E. (2008). A molecular determinant for the establishment of sister chromatid cohesion. Science *321*, 566–569.

Vernì, F., Gandhi, R., Goldberg, M. L., and Gatti, M. (2000). Genetic and molecular analysis of wings apart-like (wapl), a gene controlling heterochromatin organization in Drosophila melanogaster. Genetics *154*, 1693–1710.

Wendt, K. S. *et al.* (2008). Cohesin mediates transcriptional insulation by CCCTC-binding factor. Nature *451*, 796–801.

White, G. E., and Erickson, H. P. (2006). Sequence divergence of coiled coils--structural rods, myosin filament packing, and the extraordinary conservation of cohesins. J. Struct. Biol. *154*, 111–121.

White, G. E., and Erickson, H. P. (2009). The coiled coils of cohesin are conserved in animals, but not in yeast. PLoS ONE *4*, e4674.

Yamamoto, A., Guacci, V., and Koshland, D. (1996a). Pds1p is required for

faithful execution of anaphase in the yeast, Saccharomyces cerevisiae. The Journal of Cell Biology *133*, 85–97.

Yamamoto, A., Guacci, V., and Koshland, D. (1996b). Pds1p, an inhibitor of anaphase in budding yeast, plays a critical role in the APC and checkpoint pathway(s). The Journal of Cell Biology *133*, 99–110.

Yeh, E., Haase, J., Paliulis, L. V., Joglekar, A., Bond, L., Bouck, D., Salmon, E. D., and Bloom, K. S. (2008). Pericentric chromatin is organized into an intramolecular loop in mitosis. Curr Biol *18*, 81–90.

Zhang, J. *et al.* (2008). Acetylation of Smc3 by Eco1 is required for S phase sister chromatid cohesion in both human and yeast. Mol Cell *31*, 143–151.

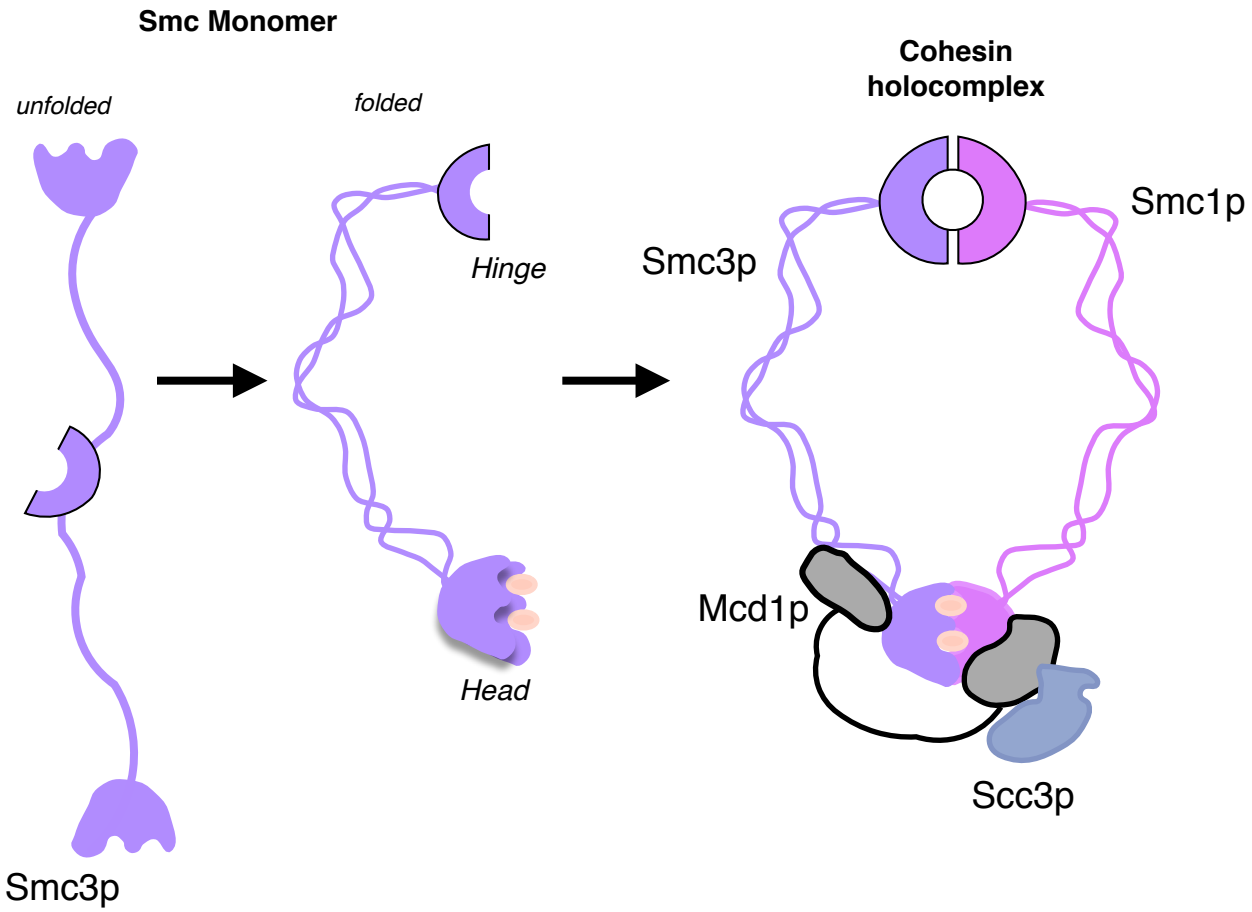

Figure 1. Topology and architecture of the cohesin complex. Left. An unfolded Smc3 monomer is composed of two head domains separated by a long coiled coil, which itself is bisected by a hinge domain. Middle. The Smc3 monomer folds back on itself at the hinge domain, bringing the two head domains together. **Right**. Smc1p and Smc3p heterodimers, associate together at the hinge and head domains, and form the cohesin holocomplex by assembling with Mcd1p and Scc3p. It is estimated that the large topological surface enclosed by Smc3 and Smc1 is 45nm wide. A second topological surface is formed by the Smc1p, Smc3p head domains and Mcd1p, which makes asymmetric contacts with the head domain of Smc3 and the base of the coiled-coils of Smc1. Scc3p associates with both the core cohesin complex as well as with a cohesin regulatory complex, composed of Pds5p, Wpl1p, and Scc3p.

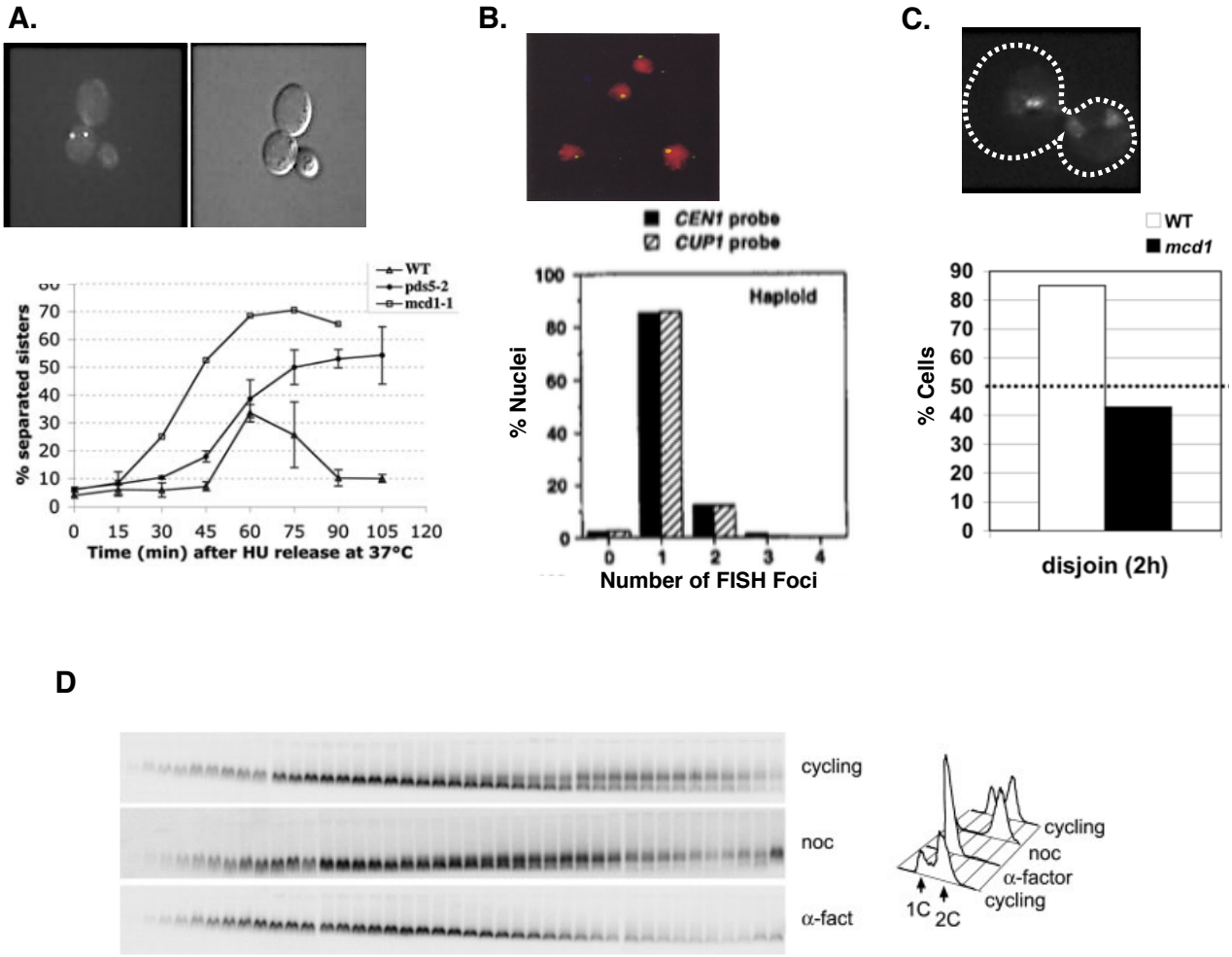

Figure 2. Comparison of Methods to Analyze Sister Chromatid Cohesion. **A.** Inset. Tandem LacO arrays integrated at genomic locus directly measures sister chromatid cohesion through the use of a LacI-GFP fusion protein. Reproduced from Straight and Murray, Current Biology, 1996. Graph. Kinetic analysis of sister chromatid cohesion of WT, *pds5-2*, and *mcd1-1* strains demonstrates clear phenotypic differences between cohesion competent (WT), cohesion establishment defective (*mcd1-1*), and cohesion maintenance defective (*pds5-2*) strains. Reproduced from Noble, Kenna, Dix, Skibbens, and Guacci, Cell Cycle, 2006. **B.** Representative image to assess cohesion state at single copy regions in the yeast genome by fluorescence in situ hybridization (FISH). Chromosomes are pseudo-colored in red (propidium iodide) and the FISH probe in yellow. Graph. Quantification of number of FISH foci detected against single copy regions in haploid yeast cells. Cells from different stages of the cell cycle cannot be readily distinguished, as no budding information can be retained after spheroplasting. Both panels reproduced from Guacci, Hogan, and Koshland, Journal of Cell Biology, 1994. **C.** Chromosome segregation assay. Cells harboring LacO arrays near the centromere are staged in M phase and preexisting spindle assembly is disrupted with nocodazole. Nocodazole is then washed away and cells are then asked to complete segregation. Only cells with sister chromatid cohesion will satisfy the spindle assembly chickpoint and show proper segregation of sister chromatids. Top. A representative cell that failed to segregate sister chromatids. The cell wall is outlined in white. Bottom. Data from wild-type and mcd1-1 cohesion dependent segregation assay. Figures reproduced from Guacci and Koshland, Molecular Biology of the Cell, 2012. **D.** Velocity gradient sedimentation and agarose gel electrophoresis analysis of large mini-chromosomes. Yeast extracts from cycling, nocodazole, and G1 arrested (a-factor) cells containing a plasmid were subjected to centrifugation through a sucrose gradient. The resulting fractions were run on agarose gels and subjected to southern blot analysis to detect the plasmid. Note the similarity of plasmid migration for all three samples from the left half of the gel, and the abundance of the slower migrating plasmid form in the asynchronous sample, where cells in telophase through G1 cannot have replicated plasmids. Fractions 21 through 75 are shown. Panel reproduced from Ivanov and Nasmyth, Molecular Cell, 2007.

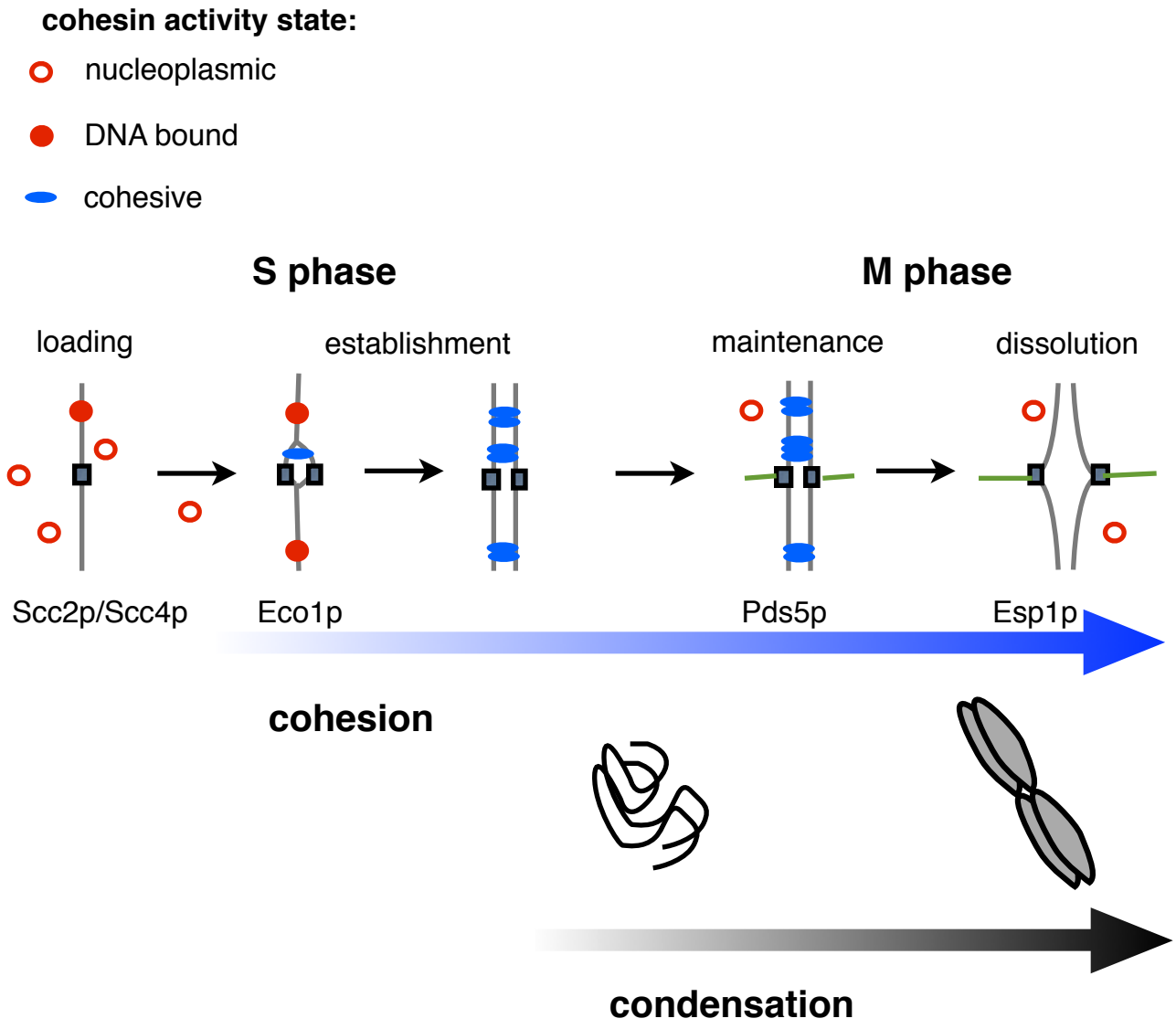

Figure 3. Schematic of cohesin's activity during the cell cycle. Cohesion. Cohesin is loaded onto chromosomes by the Scc2p/Scc4p loader complex at the G1/S boundary. Cohesion is established in concert with DNA replication during S phase, and is promoted by Eco1p-mediated acetylation. A subset of cohesin is acetylated. The cohesin accessory factor Pds5p is required for cohesion maintenance after replication until anaphase onset. Finally, cohesion is dissolved upon activation of protease Esp1, which specifically targets Mcd1p for degradation. **Condensation.** In budding yeast, condensed chromosomes, as assessed by the rDNA locus, appear soon after completion of DNA replication. Mutant alleles in both cohesin as well as condensin give rise to condensation defects in metaphase arrested cells.

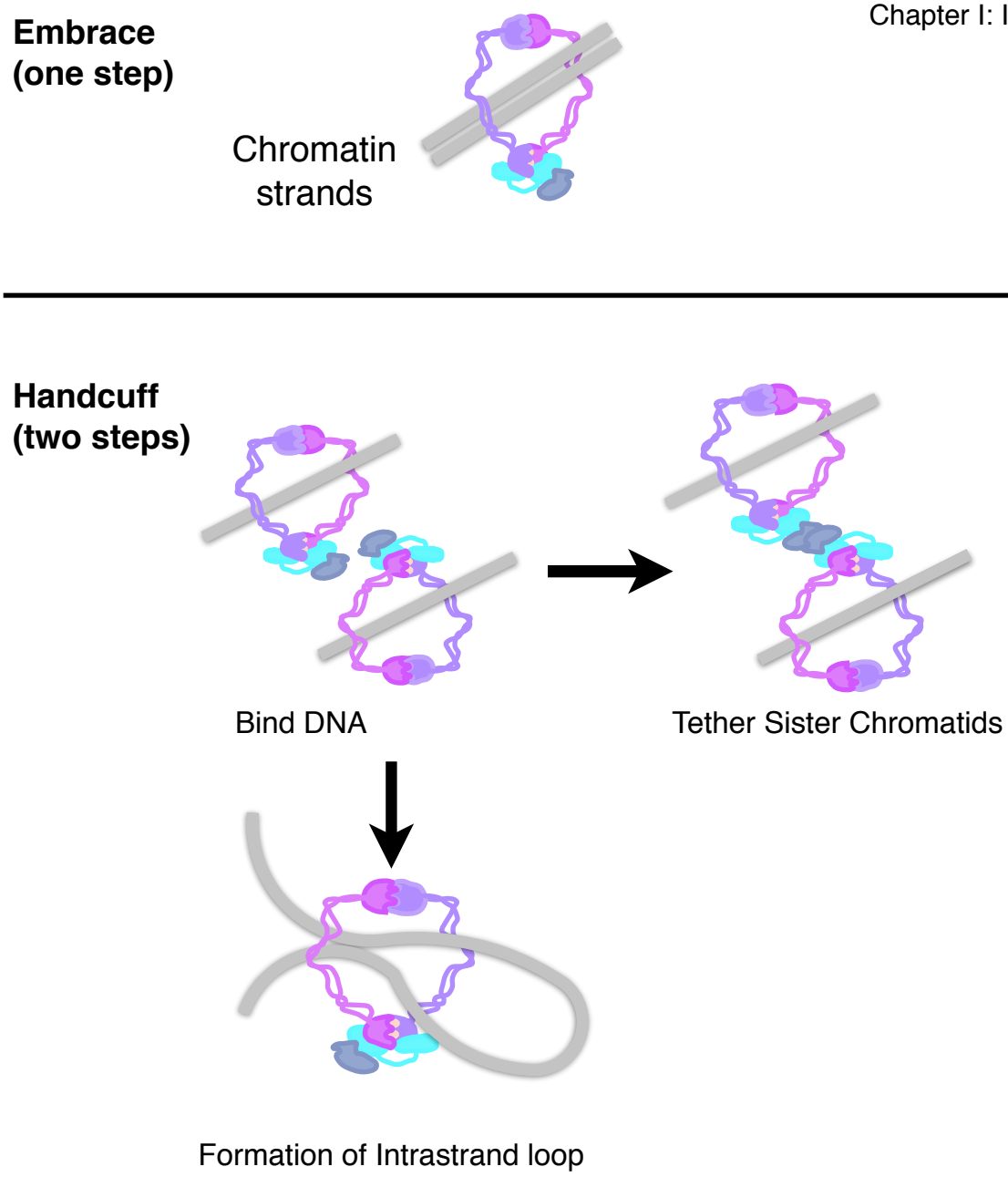

Figure 4. Proposed Models for Cohesin Function on DNA. Top. The "embrace" model posits that a single cohesin ring is necessary and sufficient to generate sister chromatid cohesion, condensation, and viability. Cohesin binds DNA before replication. As replication origins are fired, the DNA polymerase holocomplex already traps the existing sister chromatid, and its passage through the ~45nm cohesin ring ensures sister chromatids are held together from the exact onset of replication. **Bottom.** Cohesin dimer or other higher order cohesin interaction models posit that cohesin can stably bind DNA, but a second reaction is required to tether sister chromatids, such as an interaction between cohesin complexes. Different mechanisms of activation could account for cohesin's inter vs. intra strand tethering activities.

CHAPTER 2: Analysis of the ROCC Domain in the Mcd1 Subunit of Cohesin

ROCC, a conserved region in Cohesin's Mcd1 Subunit, is essential for the proper regulation of the maintenance of cohesion and establishment of condensation

Thomas Eng, Vincent Guacci, and Doug Koshland.

Published In *Molecular Biology of the Cell*
August 15, 2014 vol. 25 no. 16 pages 2351-2364
doi: 10.1091/mbc.E14-04-0929. Epub 2014 Jun 25.

Highlight

We identify and study a novel evolutionary-conserved motif termed ROCC (Regulation of Cohesion and Condensation) in the regulatory subunit of cohesin. This study shed important insights into the regulation of the maintenance of cohesion and condensation and the molecular basis for cohesin's chromatin tethering activity.

Abstract

Cohesin helps orchestrate higher order chromosome structure, thereby promoting sister chromatid cohesion, chromosome condensation, DNA repair, and transcriptional regulation. To elucidate how cohesin facilitates these diverse processes, we mutagenized Mcd1p, the Kleisin regulatory subunit of budding yeast cohesin. In the linker region of Mcd1p, we identified a novel evolutionary-conserved 10-amino acid cluster, termed ROCC (Regulation of Cohesion and Condensation). We show that ROCC promotes cohesion maintenance by protecting a second activity of cohesin that is distinct from its stable binding to chromosomes. The existence of this second activity is incompatible with the simple embrace mechanism of cohesion. In addition, we show that the ROCC motif is required for the establishment of condensation. We provide evidence that ROCC controls cohesion maintenance and condensation establishment through differential functional interactions with Pds5p and Wpl1p.

Introduction

Cohesin, a founding member of SMC-family proteins, was originally identified for its critical role in chromosome segregation (Strunnikov *et al.*, 1993). Cohesin

tethers sister chromatids in order to generate the cohesion necessary for proper chromosome segregation. However, additional studies revealed that cohesin is also important for condensation, regulation of gene expression, and DNA repair. (Guacci *et al.*, 1997; Donze *et al.*, 1999; Rollins *et al.*, 1999; Unal *et al.*, 2004; Yeh *et al.*, 2008; Guacci and Koshland, 2012). Since these different chromosomal processes have distinct spatial and temporal requirements, cohesin's activity(ies) must be strictly parsed and regulated. Many aspects of its precise regulation remain to be elucidated. For example, what are the activities of cohesin needed to maintain sister chromatid cohesion from S phase until anaphase onset? What prompts cohesin to tether chromosomes, rather than to condense them? Are these cues governed by distinct modes of regulation, through distinct regulatory factors? In this study, we address these fundamental questions by examining the regulation of cohesin in both sister chromatid cohesion and condensation using the budding yeast, *Saccharomyces cerevisiae.*

The persistence of cohesion in G2 and M phase is an active process that involves two auxiliary cohesin factors, Pds5 and Wpl1. While Pds5p promotes cohesion maintenance, Wpl1p/Rad61p (Wapl in other organisms) inhibits it (Hartman *et al.*, 2000; Kueng *et al.*, 2006; Zhang *et al.*, 2009; Peters and Nishiyama, 2012). Wpl1p's function can be explained in the context of the simple embrace model for cohesion. . In the embrace model the cohesion between sister chromatids is generated when they are topologically entrapped by a single cohesin ring during S phase. So long as the cohesin ring remains intact and closed, cohesin will continue to entrap the two sister chromatids, maintaining both cohesion and its stable binding to chromosomes. The only way to dissolve cohesion is to disrupt the integrity of the cohesin ring, causing not only the escape of the sister chromatids but also the dissociation of cohesin from the chromosome. Consistent with this model, recent studies suggest that Wpl1p opens the cohesin ring, resulting in dissociation of cohesin from the chromosomes and dissolution of cohesion. In this context, a potential positive activity for Pds5p in cohesion maintenance could be the protection of cohesin from the putative ring-opening activity of Wpl1p. However, in budding yeast, deletion of *WPL1* (*wpl1Δ*) does not rescue the cohesion maintenance defect of a *pds5* mutant (Chan *et al.*, 2013). Thus, Pds5p must preserve cohesion by antagonizing a Wpl1p-independent mechanism of cohesion dissolution. Does this alternative dissolution mechanism also destabilize cohesin binding to chromosomes, or inhibit another activity of cohesin not predicted by the embrace model?

In budding yeast, cohesin and cohesin auxiliary factors also function in mitotic chromosome condensation. Inactivation of any cohesin complex subunit as well as cohesin accessory factors Eco1p/Ctf7 and Pds5p perturbed condensation at euchromatic single-gene-copy regions and at the heterochromatic rDNA repeats

of the *RDN* locus (Guacci *et al.*, 1997; Skibbens *et al.*, 1999; Hartman *et al.*, 2000; Guacci and Koshland, 2012). Thus, factors which promote sister chromatid cohesion like cohesin, Pds5p and Eco1p also serve to promote cohesin-mediated condensation. In contrast, Wpl1p likely inhibits cohesin-mediated condensation as well as cohesion. Indeed, the deletion of *WPL1* (wpl1Δ) suppresses the condensation defect of cells lacking Eco1p, and overexpression of Wpl1p in wild-type cells induces hyper condensation (Guacci and Koshland, 2012; Lopez-Serra *et al.*, 2013). Together these results suggest a strong connection between factors that control the maintenance of cohesion and condensation. How do factors like Pds5p and Wpl1p communicate with cohesin to regulate condensation and cohesion?

Here, we investigate how cohesin is regulated to ensure that cohesion is maintained in G2 and M phase, yet still enables the establishment and maintenance of condensation. We chose to mutate the Mcd1p/Rad21p/Scc1p regulatory subunit of cohesin, due to its regulatory roles in cohesion establishment, DNA repair, and cohesion dissolution at anaphase. We have identified a cluster of conserved residues in the linker domain of Mcd1p, which we define as the ROCC (Regulation of Cohesion and Condensation) motif because they are required for the maintenance of cohesion and the establishment of condensation. The ROCC motif together with Pds5 prevents cohesion dissolution by a mechanism independent of Wpl1p. Disruption of this ROCC-mediated mechanism does not destabilize cohesin binding to chromosomes, yet abrogates cohesion maintenance. Therefore, while stable binding of cohesin to chromosomes is necessary for cohesion maintenance, it is not sufficient. The ROCC motif also promotes the establishment and maintenance of condensation by antagonizing Wpl1p's anti-condensation activity. Taken together our results suggest that ROCC controls cohesion maintenance and condensation establishment through differential functional interactions with Pds5p and Wpl1p, respectively.

Results

Q266 region of Mcd1p is required for the maintenance of sister chromatid cohesion

We sought to understand how cohesin function is coordinated in G2 and M phase to maintain sister chromatid cohesion while promoting chromosome condensation. We suspected that this coordination might be mediated by Mcd1p, the key cohesin regulatory subunit. Consequently, we sought to identify *MCD1* alleles where the maintenance of cohesion was uncoupled from the establishment of condensation. Such partially functional, separation-of-function alleles were likely to be rare. We previously showed that partially functional alleles of Smc1p, another cohesin subunit, were highly enriched in a particular mutagenic strategy called RID (Random Insertion Dominant negative) (Milutinovich *et al.*, 2007). Therefore, we subjected *MCD1* to RID mutagenesis to generate a DNA library of minichromosome-borne *mcd1* mutants, each containing a single 15 base pair (5 residue) in-frame insertion (Figure 1A & Materials and Methods). The complexity of the library was calculated to span the *MCD1* ORF with one insertion every ~2.5bp of *MCD1*. This insertion library was transformed into wild-type yeast. The RID mutagenized MCD1 was under control of the pGAL promoter. Therefore, transformants were assayed for toxicity in the presence of galactose, which induce over-expression of the RID mutant proteins, but not under non-inducing conditions on dextrose.

We identified thirty-two RID-induced mutations that led to a dominant phenotype of slow growth or inviability (Figure 1B, Supplemental Table 1). Sequencing of these dominant negative RID mutations identified ten unique alleles of *MCD1* (Figure 1C, Supplemental Table 1). Most of these RID alleles were in the amino and carboxy terminal globular domains, likely inhibiting the interaction of these domains with the head domains of the Smc3p and Smc1p respectively (Figure 1C). The dominant phenotypes of these RID proteins were easily explained. We posited that by virtue of binding to only one of the two Smc head domains, these mutant proteins could assemble into a nonfunctional complex for cohesion, preventing the assembly of a functional cohesin with wild-type Mcd1p. In contrast, one RID allele arose from an insertion immediately following residue Q266 (*mcd1-Q266*) in the linker region of Mcd1p (Figure 1C). How this allele might generate a dominant phenotype was not clear. The unusual position of this insertion allele prompted us to pursue it further as a candidate for identifying a potentially novel regulatory domain for cohesin function in M phase.

As a first step in characterizing this allele, we wanted to study its phenotypes under normal levels of expression and in the absence of Mcd1p. To eliminate Mcd1p, we generated a strain that contained *MCD1-AID* (at the *MCD1* locus) and

TIR1 (see Experimental Methods). *AID* (Auxin Inducible Degron) encodes a small domain that binds the plant hormone auxin (Nishimura *et al.*, 2009). *TIR1* encodes Tir1p, an alternative F box required for SCF mediated degradation of AID tagged proteins (Gray *et al.*, 1999). Since *TIR1* was introduced into all strains in this study bearing an AID tagged protein, it was omitted from all genotypes in the text for simplicity. In the presence of auxin, proteins coupled to AID are ubiquitinated and targeted for degradation. The effectiveness of auxin-induced degradation of MCD1-AIDp was evident by the inability of the *MCD1-AID* strain to grow in the presence of auxin and the dramatic reduction of Mcd1-AIDp within 30 minutes of auxin addition (Figure 2A, Supplemental figure 1). Into this *MCD1-AID* strain we integrated an *mcd1-Q266* allele under control of the *MCD1* promoter at the *URA3* locus. This *mcd1-Q266 MCD1-AID* strain grew normally in the absence of auxin but failed to grow in the presence of auxin (Figure 2A). Since *MCD1-AID* is degraded in response to auxin treatment, this result demonstrates that *mcd1-Q266* expressed at wild-type levels is unable to support viability on its own, and is recessive to wild-type *MCD1*. Thus, Mcd1-Q266p is defective for one or more Mcd1p activities.

We then examined cohesion in the *MCD1* strain, *MCD1-AID* strain and *mcd1-Q266 MCD1-AID* strain as cells progressed from G1 to M phase. In this experiment, G1-arrested cultures were treated with auxin, then released from their pheromone-induced arrest into media containing auxin and nocodazole (Figure 2B). This regimen allowed cells to progress synchronously through the cell cycle until they re-arrested in M phase due to the presence of nocodazole. Importantly, auxin was present in the media from G1 to M to destroy Mcd1-AIDp and prevent its accumulation over the entire cell-cycle window. During cell cycle progression aliquots of cells were fixed and assayed for cohesion using LacI-GFP tagged loci at *LYS4* and DNA content by flow cytometry.

We first compared cohesion in the *MCD1* strain and *MCD1-AID* strain to establish a basis for subsequent evaluation of *mcd1-Q266*. As expected for the *MCD1* strain, very few separated sister chromatids appeared during the course of the experiment as wild-type Mcd1p is not affected by auxin (Figure 2C). In contrast, in the *MCD1-AID* strain, there was a dramatic increase in sister chromatid separation that began during DNA replication (Figure 2C). Thus, cohesion establishment was blocked by auxin-induced depletion of Mcd1-AIDp. The fraction of cells with separated sister chromatids in the *MCD1-AID* strain (~90%) was much greater than reported previously with conditional temperature-sensitive alleles in *MCD1*, *SMC1* and *SMC3* (~65-70%) (Guacci *et al.*, 1997; Michaelis *et al.*, 1997). The significant residual cohesion seen in the t.s mutants has been interpreted to mean that cohesin-independent pathways for cohesion exist (Shimada and Gasser, 2007). The existence of these cohesin-independent pathways is challenged by the near complete loss of cohesion in *MCD1-AID*

strain. Rather, the residual cohesion in the temperature sensitive alleles likely resulted from incomplete inactivation of the mutant proteins.

Using these results as a foundation, we examined cohesion in the *mcd1-Q266 MCD1-AID* strain. The addition of auxin caused a dramatic increase in sister chromatid separation (Figure 2C). However, precocious sister separation was delayed by ~20 minutes in the *mcd1-Q266 MCD1-AID* strain as compared to the *MCD1-AID,* which importantly, also was ~20 minutes after the completion of S phase. This delay indicates that mcd1-Q266p establishes cohesion during S phase, but fails to maintain it in G2 and M phase.

To corroborate our conclusion that mcd1-Q266p has a cohesion maintenance defect, we compared the kinetics of its cohesion loss to that seen in a *Pds5-AID* strain (Figure 2C). The kinetics and degree of cohesion loss in the *PDS5-AID* and *mcd1-Q266 MCD1-AID* strains were indistinguishable. Thus, *mcd1-Q266* causes a cohesion maintenance defect very similar that seen upon inactivation of Pds5p, a protein whose characterization set the paradigm for cohesion maintenance (Noble *et al*., 2006).

We next assessed cohesion maintenance of *mcd1-Q266* by a second assay where AID tagged proteins were destroyed but only after cells had reached M phase. Cultures of four strains (*MCD1*, *mcd1-Q266 MCD1-AID*, *MCD1-AID*, and *PDS5-AID*) were first arrested in M phase using nocodazole then analyzed for cohesion (Figure 2D). All strains had robust cohesion (Figure 2E, 0 min). Auxin was added to media that still contained nocodazole to deplete Mcd1-AIDp while cells remained arrested in M phase (Figure 2D). As expected, *MCD1* cells retained cohesion, whereas the *MCD1-AID* cells rapidly lost cohesion (Figure 2E). Auxin addition also induced cohesion loss in both the *mcd1-Q266 MCD1-AID* and *PDS5-AID* strains to similar levels (Figure 2E). This result further corroborates the cohesion maintenance defect of *mcd1-Q266* as well as its similarity to the cohesion defect of *PDS5-AID.* Their cohesion loss was delayed relative to the *MCD1-AID* strain (Figure 2E), suggesting the mechanism of cohesion dissolution in *mcd1-Q266 MCD1-AID* and *PDS5-AID* strains was distinct from the rapid inactivation of Mcd1-AIDp by its artificial degradation.

mcd1-Q266 identifies a mechanism for cohesion dissolution without destabilization of cohesin binding to chromosomes

A number of possible explanations existed for the defective cohesion maintenance of the *mcd1-Q266* allele. The proximity of Q266 to the Esp1 (separase) cleavage site suggested that the Q266 residue might be part of a motif required to prevent precocious cleavage of Mcd1p by Esp1p prior to anaphase (Uhlmann *et al*., 1999). This seemed unlikely given cells were arrested

in M phase using nocodazole, a time in the cell cycle when Pds1p is present (Yamamoto *et al.*, 1996a; 1996b) so it should inhibit Esp1p. Indeed, we did not detect cleavage or any other degradation of mcd1-Q266p in nocodazole treated cells (Supplemental Figure 4). Moreover, the overall Mcd1p levels were the same for *MCD1* and *mcd1-Q266* alleles (Supplemental Figure 4). These results ruled out Mcd1p degradation as a cause for the cohesion maintenance defect.

We then turned to possibility that mcd1-Q266p caused a defect in cohesion maintenance because it disrupted the binding of cohesin to chromosomes. G1-arrested cultures of *MCD1-3FLAG MCD1-AID* strain and *mcd1-Q266-3FLAG MCD1-AID* strain were treated with auxin, then released from their pheromone-induced arrest into media containing auxin and nocodazole to allow synchronous progression through the cell cycle until M phase arrest (Figure 3A). Auxin was present in the media from G1 to M to destroy Mcd1-AIDp and prevent its accumulation, leaving only the epitope tagged versions of either Mcd1p or mcd1-Q266p in cells. After reaching M phase, when the maximal cohesion defect of *mcd1-Q266* strains is manifested (Figure 2C), both cultures were fixed. The fixed cultures were processed for chromosome spreads and chromatin immunoprecipitation (ChIP) to assess Mcd1p and mcd1-Q266p binding to chromosomes. Note the chromosomal binding of these two Mcd1p variants is a surrogate measure of cohesin's binding to chromosomes because in yeast, Mcd1p and the other three subunits of cohesin are all completely interdependent for chromosomal binding (Tóth *et al.*, 1999; Unal *et al.*, 2008; Heidinger-Pauli *et al.*, 2010b).

By chromosome spreads, we observed robust staining of Mcd1-3FLAGp and mcd1-Q266-3FLAGp on chromosomes. Thus, the general binding of cohesin to chromatin was unaffected by mcd1-Q266p (Figure 3B). The more extended nature of the spread chromosomes of *mcd1-Q266* cells compared to *MCD1* cells made quantification of the staining difficult. However, we were able to use ChIP to quantify the binding of the Mcd1-3FLAGp and mcd1-Q266p at specific loci. The pattern and amount of their binding were indistinguishable at the centromere-proximal CARC1, the centromere-distal CARL1 and at the centromeres of chromosomes 1 and 14 (Figure 3C, 3D, and 3E). Our results from both chromosome spreads and ChIP indicate that mcd1-Q266p does not compromise the total amount or the locus specific targeting of cohesin to chromosomes.

The fact that steady state levels of chromosomal binding for Mcd1-Q266p and Mcd1p were identical did not eliminate the possibility that mcd1-Q266p increased the dissociation of cohesin from chromosomes. Cohesin containing mcd1-Q266p might have been undergoing rapid cycles of disassociation and re-association with chromosomes. To assess this possibility, we decided to inactivate the

cohesin loader after cells were arrested in M phase. This strategy would allow cohesin to assemble onto chromosomes normally during S phase, but then after the loader depletion in M, any cohesin that fell off chromosomes could no longer be re-loaded onto chromosomes. Any instability in cohesin binding on chromosomes would be detected as a decrease in the amount remaining bound on chromosomes with time. The use of ChIP would enable us to monitor the stability of cohesin binding at small and specific chromosomal loci at any part of a chromosome. In previous studies, the stability of cohesin binding to chromosomes has been measured by fluorescence recovery after photobleaching. However, the bleaching method in yeast is limited to measuring the stability of cohesin bound over a cohesin barrel, which forms over a 10-15kb region flanking each of the centromeres (Yeh *et al.*, 2008).

To execute this loader-inactivation strategy, we replaced the chromosomal copy of *SCC2*, the best characterized subunit of the cohesin loader complex, with an *SCC2-AID* allele. As expected, the *SCC2-AID* strain was inviable on plates containing auxin (Supplemental Figure 3). We then assessed how effective depletion of the Scc2-AIDp was blocking cohesion generation. The *SCC2-AID* strain was staged in G1 and then depleted of Scc2-AIDp by the addition of auxin. Cells were synchronously released from G1 and in the presence of both nocodazole and auxin to continually destroy the loader and prevent its accumulation during cell cycle progression. Western blot analysis revealed that Scc2-AIDp was reduced below the level of detection (Supplemental Figure 5). We also assessed sister chromatid cohesion and cohesin binding to chromosomes (Supplemental Figure 5). Sister chromatid cohesion was reduced to levels comparable to that seen after inactivation of a cohesin subunit. In addition, cohesin binding at CARC1 was reduced to background levels. These results indicated that Scc2-AIDp function was severely compromised in the presence of auxin, making it an effective tool to study the stability of cohesin binding to chromosomes.

To ask whether inactivation of Scc2-AIDp can efficiently block cohesin loading in M phase, we generated a strain that contained the *SCC2-AID, MCD1* and *MCD1-6HA* tagged under control of the pGAL promoter (*pGAL-MCD1-6HA*). We arrested a culture of this strain in M phase using nocodazole. The culture was split and auxin was added to one half to deplete Scc2-AIDp. Western blot analysis indicate that Scc2-AIDp was reduced to undetectable levels by 15 minutes after auxin addition (Supplemental Figure 6). Thirty minutes later, galactose was added to both cultures and allowed to incubate for an additional 60 minutes. Mcd1-6HAp was induced to high levels as assayed by Western Blot in both cultures (Supplemental Figure 6). In the auxin-free culture, Mcd1-6HAp exhibited robust chromosomal binding as assayed by chromosome spreads (Supplemental Figure 6). This result is consistent with published results that the

cohesin loader is active and competent to load cohesin in M phase (Ström *et al.*, 2004). In contrast, in the auxin treated (Scc2-AIDp depleted) culture, Mcd1-6HAp failed to load onto chromosomes. Thus inactivation of the loader in M phase successfully prevented nucleoplasmic cohesin from binding chromosomes during M.

With the conditional *SCC2-AID* in hand, we analyzed the dissociation of both mcd1-Q266p and Mcd1p from chromosomes. We first generated a strain bearing the *SCC2-AID* and the *MCD1-AID* as the sole *SCC2* and *MCD1* alleles in cells. We then integrated a second copy either *MCD1-3FLAG* or an *mcd1-Q266-3FLAG* alleles at the *URA3*. We refer to these strains as the *MCD1* and *mcd1-Q266* stability strains. We arrested these two strains in M phase using nocodazole to allow normal loading of Mcd1-AIDp and MCD1-3FLAGp or mcd1-Q266-3FLAGp (Figure 4A). Cultures were split and auxin was added to one half. Auxin addition rapidly depleted the Scc2-AIDp loader within 15 minutes and the *MCD1-AID* at least within 30 minutes, leaving only the MCD1-3FLAGp or mcd1-Q266-3FLAGp on chromosomes (Supplemental Figures 1 and 6). After an additional 45 minutes in auxin, the two M phase cultures were processed for ChIP to assess the binding of Mcd1-3FLAGp and mcd1-Q266-3FLAGp to chromosomes. Because Scc2-AIDp was fully depleted by 15 minutes after auxin addition, any ChIP signal that persisted at 60 minutes reflected Mcd1-3FLAGp or mcd-Q266-3FLAGp that remained bound to their chromosomal sites for at least 45 minutes (Supplemental Figure 6). Importantly, the percent separated sister chromatids in *MCD1* (15%) and *mcd1-Q266* (50%) stability strains were the same as we observed previously in *MCD1 SCC2* and *mcd1-Q266 SCC2* strains (Figure 2E). Thus, the depletion of Scc2-AIDp did not suppress or enhance the cohesion maintenance defect in of *mcd1-Q266*.

In the *MCD1* stability strain, the amount of Mcd1-3FLAGp binding at CARC1 was unaffected by Scc2-AIDp depletion (Figure 4B, left panel), suggesting that cohesin binds very stably to this site. The proximity of CARC1 to the centromere places it likely very near or within the centromere barrel. Previous studies using fluorescence recovery after photobleaching of the centromere barrel also indicated stable cohesin binding in this region (Yeh *et al.*, 2008; Mishra *et al.*, 2010). This similarity validates our Scc2-AIDp degradation methods as a metric for assessing stably bound cohesin in M phase.

The *SCC2-AID* tool also allowed us to measure the stability of cohesin binding to chromosomal sites outside the centromere barrel, and at much finer resolution. The amount of Mcd1-3FLAGp binding at CARL1, a cohesin binding site in the middle of the arm of chromosome XII, was also unaffected by Scc2-AIDp inactivation in our *MCD1* stability strain (Figure 4B, middle panel). Thus cohesin also bound very stably to a representative arm CAR site. In contrast, Mcd1-

3FLAGp binding at two different centromeres decreased nearly three to five-fold in the absence of the loader (Figure 4B, right panel). Thus, most of the cohesin in immediate proximity of centromeres is only transiently bound.

In the *mcd1-Q266* stability strain, the mcd1-Q266-3FLAGp binding at both the arm CARL1, and the pericentric CARC1 remained at the same high levels in the presence or absence of the loader (Figure 4C, left and middle panels). Furthermore, binding at the two centromeres was reduced in the absence of loader to the same low levels seen as in the *MCD1* stability strain (Figure 4C, right). Thus, the binding of mcd1-Q266-3FLAGp to these three chromosome regions was indistinguishable from that of Mcd1p. Importantly, despite the stable binding of mcd1-Q266-3FLAGp at non-centromeric CARs, *mcd1-Q266* cells failed to maintain cohesion. Taken together, these results suggest the disruption of cohesion maintenance in *mcd1-Q266* occurs by a mechanism distinct from cohesin dissociation from chromosomes. Moreover, it suggests that the WT residues in Q266 linker region of Mcd1p are required to suppress this mechanism.

A recent study analyzed another allele of *MCD1*, *scc1-V137K*, which henceforth will be referred to as *mcd1-V137K* (Chan *et al.*, 2013). This allele had hyper-stable binding to chromosomes as assayed by fluorescent recovery after photobleaching of the cohesin barrel. This study concluded that the *mcd1-V137K* allele caused a defect in cohesion establishment based upon an endpoint assay that revealed an increased spacing of the centromeric clusters that generate the cohesin barrel (Chan *et al.*, 2013). However an endpoint assay is not suitable for distinguishing between a defect in cohesion establishment or maintenance. Therefore, we made an *mcd1-V137K MCD1-AID* strain with a GFP-LacI/LacO reporter at *LYS4* to follow cohesion through a time-course experiment. For this purpose, we utilized our assay of *MCD1-AID* depletion in G1 arrest and release into nocodazole + auxin to assess timing of cohesion loss as cells progressed from G1 to M (Supplemental Figure 7). In the *mcd1-V137K* strain, sister chromatids separated ~20 minutes after *MCD1-AID* strain and ~15 minutes after the completion of S phase. This delay is sister chromatid separation was indistinguishable from the cohesion maintenance defect observed in *PDS5-AID* and *mcd1-Q266* strains (Supplemental Figure 7 & Figure 2). Therefore, by our direct measurements, the *mcd1-V137K* allele does indeed have a cohesion defect, but its defect is in cohesion maintenance. This result also means that the maintenance defect in *mcd1-V137K*, like *mcd1-Q266*, occurs without destabilizing cohesin binding to chromosomes. Residue V137, like the Q266 region of Mcd1p, must protect against a mechanism of cohesion dissolution that disrupts a cohesin activity other than stable chromosome binding. Furthermore, stable binding of cohesin to chromosomes is insufficient to maintain cohesion.

Q266 inhibits a Wpl1-independent mechanism for cohesion dissolution

The phenotypic similarities of *mcd1-Q266*, and *PDS5-AID* prompted us to test whether the cohesion maintenance defect in these two mutants resulted from a failure to suppress a common process of cohesion dissolution. An obvious choice for this process was one mediated by Wpl1p, the only cohesin inhibitor known to be active prior to anaphase (Uhlmann *et al.*, 1999; Heidinger-Pauli *et al.*, 2010b). If so a deletion of *WPL1* (*wpl1Δ)* should suppress the precocious cohesion dissolution found in both *PDS5-AID* and *mcd1-Q266* strains. However, a previous study revealed that cohesion dissolution in *pds5* mutants was not suppressed by *wpl1Δ* (Chan *et al.*, 2013). To test whether cohesion dissolution in *mcd1-Q266* cells also occurs by a *WPL1*-independent mechanism, we deleted *WPL1* in our *mcd1-Q266 MCD1-AID* strain. We assayed cohesion in these cells as they progressed from G1 to M to test cohesion establishment and maintenance (Figure 5).

The *wpl1Δ mcd1-Q266 MCD1-AID* mutant exhibited the partial defect in cohesion establishment characteristic of *wpl1Δ* alone (Rowland *et al.*, 2009; Sutani *et al.*, 2009; Guacci and Koshland, 2012) (Figure 5A, 75 min time point). Importantly, the cohesion maintenance defect in the *wpl1Δ mcd1-Q266* strain was as severe, as or possibly exacerbated, as compared to the *mcd1-Q266* strain (Figure 5A, time points 90 to 150 min). These results indicated that the precocious cohesion dissolution in *mcd1-Q266*, like *pds5* mutants, occurred by a Wpl1p-independent mechanism. This independence fit with our observations that the mechanism of cohesion dissolution in *mcd1-Q266* and *pds5* compromised cells was inconsistent with Wpl1p's known inhibitory activity, promoting cohesin dissociation from chromosomes (Sutani *et al.*, 2009). Taken together, our results are consistent with Pds5p and the Q266 region inhibiting a common but novel Wpl1p-independent process of cohesion dissolution.

The next question we addressed was whether the *mcd1-Q266*, *pds5* and *mcd1-V137K* mutants failed to suppress this novel process because they shared a common molecular defect. In a previous study, *mcd1-V137K* strains were shown to be defective in the binding of Mcd1p to Pds5p by their failure to co-immunoprecipitate from soluble extracts (Chan *et al.*, 2013). To characterize this defect further, we took advantage of the fact that Pds5p was known to be recruited to chromosomes by cohesin and this binding was dependent upon Mcd1p (Hartman *et al.*, 2000; Panizza *et al.*, 2000). We assayed the ability of *mcd1-V137K* to impair binding of Pds5p to chromosomes by chromosome spreads (Supplemental Figure 7). The staining of Pds5p to chromosomes was dramatically reduced, indicating that *mcd1-V137K* blocked Pds5p binding to chromosome-bound cohesin as well as soluble cohesin. Thus, *mcd1-V137K* and Pds5 mutants both impinge on Pds5 activity.

We then asked whether *mcd1-Q266* also compromised Pds5p recruitment to chromosomes. We allowed *mcd1-Q266 MCD1-AID* and *MCD1* strains to progress from G1 to M in the presence of auxin to generate chromosomes bound only with mcd1-Q266p or Mcd1p. We assessed Pds5p recruitment to chromosomes by chromosome spreads and ChIP. By chromosome spreads, Pds5p was bound to chromosomes containing only mcd1-Q226p, and its staining was similar to that of chromosomes containing wild-type Mcd1p (Figure 5B). Furthermore, by ChIP, the amount and position of Pds5p binding was indistinguishable at CARC1, CARL1 and two centromeres in wild-type *MCD1* and mcd1-Q266 cells (Figure 5C, 5D, 5E). Thus, the difference in Pds5p recruitment to chromosomes and CARs in *mcd1-V137K* and *mcd1-Q266* suggest that these mutants have different molecular defects that lead to inappropriate activation of the novel cohesion dissolution process.

The Q266 region promotes the establishment of chromosome condensation by antagonizing Wpl1p.

A deletion of *WPL1* suppresses the auxin-induced lethality of the *mcd1-Q266 MCD1-AID* strain (Figure 6A). However, this suppression of inviability could not have been caused by suppression of the cohesion defect since *wpl1Δ* exacerbated rather than suppressed the cohesion defect of *mcd1-Q266 MCD1-AID* (Figure 5A). Previously it was shown that *wpl1Δ* could suppress the lethality of eco1Δ (Rolef Ben-Shahar *et al.*, 2008; Rowland *et al.*, 2009; Sutani *et al.*, 2009; Guacci and Koshland, 2012). Importantly, while *wpl1Δ* suppresses the lethality of an *eco1Δ (wpl1Δ eco1Δ)*, it fails to suppress the cohesion establishment defect; rather it correlates with suppression of condensation defects characteristic of *eco1* mutants (Guacci and Koshland, 2012). The surprising viability in the absence of robust cohesion establishment is thought to result from a surrogate pathway for bipolar attachment that results from the unusual assembly of the spindle during S phase in budding yeast (Guacci and Koshland, 2012). The correlation between the restoration of condensation and viability in *eco1Δ wpl1Δ* double mutants suggested that the condensation function of cohesin was essential for viability. By analogy, we wondered whether *mcd1-Q266* caused a defect in condensation as well as cohesion maintenance, and if so, did *wpl1Δ* restore viability of the *mcd1-Q266 MCD1-AID* strain by suppressing its condensation defect.

Most budding yeast chromosomes condense only about 1.7 fold between interphase and mitosis (Guacci *et al.*, 1994). Hence, the chromosomes are indistinguishable in interphase and mitosis, exhibiting the same tight circular mass in DAPI-stained chromosome spreads. However the 500kb *rDNA* locus undergoes a dramatic shift in morphology from a diffuse puff in interphase to a

short line-like loop in mitosis (Figure 6B). We have shown that this change in morphology is dependent on cohesin and condensin (Guacci *et al.*, 1997; Lavoie *et al.*, 2000).

To analyze the effect of mcd1-Q266p on condensation, we compared *rDNA* morphology in *mcd1-Q266 MCD1-AID*, *MCD1-AID*, and *MCD1* strains. We followed *rDNA* morphology by chromosome spreads as cells progressed from G1 to M in the presence of auxin (Figure 6C). In the *MCD1* strain, the compacted loops of the *rDNA* appeared at the exit from S and was maintained through M (Figure 6D). In the *MCD1-AID* strain, the *rDNA* in most cells never formed short line-like loops but rather remained as non-descript puffs (Figure 6D). These results corroborate previous studies linking cohesin function with proper condensation (Guacci *et al.*, 1997; Heidinger-Pauli *et al.*, 2010a; Guacci and Koshland, 2012). In the *mcd1-Q266 MCD1-AID* strain, the *rDNA* never condensed (Figure 6D). In addition, the morphology of the entire chromosome mass, as well as the *rDNA*, became distended as cells progressed longer into M (Figure 3B and 5B). Thus, the establishment of *rDNA* condensation requires the Q266 region of Mcd1p.

Having established a condensation defect for *mcd1-Q266* strains, we asked whether condensation was restored in the absence of Wpl1p. We examined *rDNA* morphology in the *wpl1Δ mcd1-Q266 MCD1-AID* strain by chromosome spreads (Figure 6E). We observed that *rDNA* condensation was restored to near wild-type levels albeit with delayed kinetics (Figure 6E). This result leads to three important conclusions. First, the Q266 region of Mcd1p promotes the establishment of chromosome condensation by antagonizing Wpl1p. Second, it corroborates previous observations that Wpl1p is an inhibitor of chromosome condensation in yeast, and finally, further correlates an essential function of cohesin with chromosome condensation.

Partially conserved residues adjacent to Mcd1-Q266 define a Q266-inclusive motif termed ROCC, for regulator of cohesion and condensation.

The *mcd1-Q266* allele had a unique combination of phenotypes including defects in condensation establishment and cohesion maintenance but not cohesion establishment. To assess whether these phenotypes were a peculiarity of this specific allele, or representative of alleles in this region of Mcd1p, we subjected fourteen residues flanking mcd1-Q266 to oligo-based mutagenesis (Materials and Methods). Mutants were screened for the inability to support viability in the absence of *MCD1* and for defects in cohesion and condensation.

One allele, *mcd1-m0* caused inviability and defects in cohesion and condensation (Figure 7A and B). This allele changed seven residues (258-264) amino terminal

to Q266 (Figure 7A). To help identify particularly important residues within the *m0* allele for its phenotype, we asked whether any of these residues were conserved among Mcd1p orthologs. Alignments of yeast Mcd1p orthologs showed that the linker region including the Mcd1-Q266 residue have overall very poor conservation. However, a five amino acid sequence DDDDN (258-262) mutated in the *m0* allele has an identical or near identical match at very similar positions from the amino termini in mitotic Mcd1p orthologs in most species including humans (Figure 7C). Using this sequence to align the adjacent sequences revealed potentially additional conserved residues. This conservation in the midst of otherwise highly divergent linker sequence suggested that Q266 might alter an evolutionarily conserved motif that participates in the regulation of cohesin function.

To assess the cohesion and condensation phenotypes further, we assessed cohesion and condensation in *mcd1-m0 MCD1-AID* cells after it had progressed from G1 to M in the presence of auxin. Both mutants exhibited defects in condensation and cohesion (Figure 7B). We then assayed cohesion in the *mcd1-m0 MCD1-AID* cells. Like *mcd1-Q266*, the *m0* allele failed to maintain cohesion (Figure 7D). Moreover, the timing of cohesion loss was indistinguishable from the *Q266* allele (Figure 2C & Figure 7D). Thus, the unique combination of defects in condensation and cohesion maintenance are shared between the Q266 allele and at least *m0*. Thus, multiple residues proximal to Q266 contribute to the maintenance of cohesion and the establishment of condensation in budding yeast. We propose that this region comprises a new motif, which we term ROCC, for regulation of cohesion and condensation.

Discussion

In order for cohesin to mediate its diverse biological functions, its activity(ies) must be parsed and coordinated through complex regulation. To begin to elucidate the mechanism(s) of this complex regulation, we focused on how cohesin is regulated in budding yeast during M phase to ensure the maintenance of sister chromatid cohesion and the establishment of condensation. Here we identified and characterized the ROCC (Regulator of Cohesion and Condensation) motif, a ten residue region within the linker region of the Mcd1p subunit of cohesin. Our data indicates that the ROCC domain regulates both the maintenance of cohesion and the establishment of condensation.

The study of the ROCC motif revealed that *rocc* mutants establish but cannot maintain cohesion. The kinetics of loss of cohesion in the *rocc* mutants is very similar to that seen in cells defective for Pds5p function, either *pds5* mutants or *mcd1*/*scc1* (*scc1-V137K*) (this study). In all these mutants, sister chromatids start

separating approximately 20 minutes after a cohesin null mutant and 15-20 minutes after the completion of S phase. This temporal similarity of the cohesion maintenance defect caused by *rocc* and *pds5* mutants suggests that their dysfunction leads to a failure to inhibit a common cohesion dissolution process in G2. One candidate for a dissolution inducer is Wpl1p (Wapl in vertebrates) as its over-expression in mammalian cells induces precocious sister separation (Gandhi *et al.*, 2006). However, deletion of *WPL1* does not suppress the cohesion maintenance defects of either *rocc* or *pds5* mutants (this study and Chan *et al.*, 2013). The Wpl1p-independent cohesion defects in these two mutants not only further ties together Pds5p and ROCC function, but also reinforces the existence of a novel mechanism of cohesion dissolution yet to be discovered. We suggest that Pds5p bound to cohesin protects the core complex against this novel cohesion dissolution process. This is akin to the idea of Pds5p as a molecular shield to protect cohesin and cohesion maintenance (Stead *et al.*, 2003; D'Ambrosio and Lavoie, 2014)**.** Abrogation of Pds5p function makes cohesin susceptible to this dissolution process. We suggest that *mcd1-V137K* blocks Pds5p binding to cohesin, while *mcd1-Q266* perturbs a Pds5p-associated activity (either Pds5p itself or another protein) that acts after Pds5p binds to cohesin.

Here, we began to elucidate the mechanism of this novel Wpl1p-independent process for cohesion dissolution. Wpl1p disrupts the integrity of the cohesin complex which in turn increases cohesin dissociation from chromosomes and dissolution of cohesion (Sutani *et al.*, 2009). In contrast, we show that the novel Wpl1p-independent mechanism disrupts cohesion in *rocc* and *mcd1-V137K* mutants without altering the stable binding of cohesin to chromosomes (this study; Chan *et al.*, 2013). Indeed, we observed almost no cohesin dissociated from chromosomes during a thirty minute window following inhibition of the cohesin loader. Importantly, this low rate of cohesin dissociation from chromosomes in *rocc* mutants was measured at many chromosomal loci/regions. Furthermore, the persistent binding of cohesin to chromosomes in the *scc1-V137K* mutant was demonstrated by completely different method of fluorescence recovery after photobleaching (Chan *et al.*, 2013). Finally, in these studies of the *rocc* and *scc1-V137K* mutants, the stable cohesin binding to chromosomes was monitored using different cohesin subunits as reporters, making it highly unlikely that a lone cohesin subunit could be functioning independent of a functional complex (Chan *et al.*, 2013). Taken together, we showed that cohesion dissolution can occur without increasing cohesin dissociation from chromosomes through the study of two different mutants, two independent methods, and two different reporters of the cohesin complex.

The observation that cohesion can be dissolved without dissociating cohesin from chromosomes provides a key mechanistic insight into understanding how

sister chromatids are tethered. In the simple embrace model, the only mechanism capable of dissolving cohesion is the disruption of the ring's integrity either by opening or cleaving it. This disruption of ring's integrity would not only allow the entrapped sister chromatids to escape, but also cause cohesin dissociation from chromosomes. Clearly, this obligatory coupling of cohesion dissolution with cohesin dissociation from chromosomes does not fit the properties of dissolution observed in the *rocc* and *mcd1-V137K* mutants (this study). Rather, the cohesion dissolution in these mutants demands a second function of cohesin that can be disrupted besides its chromosome binding activity. One of several possibilities for this second activity is cohesin oligomerization as suggested by the handcuff model (Petrushenko *et al.*, 2010). In this model, cohesion arises from the oligomerization of two cohesins, each of which topologically entraps a single sister chromatid. Additional models of tethering involving oligomerization have been proposed based upon studies of bacterial SMC complexes (Gloyd *et al.*, 2011). Further analysis of cohesion dissolution in *rocc* and *pds5* mutants provides a potentially powerful tool to elucidate the molecular nature of this second step.

Our analyses of *rocc* mutants revealed a second important and unique phenotype; an ability to establish cohesion but not condensation of the *rDNA*. This result demonstrated a role for ROCC in the regulation of the establishment of condensation. This *rocc* phenotype suggests that while cohesin is required for both cohesion and condensation, its activity(ies) in the establishment of cohesion and condensation can be uncoupled. Previously we reported evidence for this uncoupling as the introduction of *wpl1Δ* into *eco1Δ* suppressed its condensation but not its cohesion defect (Guacci and Koshland, 2012). Interestingly, a *wpl1Δ* also suppressed the condensation defect of *rocc* strains but not the cohesion-maintenance defect. Thus ROCC and Eco1p appear to antagonize an anti-condensation activity of Wpl1p. Since *rocc* mutants do not destabilize cohesin binding to chromosomes, this anti-condensation activity of Wpl1p must be distinct from its ability to dissociate cohesin from chromosomes. We suggest that ROCC with Eco1p modulate the multiple activities of Pds5p, Wpl1p, or other yet to be defined factors as part of a key regulatory network that controls cohesin's function in cohesion and condensation.

The role of cohesin and Pds5p in condensation is evolutionarily conserved, as they modulate meiotic chromosome condensation in budding yeast, fission yeast as well as vertebrates (Ding *et al.*, 2006; Novak *et al.*, 2008; Jin *et al.*, 2009). The role of Wpl1p in regulating condensation may also be conserved in vertebrates. A recent study showed that depletion of the *WPL1* homolog (*WAPL*) in vertebrate cells led to cohesin-dependent chromosome compaction in serum starved G_0 cells (Tedeschi *et al.*, 2013). As we observed in yeast, the presence or absence of WAPL in these G_0 cells did not change the binding of cohesin to

chromosomes, implying that the anti-condensation function of Waplp in vertebrates is also distinct from its ability to dissociate cohesin from chromosomes. In this context, the apparent conservation of the ROCC motif in mammalian orthologs of Mcd1p is very intriguing (this study). One possibility is that ROCC, Eco1p and Wpl1p regulate a signal cascade, independent of any cohesin tethering activity, which triggers condensation, such as by activating condensin. Alternatively, cohesin may promote condensation by its proposed ability to generate intra-strand tethers as well as the inter-strand tethers needed for cohesion (Kagey *et al.*, 2010; Tedeschi *et al.*, 2013). In this scenario, ROCC, Eco1p and Wpl1p may be part of a second pathway that regulates intra-strand tethers. Distinguishing between these models by further characterization of ROCC should provide important new insights into the fascinating complexity of cohesin function and regulation.

Acknowledgements.

We thank Koshland lab members for helpful discussions, reagents, and constructive feedback on the manuscript. Katie Hogan and Carol Davenport conducted the initial RID overexpression screen. This work was supported by grant R01 GM092813from NIGMS/NIH to DEK and a NSF Graduate Research Fellowship to TE.

Materials and Methods

Yeast strains, media, and reagents.

Yeast strains used in this study are the A346a background, and their genotypes are listed in supplemental table 1. Synthetic dropout and YPD media were prepared as previously described (Guacci *et al.*, 1997). For experiments using the AID system, a 1M stock of 3-indoleacetic acid (Sigma-Aldrich, St. Louis, MO) was made in DMSO and added to plates or liquid cultures at a final concentration of 500µM, cooling agar used in plates to ~55˚C before adding auxin to each batch. 5-Fluoroorotic (5-FOA) was purchased from BioVectra (Charlottetown, PE).

Dilution Plating Assays.

Cells were grown to saturation in YPD media at 23°C (or 30°C when listed), diluted to OD_{660} 1.0 using YPD, and then plated in 10-fold serial dilutions. Cells were incubated on plates at relevant temperatures as described.

Cohesion Assays.

To monitor cohesion from G1 to M, haploid yeast cells were initially grown to mid log phase at 23°C in YPD culture. Cells were staged to G1 by addition α factor (Sigma-Aldrich) to 10^{-8}M final conc. and incubation for 3hr. Cells were examined by light microscopy to confirm the presence of the schmoo morphology in 95% of the cells, at which point auxin was added (500µM final) to induced degradation of AID tagged proteins and cells incubated 1h more. Cells were released from G1 arrest by washing six times in YPD containing auxin and 0.1 mg/ml Pronase E (Sigma-Aldrich), then resuspended in fresh YPD containing auxin and nocodazole (Sigma-Aldrich) at 15 µg/ml final and incubated at 23˚C to allow cell-cycle progression until arrest in mid-M phase. To monitor cohesion and cell cycle progression and cohesion, cell aliquots were fixed every 15 minutes for DNA content by FACS and for cohesion via the LacI-GFP cohesion assay.
To monitor cohesion in M phase arrested cells, haploid yeast cells were grown at 23˚C to mid-log phase, and then nocodazole (15µg/ml) was added and cells incubate 3h at 23°C to arrest at mid-M phase. Arrests were confirmed by light microscopy for the classical large budded cellular phenotype (~95% of the population). Auxin (500µM final) was added to cultures and cells were incubated at 23°C. Aliquots were fixed and processed at various timepoints after auxin addition to assess cohesion via the GFP-LacI system.

Microscopy.

Images were acquired with an Axioplan2 microscope (100× objective, numerical aperture 1.40; Zeiss Thornwood, NY) equipped with a Quantix charge-coupled device camera (Photometrics, Tucson, AZ).

Chromosome spreads and microscopy.

Chromosome spreads were performed as previously described (Wahba *et al.*, 2013). Slides were incubated with a mouse anti-FLAG monoclonal (Sigma) at 1:2,000, mouse anti-V5 (Life Technologies) at 1:2,000, polyclonal rabbit anti-Pds5 at 1:2,000, or polyclonal rabbit anti-Mcd1 at 1:2,000 dilutions. The primary antibody was diluted in blocking buffer (5% BSA, 0.2% milk, 1× PBS, 0.2% Triton X-100). The secondary Cy3-conjugated goat anti-mouse antibody (No. 115-165-003) was obtained from Jackson ImmunoResearch (West Grove, PA) and diluted 1:2000 in blocking buffer. Indirect immunofluorescence (IF) was observed using an Olympus IX-70 microscope with a 100×/NA 1.4 objective, and Orca II camera (Hamamatsu, Bridgewater, NJ).

Chromatin immunoprecipitation (ChIP).

Cells used for ChIP experiments were processed in the same manner as cells examined for cohesion assays as described in (Wahba *et al.*, 2013). Briefly, after synchronous release from G1 into mitotic arrest, $5x10^8$ large-budded cells were fixed for two hours with 1% formaldehyde. After cell lysis, chromatin was sheared 20 times for 45 s each (settings at duty cycle: 20%, intensity: 10, cycles/burst: 200; 30s of rest between cycles) using a Covaris S2. Immunoprecipitation of epitope tagged proteins were isolated using anti-Pds5 polyclonal antibody (Covance Biosciences, NY). Mcd1p was alternatively immunoprecipitated with a polyclonal rabbit anti-Mcd1 antibody (Covance Biosciences, NY). A no primary antibody control was also run to ensure specificity. Appropriate dilutions of input and immunoprecipitated DNA samples were used for PCR analysis to ensure linearity of the PCR signal. PCR and data analysis was carried out as described previously (Wahba *et al.*, 2013). All experiments were done at least twice and a representative data set is shown. ChIP primers are available upon request.

Flow Cytometry.

Flow cytometry was conducted as described previously (Yamamoto *et al.*, 1996a) with slight modifications. SYBR Green DNA I dye was used to examine DNA content (Life Technologies) at a 1:10,000 dilution in sodium citrate buffer (pH 7.4, 50mM). Twenty thousand events were collected for each timepoint.

Generation of Auxin Degron Cassettes.

The original auxin degron cassettes from Nishimura and colleagues were modified as followed. A 3V5 epitope tag and five amino acid polylinker was added at the N terminus of the AID open reading frame by standard cloning techniques.

Random Insertion Screen for Dominant Negative Alleles (RID Screening).

Briefly, linker scanning mutagenesis was performed essentially as described in Milutinovich 2007. Plasmid pVG385, a *CEN URA3* plasmid which contains a *MCD1* under control of the *pGAL* promoter was mutagenized in vitro using the TnABC transposase following manufacturer's protocol (GPS-LS Linker Scanning System, NEB). The in vitro mutagenized pVG385 was transformed into bacteria and a Tn7 random insertion DNA library (from ~4000 bacterial colonies) was generated. Tn7 inserts at only one site in each plasmid and generates a PmeI site at each end of the Tn7. This Tn7 library DNA was digested with PmeI to excise Tn7, and the linearized plasmid was gel purified and re-circularized (ligated at low density). This re-circularized DNA has a 15bp insertion at the site of Tn7 excision, and was transformed into *E. coli*. DNA from ~12,000 individual bacterial colonies were harvested to form the bacterial *MCD1-RID* library. This pVG385-RID library was then transformed into either *MCD1* or *mcd1-1* haploid yeast strains and plated onto URA- dextrose media to select URA+ transformants. Approximately 6000 transformants from wild-type yeast and 2300 transformants from *mcd1-1* yeast were transformants were screened by replica plating to both URA- dextrose and URA- galactose media. Transformants which were inviable or slow growing on galactose but grew well on dextrose were selected for further analysis. These candidate clones were patched onto URA- dextrose plates then replica plated to URA- galactose and 5'FOA galactose media to confirm linkage of the inviable phenotype on galactose media without the candidate plasmid. Plasmids from these candidates were isolated and re-transformed into yeast to confirm the pVG385-MCD1-RID lethality. Thus confirmed, plasmids were sequenced using standard methods to identify the site of insertion.

Oligo Based Mutagenesis of the ROCC Domain.

Briefly, we generated mutagenized PCR fragments of the MCD1 reading frame at codons specifying amino acids 258-265, and separately, 265-272. These mutated MCD1 fragments were cotransformed with a gapped MCD1 plasmid (pVG164 CEN TRP MCD1) into DK5521 (mcd1Δ CEN URA mcd1-1) such that resulting TRP+ colonies repaired the *CEN TRP1* plasmid using the mutagenized

MCD1 fragment as template. About 4,000 TRP+ independent transformants were recovered, and of these, fifty candidate transformants were inviable on 5'FOA. Sequenced plasmids were rebuilt and retested in a MCD1-AID background for cohesion and condensation analysis.

Strains Used in This Study.

Strain	Genotype	Reference
VG3349-1B	*MATa LacO(DK)-NAT::lys4 pHIS3-GFP-LacI-HIS3::his3-11,15 trp1-1 ura3-52 leu2-3,112 bar1 GAL+*	Guacci, 2012
VG3465-1A	*pGAL-MCD1-6MYC-URA3::ura3-52* in 3349-1B	This study
VG3691-2A	*MATa SCC2-3V5-AID2:KanMx6 GPD1-TIR1-CaTRP1::trp1-1 pGAL-MCD1-6HA-URA3::ura3-52 bar1 LacO(DK)-NAT::lys4 leu2-3,112 pHIS3-GFPLacI-HIS3::his3-11,15 GAL+*	This study
DK5501	*MCD1-AID:KanMx6 pGPD1-OsTIR1-CanLEU2::leu2-3,112* in 3349-1B	This study
DK5503	*pMCD1-MCD1-6MYC-URA3::ura3-52* in DK5501	This study
DK5521	*mcd1Δ::KanMx6 {pVG209 CEN URA mcd1-1}* in 3349-1B	This study
DK5530	*MCD1-Q266-6MYC-URA3::ura3,52* in DK5501	This study
DK5531	*pADH1-TIR1-URA3::ura3-52* in 3349-1B	This study
DK5532	*pGPD1-TIR1-CanLEU2::leu2-3,112* in 3349-1B	
DK5535	*mcd1-Q266-3FLAG-URA3::ura3-52* in DK5501	This study
DK5536	*MCD1-3FLAG-URA3::ura3-52* in DK5501	This study
DK5539	*SCC2-3V5-AID2:KanMx6 MCD1-AID:KanMx6 MCD1-Q266-3FLAG-URA3::ura3-52 pGPD1-TIR1-CanLEU2::leu2-3,112* in 3349-1B	This study

DK5540	*PDS5-3V5-AID2:KanMx6 ADH1-TIR1-URA3* in DK5531	This study
DK5542	*MCD1-AID:KanMx6* in DK5531	This study
DK5543	*{pVG164 CEN TRP mcd1-mut #m0 ROCC mutant} MCD1-AID::KanMX ADH1-TIR1-URA3::ura3-52* in DK5542	This study
DK5550	*mcd1-Q266-6MYC-URA3::ura3-52 MCD1-AID::KanMX rad61Δ::HPH GPD1-TIR1-CanLEU2::leu2-3,112* in DK5530	This study
DK5557	*MCD1-TRP1::trp1-1 MCD1-AID pADH1-TIR1-URA3::ura3-52* in DK5531	This study
DK5558	*MCD1-V137K-TRP1::trp1-1 MCD1-AID pADH1-TIR1-URA3::ura3-52* in DK5531	This study
DK5560	*pGAL1-mcd1-Q266-6MYC-URA3::ura3-52* in 3349-1B	This study
DK5560	*SCC2-3V5-AID2:KanMx6 MCD1-AID:KanMx6 MCD1-3FLAG-URA3 pGPD1-TIR1-CanLEU2::leu2-3,112* in 3349-1B	This study

Note: AID2 is a custom AID cassette that was identified, cloned, and verified for function by T. Eng and Leon Chan.

References.

Chan, K.-L., Gligoris, T., Upcher, W., Kato, Y., Shirahige, K., Nasmyth, K., and Beckouët, F. (2013). Pds5 promotes and protects cohesin acetylation. Proc Natl Acad Sci USA *110*, 13020–13025.

D'Ambrosio, L. M., and Lavoie, B. D. (2014). Pds5 Prevents the PolySUMO-Dependent Separation of Sister Chromatids. Curr Biol *24*, 361–371.

Ding, D.-Q., Sakurai, N., Katou, Y., Itoh, T., Shirahige, K., Haraguchi, T., and Hiraoka, Y. (2006). Meiotic cohesins modulate chromosome compaction during meiotic prophase in fission yeast. The Journal of Cell Biology *174*, 499–508.

Donze, D., Adams, C. R., Rine, J., and Kamakaka, R. T. (1999). The boundaries of the silenced HMR domain in Saccharomyces cerevisiae. Genes Dev *13*, 698–708.

Gandhi, R., Gillespie, P. J., and Hirano, T. (2006). Human Wapl is a cohesin-binding protein that promotes sister-chromatid resolution in mitotic prophase. Curr Biol *16*, 2406–2417.

Gloyd, M., Ghirlando, R., and Guarné, A. (2011). The role of MukE in assembling a functional MukBEF complex. J. Mol. Biol. *412*, 578–590.

Gray, W. M., del Pozo, J. C., Walker, L., Hobbie, L., Risseeuw, E., Banks, T., Crosby, W. L., Yang, M., Ma, H., and Estelle, M. (1999). Identification of an SCF ubiquitin-ligase complex required for auxin response in Arabidopsis thaliana. Genes Dev *13*, 1678–1691.

Guacci, V., and Koshland, D. (2012). Cohesin-independent segregation of sister chromatids in budding yeast. Mol Biol Cell *23*, 729–739.

Guacci, V., Hogan, E., and Koshland, D. (1994). Chromosome condensation and sister chromatid pairing in budding yeast. The Journal of Cell Biology *125*, 517–530.

Guacci, V., Koshland, D., and Strunnikov, A. (1997). A direct link between sister chromatid cohesion and chromosome condensation revealed through the analysis of MCD1 in S. cerevisiae. Cell *91*, 47–57.

Hartman, T., Stead, K., Koshland, D., and Guacci, V. (2000). Pds5p is an essential chromosomal protein required for both sister chromatid cohesion and condensation in Saccharomyces cerevisiae. The Journal of Cell Biology *151*, 613–626.

Heidinger-Pauli, J. M., Mert, O., Davenport, C., Guacci, V., and Koshland, D. (2010a). Systematic reduction of cohesin differentially affects chromosome segregation, condensation, and DNA repair. Curr Biol *20*, 957–963.

Heidinger-Pauli, J. M., Onn, I., and Koshland, D. (2010b). Genetic evidence that the acetylation of the Smc3p subunit of cohesin modulates its ATP-bound state to promote cohesion establishment in Saccharomyces cerevisiae. Genetics *185*, 1249–1256.

Jin, H., Guacci, V., and Yu, H.-G. (2009). Pds5 is required for homologue pairing and inhibits synapsis of sister chromatids during yeast meiosis. The Journal of Cell Biology *186*, 713–725.

Kagey, M. H. *et al.* (2010). Mediator and cohesin connect gene expression and chromatin architecture. Nature *467*, 430–435.

Kueng, S., Hegemann, B., Peters, B. H., Lipp, J. J., Schleiffer, A., Mechtler, K., and Peters, J.-M. (2006). Wapl Controls the Dynamic Association of Cohesin with Chromatin. Cell *127*, 955–967.

Lavoie, B. D., Tuffo, K. M., Oh, S., Koshland, D., and Holm, C. (2000). Mitotic chromosome condensation requires Brn1p, the yeast homologue of Barren. Mol Biol Cell *11*, 1293–1304.

Lopez-Serra, L., Lengronne, A., Borges, V., Kelly, G., and Uhlmann, F. (2013). Budding yeast Wapl controls sister chromatid cohesion maintenance and chromosome condensation. Curr Biol *23*, 64–69.

Michaelis, C., Ciosk, R., and Nasmyth, K. (1997). Cohesins: chromosomal proteins that prevent premature separation of sister chromatids. Cell *91*, 35–45.

Milutinovich, M., Unal, E., Ward, C., Skibbens, R. V., and Koshland, D. (2007). A multi-step pathway for the establishment of sister chromatid cohesion. PLoS Genet *3*, e12.

Mishra, A., Hu, B., Kurze, A., Beckouët, F., Farcas, A.-M., Dixon, S. E., Katou, Y., Khalid, S., Shirahige, K., and Nasmyth, K. (2010). Both Interaction Surfaces within Cohesin's Hinge Domain Are Essential for Its Stable Chromosomal Association. Current Biology *20*, 279–289.

Nishimura, K., Fukagawa, T., Takisawa, H., Kakimoto, T., and Kanemaki, M. (2009). An auxin-based degron system for the rapid depletion of proteins in nonplant cells. Nat. Methods *6*, 917–922.

Noble, D., Kenna, M. A., Dix, M., Skibbens, R. V., Unal, E., and Guacci, V.

(2006). Intersection between the regulators of sister chromatid cohesion establishment and maintenance in budding yeast indicates a multi-step mechanism. Cell Cycle *5*, 2528–2536.

Novak, I., Wang, H., Revenkova, E., Jessberger, R., Scherthan, H., and Hoog, C. (2008). Cohesin Smc1beta determines meiotic chromatin axis loop organization. The Journal of Cell Biology *180*, 83–90.

Panizza, S., Tanaka, T., Hochwagen, A., Eisenhaber, F., and Nasmyth, K. (2000). Pds5 cooperates with cohesin in maintaining sister chromatid cohesion. Curr Biol *10*, 1557–1564.

Peters, J.-M., and Nishiyama, T. (2012). Sister chromatid cohesion. Cold Spring Harb Perspect Biol *4*, a011130.

Petrushenko, Z. M., Cui, Y., She, W., and Rybenkov, V. V. (2010). Mechanics of DNA bridging by bacterial condensin MukBEF in vitro and in singulo. Embo J *29*, 1126–1135.

Rolef Ben-Shahar, T., Heeger, S., Lehane, C., East, P., Flynn, H., Skehel, M., and Uhlmann, F. (2008). Eco1-dependent cohesin acetylation during establishment of sister chromatid cohesion. Science *321*, 563–566.

Rollins, R. A., Morcillo, P., and Dorsett, D. (1999). Nipped-B, a Drosophila homologue of chromosomal adherins, participates in activation by remote enhancers in the cut and Ultrabithorax genes. Genetics *152*, 577–593.

Rowland, B. D. *et al.* (2009). Building sister chromatid cohesion: smc3 acetylation counteracts an antiestablishment activity. Mol Cell *33*, 763–774.

Shimada, K., and Gasser, S. M. (2007). The origin recognition complex functions in sister-chromatid cohesion in Saccharomyces cerevisiae. Cell *128*, 85–99.

Skibbens, R. V., Corson, L. B., Koshland, D., and Hieter, P. (1999). Ctf7p is essential for sister chromatid cohesion and links mitotic chromosome structure to the DNA replication machinery. Genes Dev *13*, 307–319.

Stead, K., Aguilar, C., Hartman, T., Drexel, M., Meluh, P., and Guacci, V. (2003). Pds5p regulates the maintenance of sister chromatid cohesion and is sumoylated to promote the dissolution of cohesion. The Journal of Cell Biology *163*, 729–741.

Ström, L., Lindroos, H. B., Shirahige, K., and Sjögren, C. (2004). Postreplicative recruitment of cohesin to double-strand breaks is required for DNA repair. Mol Cell *16*, 1003–1015.

Strunnikov, A. V., Larionov, V. L., and Koshland, D. (1993). SMC1: an essential yeast gene encoding a putative head-rod-tail protein is required for nuclear division and defines a new ubiquitous protein family. The Journal of Cell Biology *123*, 1635–1648.

Sutani, T., Kawaguchi, T., Kanno, R., Itoh, T., and Shirahige, K. (2009). Budding yeast Wpl1(Rad61)-Pds5 complex counteracts sister chromatid cohesion-establishing reaction. Curr Biol *19*, 492–497.

Tedeschi, A. *et al.* (2013). Wapl is an essential regulator of chromatin structure and chromosome segregation. Nature *501*, 564–568.

Tóth, A., Ciosk, R., Uhlmann, F., Galova, M., Schleiffer, A., and Nasmyth, K. (1999). Yeast cohesin complex requires a conserved protein, Eco1p(Ctf7), to establish cohesion between sister chromatids during DNA replication. Genes Dev *13*, 320–333.

Uhlmann, F., Lottspeich, F., and Nasmyth, K. (1999). Sister-chromatid separation at anaphase onset is promoted by cleavage of the cohesin subunit Scc1. Nature *400*, 37–42.

Unal, E., Arbel-Eden, A., Sattler, U., Shroff, R., Lichten, M., Haber, J. E., and Koshland, D. (2004). DNA Damage Response Pathway Uses Histone Modification to Assemble a Double-Strand Break-Specific Cohesin Domain. Mol Cell *16*, 991–1002.

Unal, E., Heidinger-Pauli, J. M., Kim, W., Guacci, V., Onn, I., Gygi, S. P., and Koshland, D. E. (2008). A molecular determinant for the establishment of sister chromatid cohesion. Science *321*, 566–569.

Wahba, L., Gore, S. K., and Koshland, D. (2013). The homologous recombination machinery modulates the formation of RNA-DNA hybrids and associated chromosome instability. Elife *2*, e00505.

Yamamoto, A., Guacci, V., and Koshland, D. (1996a). Pds1p is required for faithful execution of anaphase in the yeast, Saccharomyces cerevisiae. The Journal of Cell Biology *133*, 85–97.

Yamamoto, A., Guacci, V., and Koshland, D. (1996b). Pds1p, an inhibitor of anaphase in budding yeast, plays a critical role in the APC and checkpoint pathway(s). The Journal of Cell Biology *133*, 99–110.

Yeh, E., Haase, J., Paliulis, L. V., Joglekar, A., Bond, L., Bouck, D., Salmon, E. D., and Bloom, K. S. (2008). Pericentric chromatin is organized into an intramolecular loop in mitosis. Curr Biol *18*, 81–90.

Zhang, B. *et al.* (2009). Dosage effects of cohesin regulatory factor PDS5 on mammalian development: implications for cohesinopathies. PLoS ONE *4*, e5232.

Figure Legends.

Figure 1. Isolation of RID mutants in MCD1.
(A) Schematic of RID mutagenesis. Plasmid pVG385 containing *MCD1* driven by the *GAL1* promoter (*pGAL-MCD1*) was subjected to Tn7 transposition in vitro. The inserted transposon was removed by *PmeI* digestion, leaving random 15bp insertions. The library was transformed into either haploid WT (VG3349-1B) or *mcd1-1* (VG3312-7A) strains and transformants were screened for inviability or slow growth on galactose.
(B) Haploid WT (VG3349-1B) yeast bearing *pGAL-MCD1* or *pGAL-mcd1-Q266* were grown at 23˚C to saturation, then plated in ten fold serial dilutions onto media containing galactose (YPGAL) or dextrose (YPD) and incubated at 23°C for 3 days. pGAL-Mcd1-Q266 is semi-dominant over *MCD1* and more penetrant at 16˚C (data not shown).
(C) Schematic of cohesin structure and map of RID mutation positions in *MCD1*. The four subunits of the cohesin complex are represented. The head domains of Smc1p and Smc3p are shown as large grey balls at the base of these proteins. The amino and carboxy globular domains of Mcd1p are shown as green balls to the left and right with the intervening green bar representing the linker region. Map of Rid mutations is shown to the right. Grey areas indicate globular domains as determined by sequence conservation.

Figure 2. *mcd1-Q266* is recessive to *MCD1* but exhibits a defect in cohesion maintenance after Mcd1p is removed via the auxin degron system.
(A) Haploid yeast strains *MCD1* (DK5531), *MCD1-AID* (DK5501), and *mcd1-Q266 MCD1-AID* (DK5535) were grown at 23˚C to saturation, plated in ten fold serial dilutions onto onto rich media (YPD) or rich media + 500µM auxin (YPD + auxin) then incubated for 3 days at 23°C.
(B) Schematic to measure cohesion establishment and maintenance as cells progress from G1 to M. Early log phase cells growing at 23°C in YPD were arrested in G1 using xF then auxin (500µM) added and cells incubated 1h more in G1. Cells were then released from G1 arrest into YPD media containing auxin (500µM) and nocodazole (15µg/mL) to allow cell-cycle progression until arrest in M phase. Cell aliquots were fixed and processed every 15min to assess cohesion and DNA content (see Figure S2 and Material and Methods).
(C) Analysis of cohesion in *mcd1-Q266* cells during progression from G1 to M. Haploid *MCD1* (DK5531, solid black crosses), *PDS5-AID* (DK5540, gray circles), *MCD1-AID* (DK5542, open diamonds), and *mcd1-Q266 MCD1-AID* (DK5535, red squares) were assessed for cohesion as described in (B). The percentage of cells with two GFP foci at a *CEN*-distal locus (*LYS4*) is plotted. S phase is marked with a gray box. 200-300 cells were counted at each time-point and the experiment was repeated three times. A representative time-course is shown.

(D) Schematic to measure cohesion maintenance in M phase arrested cells. Early log phase cells growing at 23°C in YPD were arrested by addition of nocodazole (15µg/mL) and incubation for 2.5h. Auxin (500µM) was added and cells incubated an additional 90min. Cell aliquots were processed for the GFP cohesion assay prior to Auxin addition (T=0) and at 15min intervals after auxin addition. (E) Analysis of cohesion in *mcd1-Q266* strains in M phase arrest. Haploid *MCD1* (DK5531, solid black crosses), *PDS5-AID* (DK5540, gray circles), *MCD1-AID* (DK5542, open diamonds), and *mcd1-Q266 MCD1-AID* (DK5535, red squares) were treated and assessed for cohesion as described in (D). The percentage of cells with two GFP foci at a *CEN*-distal locus *LYS4* is plotted. 100-300 cells were counted at each timepoint. Data was generated from two independent experiments and error bars show standard deviation.

Figure 3. mcd1-Q266p and Mcd1p exhibit similar & robust binding to chromosomes. (A) Schematic for analysis of cohesin binding as determined by chromatin immunoprecipitation. Early log phase cells were arrested in G1, treated with auxin to deplete MCD1-AID and released from G1 and re-arrested in M phase using nocodazole at 23°C as described in Figure 2A & 2B. Cells were processed for for chromosome spreads (B) and for chromatin immunoprecipitation (C-E). For ChIP experiments, the average cohesin binding from two biological replicates is plotted. Error bars represent standard deviation between both experiments.
(B) Chromosome spreads. Mcd1-3FLAG MCD1-AID (DK5536, upper panels) and mcd1-Q266-3FLAG MCD1-AID (DK5535, lower panels) cells were processed for chromosome spreads (see Materials and Methods). MCD1-Q266-3FLAGp or MCD1-3FLAGp were visualized using mouse anti-FLAG antibody (anti-FLAG) and DNA (DAPI). Data shown is from one of three independent experiments.
(C-E) Chromatin Immunoprecipation (ChIP). Strains in B were processed for ChIP to assess FLAG tagged Mcd1p binding using rabbit anti-Mcd1p antibodies (Materials and Methods). Mcd1p (black lines or black bars) or mcd1-Q266p (red lines or red bars).
(C) Chromosome III pericentric domain ChIP. Mcd1p binding was assessed by qPCR using primers spanning a 10kb region. Primer pairs were spaced every ~500bp.
(D) Chromosome XII ChIP at a single copy domain near the *rDNA*. Mcd1p binding over a 10kb region was assessed by qPCR using primer pairs spaced every ~500bp.
(E) *CEN*1 and *CEN14* ChIP. Mcd1p binding at 3 loci immediately flanking *CEN1* and *CEN14*. All primer sets examine DNA sequences within 500bp of either centromere.

Figure 4. *mcd1-Q266* and Wild-Type cohesin are stably bound on chromosomes at CAR sites, but equally unstable at *CENs*.

(A) Schematic to assess stability of the cohesin complex on chromosomes in M phase cells. Cells were arrested in M phase as describe in Figure 2D legend. The culture was split in half and auxin (500μM) added to one half then each half was incubated for 1h in M phase then samples processed for ChIP using rabbit anti-Mcd1 antibody (see Materials and Methods).
(B & C) Analysis of cohesin binding to chromosomes in M phase after Scc2p loader depletion (*stability* strains). We utilized two haploid *MCD1* stability strains which contained (*SCC2-AID MCD1-AID*) and either *MCD1-3FLAG* (DK5560) or *mcd1-Q266-3FLAG* (DK5539). Strains were grown and processed as described in A. FLAG tagged Mcd1p binding at specific chromosomal sites was assessed by ChIP using qPCR. Two independent experiments were performed and gave equivalent results, one of which is shown here.
(B) Effect of Loader depletion on Mcd1-3FLAGp cohesin binding to chromosomes. ChIP of Mcd1-3FLAGp stability strain DK5560 when Scc2p was active (No Auxin; solid line) or after Scc2p loader was depleted (+ Auxin, dotted black line). Chip analysis at chromosome III peri-centric region (left Panel), chromosome XII single copy arm region (middle panel) and within 500bp of *CEN3* and *CEN14* (right panel). Data is the average of two qPCR replicates for each primer pair.
(C) Effect of loader depletion on mcd1-Q266p cohesin binding to chromosomes. ChIP of Mcd1-Q266-3FLAG stability strain DK5539 when Scc2p was active (no auxin, solid red line) or after Scc2p loader was depleted (+ Auxin, dotted red line). ChIP analysis was performed at same loci as in B.

Figure 5. Mechanism of Cohesion Maintenance.
(A) Effect of *wpl1Δ* on the cohesion maintenance defect of *mcd1-Q266*. Four haploid strains were subjected to auxin depletion in G1 phase then allowed to progress into M phase arrest under auxin depletion as described in Figure 2B legend to assess whether *WPL1* affects the *mcd1-Q266* cohesion defect. Cohesion loss in *MCD1* (DK5531, solid black circles), *wpl1Δ* (DK5561, gray diamonds), *mcd1-Q266 MCD1-AID* (DK5530, solid red squares), and *wpl1Δ mcd1-Q266 MCD1-AID* (DK5535, dotted red squares) was assessed by plotting the percentage of cells with two GFP foci at a *CEN*-distal locus (*LYS4*). S phase is marked with a gray box. 200-300 cells were counted at each time-point. Data is from 2 independent experiments.
(B-E). Effect of mcd1-Q266 on Pds5p binding to chromosomes. Haploids *MCD1* (DK5531) and *mcd1-Q266 MCD1-AID* (DK5501, lower panels) were grown as described in A and then processed for chromosome spreads (B) and ChIP (C-E).
(B) Chromosome spreads to detect Pds5p. The Pds5p staining in *MCD1* cells (top panels) and in *mcd1-Q266* cells (bottom panels). Pds5p was detected using rabbit anti-Pds5p antibodies (right panels) and DNA detected using DAPI (left panels). Data was generated from two independent experiment, which gave similar results. A representative field is shown.

(C-E) Pds5p Chromatin Immunoprecipation (ChIP). Strains in B were processed for ChIP to assess Pds5p binding using rabbit anti-Pds5p antibodies (Materials and Methods). Strains containing WT Mcd1p cohesin (DK5531, black lines) or *mcd1-Q266* cohesin (DK5535, red lines) as shown. (C) Chip analysis at chromosome III peri-centric region (D) ChIP at chromosome XII single copy arm region (middle panel) and (E) ChIP within 500bp of *CEN3* and *CEN14* (right panel). Data from average cohesin binding from two biological replicates is plotted. Error bars represent standard deviation between both experiments.

Figure 6. *Wpl1Δ* deletion suppresses both the inviability and condensation defects of *mcd1-Q266*.

(A) Haploid yeast strains *mcd1-Q266 MCD1-AID* (DK5530) and *wpl1Δ mcd1-Q266 MCD1-AID* (DK5550) were grown at 23˚C and plated in ten fold serial dilutions onto rich media (YPD) or rich media with 500µM auxin (YPD+auxin).
(B) Effect of *wpl1Δ* on the cohesion maintenance defect of *mcd1-Q266*. Four haploid strains were subjected to auxin depletion in G1 phase then allowed to progress into M phase arrest under auxin depletion as described in Figure 2B legend. Cohesion loss in *MCD1* (DK5531, solid black circles), *wpl1Δ* (DK5561, gray diamonds), *mcd1-Q266 MCD1-AID* (DK5530, solid red squares), and *wpl1Δ mcd1-Q266 MCD1-AID* (DK5535, dotted red squares) was assessed by plotting the percentage of cells with two GFP foci at a *CEN*-distal locus (*LYS4*). S phase is marked with a gray box. 200-300 cells were counted at each time-point. A representative timecourse is shown from two independent biological replicates.
(B) Representative cytological morphology of the *rDNA* locus, as prepared by chromosome spreads and stained with DAPI (see Materials and Methods, and Lavoie *et al*., 2000). Decondensed *rDNA* (left panel), Condensed *rDNA* (right panel) Arrow indicates the location of *rDNA*.
(C-F) Assessment of chromosome condensation in budding yeast. Samples were collected at fifteen minute intervals and processed to examine rDNA morphology by chromosome spreads stained with DAPI. At least 100 chromosome masses were scored per timepoint.
(C) Schematic of auxin depletion in G1 and subsequent release to M phase arrest. (D) Effect of *mcd1-Q266* on *rDNA* condensation as described in C. Haploids *MCD1* (DK5531, solid black crosses), *MCD1-AID* (DK5542, dashed black circles), and *mcd1-Q266 MCD1-AID* (DK5535, red squares) were subjected to auxin depletion in G1 phase then allowed to progress into M phase arrest under auxin depletion as described in Figure 2B legend. *rDNA* condensation was assessed at various times points after G1 phase release. The percent of cells where the *rDNA* “loop” was well formed is plotted. S phase as determined by flow cytometry is marked with a gray box. A representative biological replicate is shown from two biological replicates.
(E) Effect of *wpl1Δ* on the *rDNA* condensation defect of *mcd1-Q266* during

progression from G1 to M. Haploids *mcd1-Q266* (DK5530) and *wpl1Δ mcd1-Q266* (DK5550) strains were grown, treated then the *rDNA* scored for condensation as described in (D-E). Right panel. A representative plot is shown from two biological replicates with similar results. Left panel. Representative DAPI stained chromosome masses from *mcd1-Q266* (DK5530) (upper image) and *wpl1Δ mcd1-Q266* (DK5550) (bottom image) from the 150 minutes post release timepoint.

Figure 7. Mutagenesis of Residues Adjacent to Q266 Identify an Evolutionarily Conserved Motif, Termed ROCC.

(A) Residues in region adjacent to Q266 were mutagenized and subjected to screening to identify mutant alleles that cannot support viability on their own but form a full-length Mcd1p (see Materials and Methods). One such allele, termed *mcd1-m0*, had a seven amino acid substitution.

(B) Assessment of cohesion and condensation of *mcd1-m0* allele. Plasmids bearing mutant alleles generated in A were transformed into a *MCD1-AID* background (*mcd1-m0 MCD1-AID*: DK5543.). Cells were depleted for Mcd1-AIDp in G1 phase then released into M phase arrest as described in figure 2D. Cohesion (at *LYS4*) and condensation (at *rDNA*) were scored in M phase as described in Figure 6B and 6D respectively .

(C) Sequences of Mcd1p homologs were imported from GENBank into ClustalW and N terminus aligned. No major homology was predicted by ClustalW. We manually aligned the homologs by shifting amino acids from Mcd1p homologs by several bases to highlight the presence of a poly-aspartic acid patch located in similar distances from the N terminus.

(D) Analysis of cohesion in *mcd1-m0* strain during progression from G1 to M phase. Haploid *MCD1* (DK5542) and *mcd1-m0 mcd1-AID* (DK5543) strains during progression from G1 to M and were subjected to auxin depletion in G1 phase then allowed to progress into M phase arrest under auxin depletion as described in Figure 2B legend. The percentage of cells with two GFP foci at a CEN-distal locus *LYS4* was plotted to assess cohesion loss. S phase is marked with a gray box. A representative plot is shown from two biological replicates.

Supplemental Table 1.
RID Alleles Recovered from Insertion Screen.

MCD1 RID alleles in VG3349-1B were recovered from the over-expression screen in haploid yeast cells and sequenced using standard techniques (See Materials and Methods). The insertions in Mcd1 are named after the residue the insertion follows. Two recovered mutants in RID-L74 had silent codon changes specifying lysine 74. Alleles were recovered in both the wild-type MCD1 background as well as the *mcd1-1* background.

Supplemental Figure 1.
MCD1-AID as a Tool to Study Cohesion.
Left panel: Early log haploid yeast cells carrying *MCD1-AID* (DK5542) were treated with hydroxyurea (0.2M final) for 2 hours to induce S phase arrest. The culture was treated with auxin (500μM) immediately following time 0. Samples were taken at timepoints indicated. Denaturing cell extracts were prepared from each timepoint and separated by SDS-PAGE electrophoresis. Protein levels of Mcd1-AIDp were tracked with a rabbit anti-Mcd1 antibody. A rabbit anti-tubulin antibody was used as a loading control.
Right panel: Early log haploid yeast cells carrying *MCD1-AID* (DK5542) were arrested in M phase with nocodazole (15μg/mL) for 2.5 hours. Immediately following the zero minute timepoint, auxin was added to the culture (500μM). A sample was collected before auxin and 30 minutes post auxin addition. Denaturing cellular extracts were separated by SDS-PAGE electrophoresis and Mcd1-AIDp was identified with a rabbit anti-Mcd1 antibody. Tubulin was used as a loading control.

Supplemental Figure 2.
Cell cycle profiles from G1 to M phase in cohesin mutants from this study.
As described in 2A, cells released from G1 arrest were also prepared for flow cytometry (see Materials and Methods). Ethanol fixed cells were treated with RNase and proteinase K before staining with SYBR Green DNA I on a Millipore Guava EasyCyte flow cytometer.
(A) Samples from *MCD1* (DK5531), *mcd1-Q266 MCD1-AID* (DK5535), and Pds5-AID (DK5540) strains were processed as described above. All strains completed DNA replication by 75 minutes. At least 20,000 events were counted from each timepoint.
(B) *mcd1-V137K MCD1-AID (*DK5558) and *MCD1-AID MCD1* (DK5557) analyzed by flow cytometry as described above. At least 20,000 events were counted from each timepoint.

Supplemental Figure 3.
Auxin tagged essential yeast genes are not viable on auxin media.
Haploid strains (MCD1: DK5532; MCD1-AID: DK5542; *SCC2-AID*: DK5539; *PDS5-AID*: DK5540; *MCD1-AID MCD1:* DK5503) were grown at 23˚C to saturation, then plated in ten fold serial dilutions onto media lacking or supplemented with auxin (YPD or YPD +Auxin) and incubated at 23°C for 3 days.

Supplemental Figure 4.
mcd1-Q266 is not precociously degraded.
Haploid early log phase yeast strains *MCD1-6MYC* (*DK5503*) and *mcd1-Q266-6MYC* (DK5530) were arrested in M-phase with nocodazole and denaturing cellular extracts were separated by SDS-PAGE electrophoresis. Epitope tagged

alleles of Mcd1 were visualized using an anti-Myc antibody (1:10,000 dilution). Tubulin was used as a loading control.

Supplemental Figure 5.
SCC2-AID As a Tool to Study Cohesin Loading.
(A) Early log phase haploid cells growing at 23°C in YPD were arrested in G1 using xF then auxin (500μM) added and cells incubated 1h more in G1. Cells were then released from G1 arrest into YPD media containing auxin (500μM) and nocodazole (15μg/mL) to allow cell-cycle progression until arrest in M phase. Cells were examined ~150 minutes post release (95% large budded cells) for cohesion, western blot analysis, and chIP.
(B) Scc2-3V5-AIDp (DK5539) was assessed as described in (A) in the presence or absence of auxin. Denatured total cell extracts were separated by SDS-PAGE. The membrane was probed with a mouse anti-V5 antibody to identify Scc2-3V5-AID. Anti-V5 blot is overexposed to detect any signal in the + auxin lane. Tubulin was used as a loading control.
(C) Strains (SCC2: DK5532; SCC2-3V5-AID: DK5539) were prepared as described in (A) were assessed for sister chromatid separation at *LYS4.*
(D) SCC2-3V5-AID2 (DK5539) was prepared for chromatin immunoprecipitation as described in (A) using a rabbit anti-Mcd1 antibody.

Supplemental Figure 6.
Scc2-AID is Required for *de novo* cohesin loading.
(A) Haploid strain SCC2-3V5-AID pGAL-MCD1-6HA (VG3691-2A) was grown in lactic acid + glycerol media to early log phase and staged in G1 with mating pheromone. Cells were then released from G1 arrest into YPD media containing auxin (500μM) and nocodazole (15μg/mL) to allow cell-cycle progression until arrest in M phase. When the culture was 95% large budded, the sample was split in half. One half of the sample was treated with auxin for 1 hour. Afterwards, galactose was added to both halves to induce PGAL-MCD1-6HA. An untagged *SCC2* strain (*DK5532*) was also examined with this regiment. Denaturing cellular extracts were generated from samples treated only with auxin, only with galactose, or both auxin and galactose, and visualized by SDS-PAGE electrophoresis. Scc2-3V5-AIDp was visualized with a mouse anti-V5 antibody. Mcd1 was visualized with a rabbit anti-Mcd1 antibody. Tubulin was used as a loading control.
(B) Timecourse of SCC2-3V5-AID degradation. Haploid *SCC2-3V5-AID* (VG3691-2A) was grown to early log phase in YPD and arrested in M phase to 95% large budded cells. Immediately following the zero minute timepoint, auxin was added to the culture (500μM). Samples were taken at fifteen minute intervals. Denaturing cellular extracts from each timepoint were visualized by SDS-PAGE electrophoresis. V5 tagged proteins were visualized with a mouse anti-V5 antibody. Similar kinetics were observed for cells staged in M phase but

grown in lactic acid + glycerol.
(C) Analysis of cohesin binding to chromosomes in the absence of Scc2. Chromosome spreads prepared from M phase arrested samples as described in (A) were subjected to indirect immunofluorescence using an anti-HA antibody under different experimental regiments. Note that Mcd1-6HA is equally expressed in both the presence or absence of auxin (see A, anti-HA, third and sixth lanes).

Supplemental Figure 7. Like Mcd1-Q266, Mcd1-V137K Can Establish, but Cannot Maintain Cohesion.
(A) Haploid yeast strains were grown to early log (*mcd1-V137K MCD1-AID*: DK5558. *MCD MCD1-AID*: DK5557. *PDS5-AID*: DK5540. *MCD1-AID*: DK5501.) Their ability to generate cohesion from G1 to M phase was examined as completed in Figure 2B. The percentage of cells with two GFP foci at a *CEN*-distal locus (*LYS4*) is plotted. S phase is marked with a gray box. MCD1: black crosses. PDS5-AID: gray circles. mcd1-V137K MCD1-AID: blue squares. MCD1-AID: dashed diamonds. Three hundred cells were counted at each time-point and the experiment was repeated twice. A representative time-course is shown. All cultures completed replication by 75 minutes, as assessed by flow cytometry (see Supplemental Figure S2).
(B) Haploid yeast strains (*mcd1-V137K MCD1-AID*: DK5558. *MCD MCD1-AID*: DK5557) were grown to early log phase and prepared arrested in M phase as in (A). Chromosome spreads were prepared from both cultures and a rabbit anti-Pds5 antibody was used for indirect immunofluorescence to determine Pds5 localization. A representative field is shown.

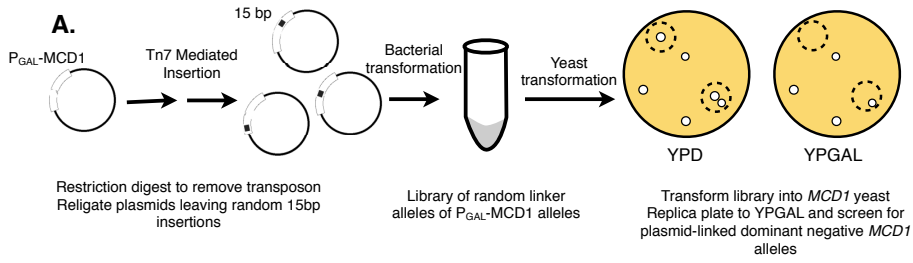
A.
15 bp
P_{GAL}-MCD1
Tn7 Mediated Insertion
Bacterial transformation
Yeast transformation
YPD
YPGAL
Restriction digest to remove transposon
Religate plasmids leaving random 15bp insertions
Library of random linker alleles of P_{GAL}-MCD1 alleles
Transform library into *MCD1* yeast
Replica plate to YPGAL and screen for plasmid-linked dominant negative *MCD1* alleles

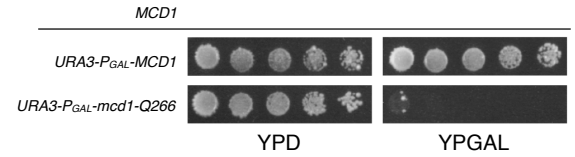
B.
MCD1
URA3-P_{GAL}-MCD1
URA3-P_{GAL}-mcd1-Q266
YPD
YPGAL

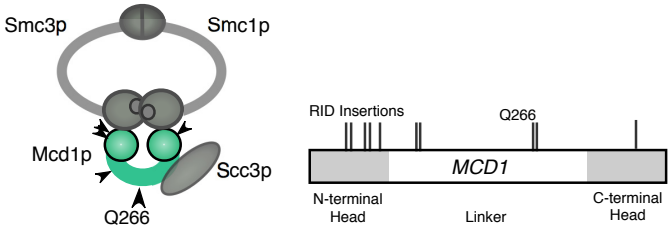
C.
Smc3p
Smc1p
Mcd1p
Scc3p
Q266
RID Insertions
Q266
MCD1
N-terminal Head
Linker
C-terminal Head

Figure 1.

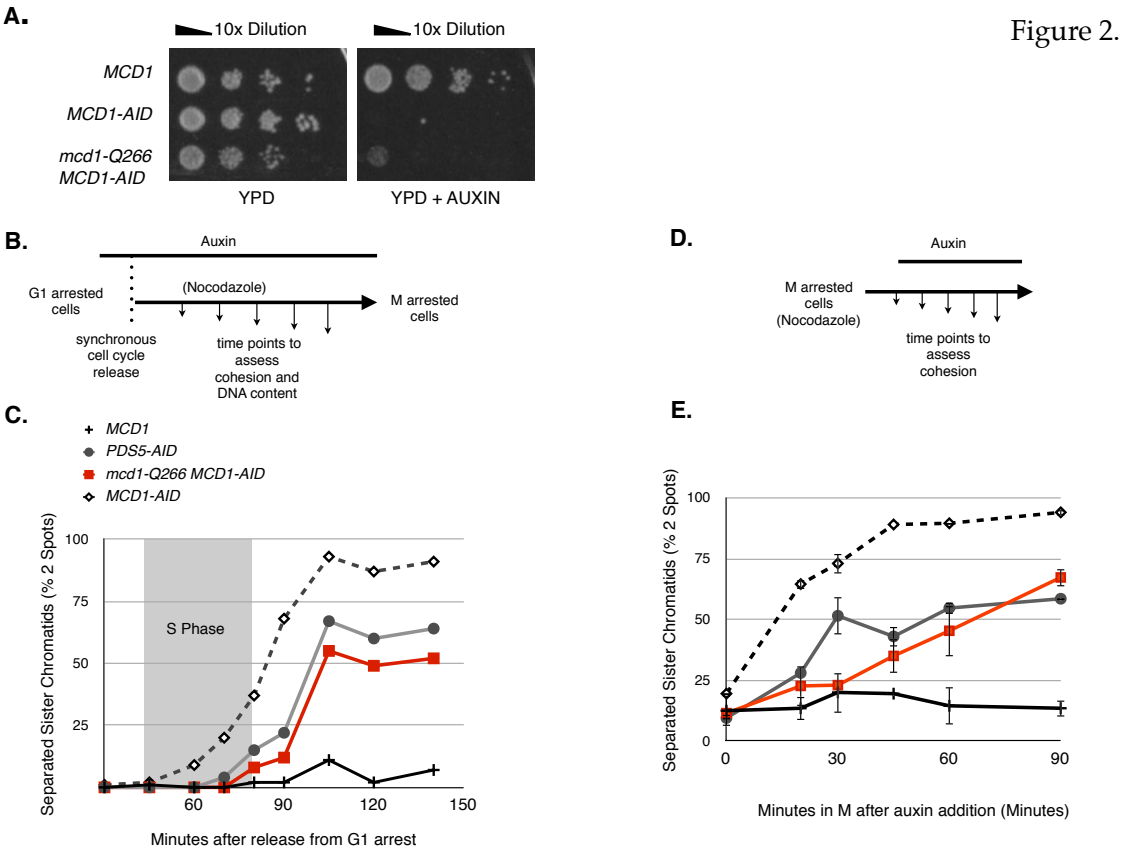
A.
10x Dilution
10x Dilution
MCD1
MCD1-AID
mcd1-Q266
MCD1-AID
YPD
YPD + AUXIN
B.
Auxin
G1 arrested cells
(Nocodazole)
M arrested cells
synchronous cell cycle release
time points to assess cohesion and DNA content
C.
MCD1
PDS5-AID
mcd1-Q266 MCD1-AID
MCD1-AID
Separated Sister Chromatids (% 2 Spots)
S Phase
Minutes after release from G1 arrest
D.
Auxin
M arrested cells (Nocodazole)
time points to assess cohesion
E.
Separated Sister Chromatids (% 2 Spots)
Minutes in M after auxin addition (Minutes)

Figure 2.

Figure 3.

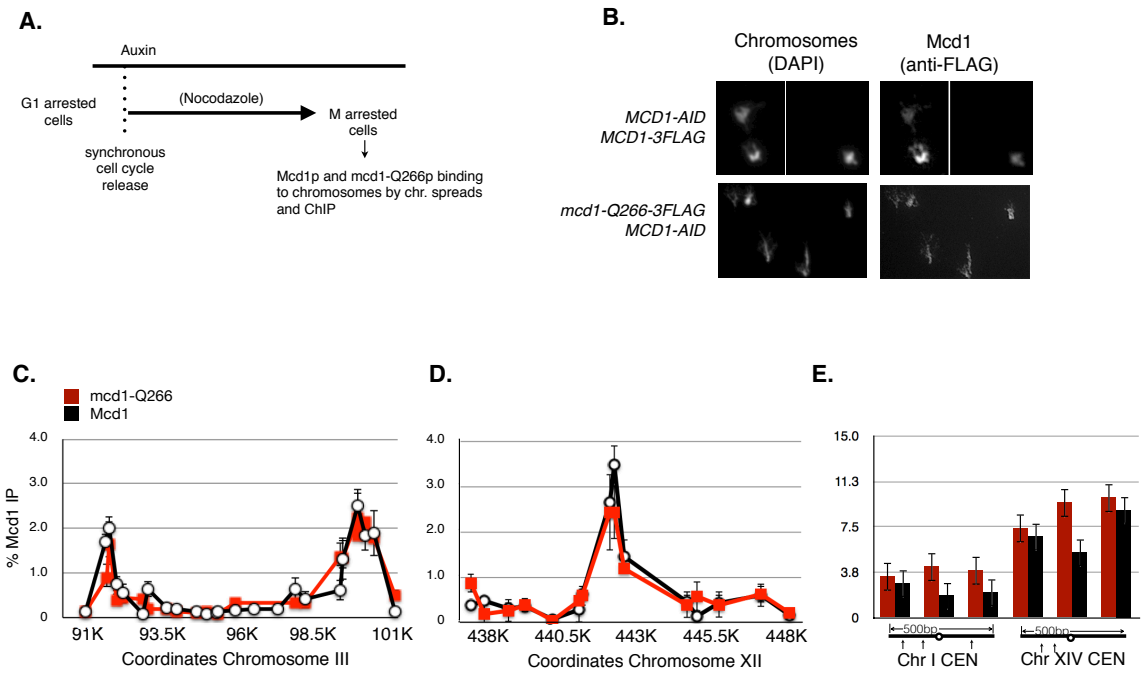
A.
Auxin
G1 arrested cells
(Nocodazole)
M arrested cells
synchronous cell cycle release
Mcd1p and mcd1-Q266p binding to chromosomes by chr. spreads and ChIP
B.
Chromosomes (DAPI)
Mcd1 (anti-FLAG)
MCD1-AID
MCD1-3FLAG
mcd1-Q266-3FLAG
MCD1-AID
C.
mcd1-Q266
Mcd1
% Mcd1 IP
4.0
3.0
2.0
1.0
0
91K
93.5K
96K
98.5K
101K
Coordinates Chromosome III
D.
438K
440.5K
443K
445.5K
448K
Coordinates Chromosome XII
E.
15.0
11.3
7.5
3.8
0
500bp
Chr I CEN
Chr XIV CEN

Figure 4.

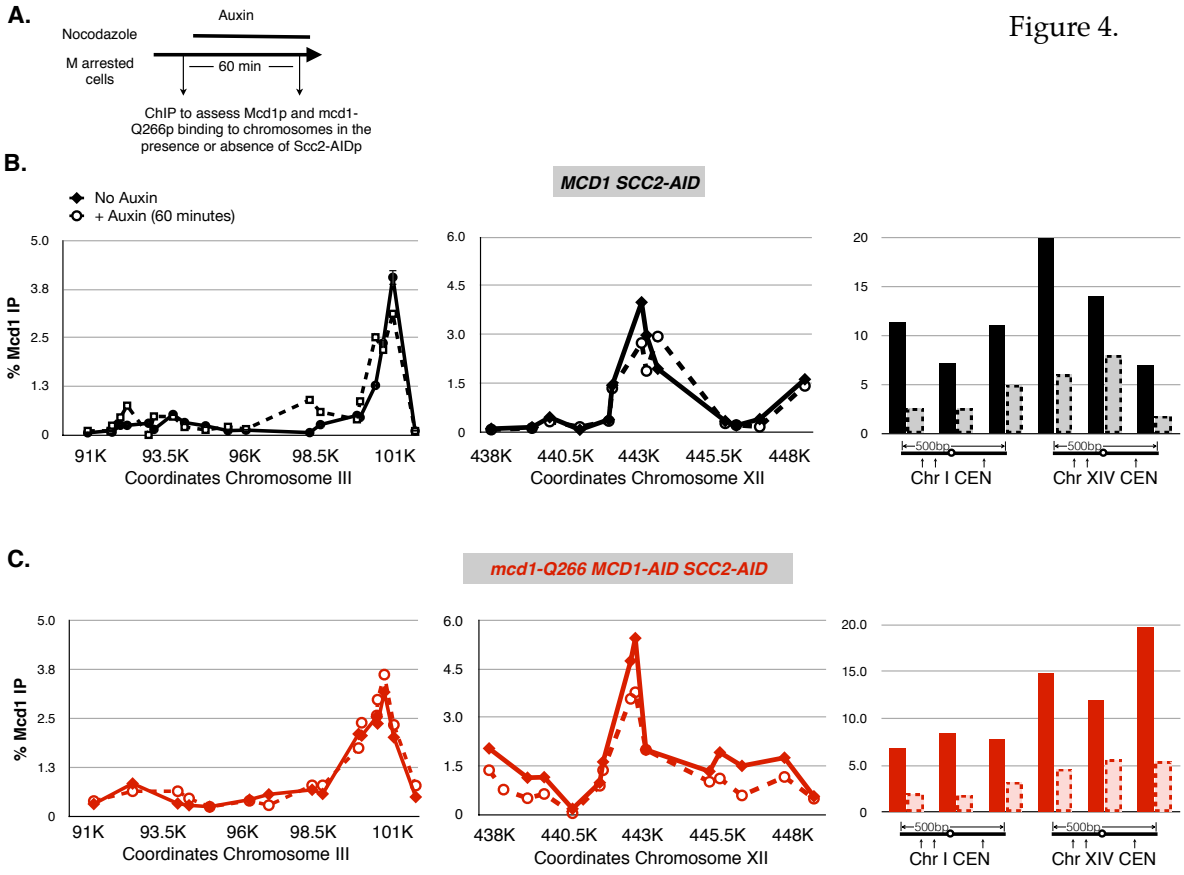
A.
Auxin
Nocodazole
M arrested cells
60 min
ChIP to assess Mcd1p and mcd1-Q266p binding to chromosomes in the presence or absence of Scc2-AIDp
B.
MCD1 SCC2-AID
No Auxin
+ Auxin (60 minutes)
% Mcd1 IP
Coordinates Chromosome III
Coordinates Chromosome XII
Chr I CEN
Chr XIV CEN
500bp
C.
mcd1-Q266 MCD1-AID SCC2-AID
% Mcd1 IP
Coordinates Chromosome III
Coordinates Chromosome XII
Chr I CEN
Chr XIV CEN
500bp

Figure 5.

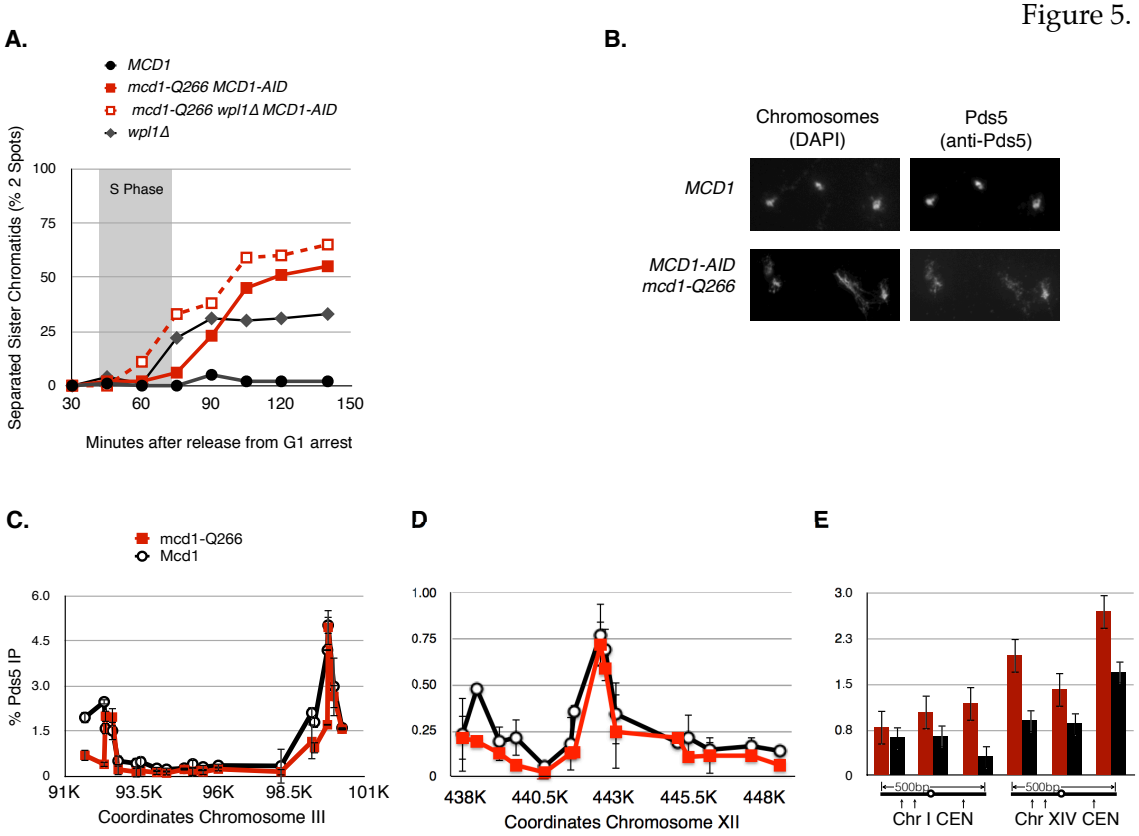
A.
MCD1
mcd1-Q266 MCD1-AID
mcd1-Q266 wpl1Δ MCD1-AID
wpl1Δ
Separated Sister Chromatids (% 2 Spots)
S Phase
Minutes after release from G1 arrest
B.
Chromosomes (DAPI)
Pds5 (anti-Pds5)
MCD1
MCD1-AID mcd1-Q266
C.
mcd1-Q266
Mcd1
% Pds5 IP
Coordinates Chromosome III
D
Coordinates Chromosome XII
E
Chr I CEN
Chr XIV CEN

Figure 6

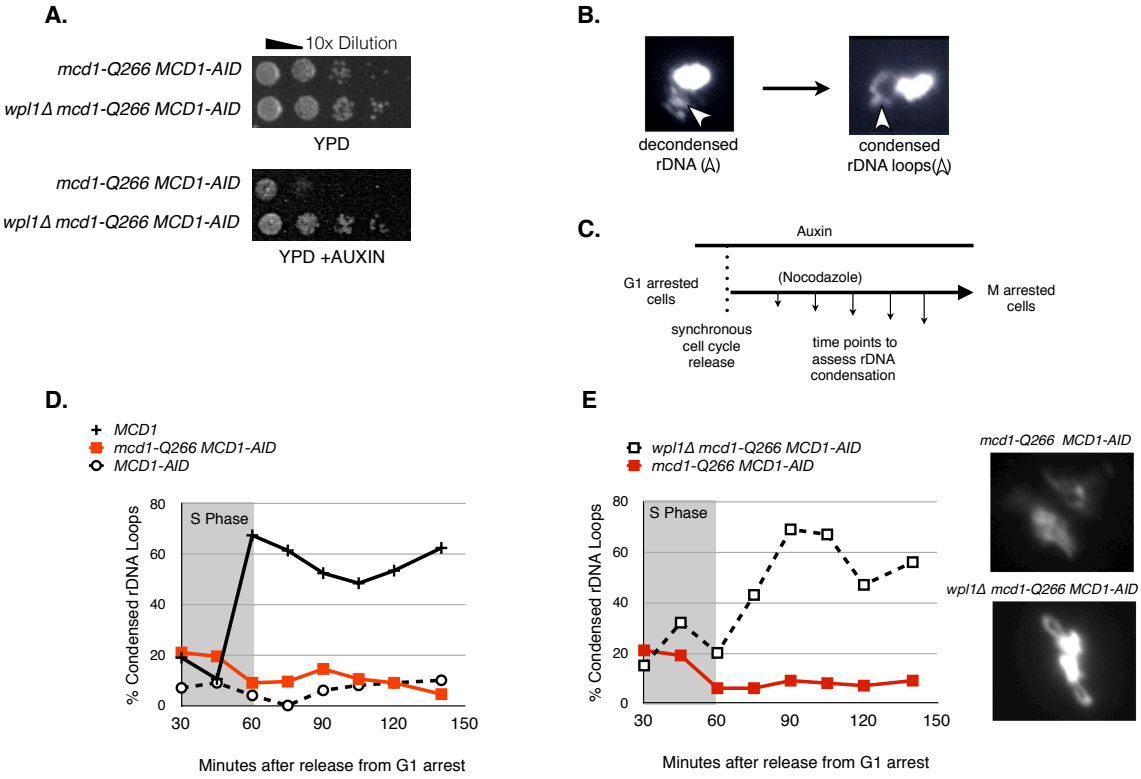
A.
10x Dilution
mcd1-Q266 MCD1-AID
wpl1Δ mcd1-Q266 MCD1-AID
YPD
mcd1-Q266 MCD1-AID
wpl1Δ mcd1-Q266 MCD1-AID
YPD +AUXIN
B.
decondensed rDNA (A)
condensed rDNA loops(A)
C.
Auxin
G1 arrested cells
(Nocodazole)
M arrested cells
synchronous cell cycle release
time points to assess rDNA condensation
D.
MCD1
mcd1-Q266 MCD1-AID
MCD1-AID
% Condensed rDNA Loops
S Phase
Minutes after release from G1 arrest
E
wpl1Δ mcd1-Q266 MCD1-AID
mcd1-Q266 MCD1-AID
% Condensed rDNA Loops
S Phase
Minutes after release from G1 arrest
mcd1-Q266 MCD1-AID
wpl1Δ mcd1-Q266 MCD1-AID

Figure 7.

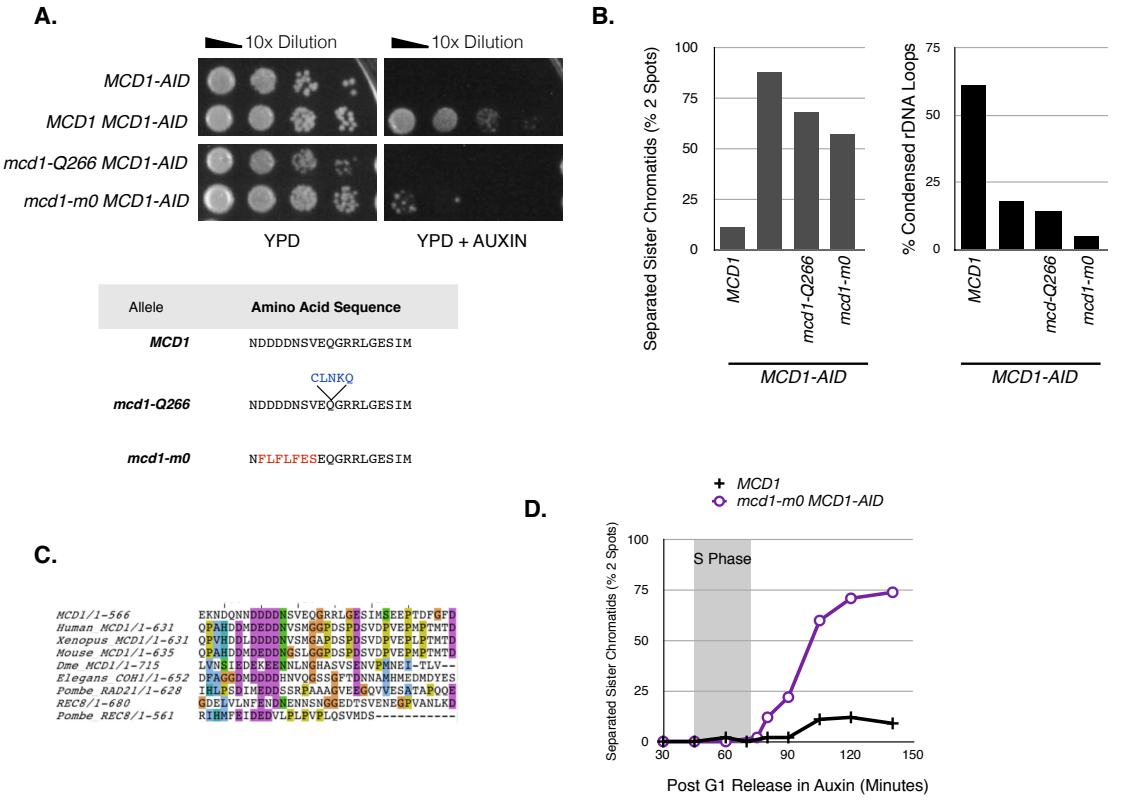
A.
10x Dilution
10x Dilution
MCD1-AID
MCD1 MCD1-AID
mcd1-Q266 MCD1-AID
mcd1-m0 MCD1-AID
YPD
YPD + AUXIN
Allele
Amino Acid Sequence
MCD1
NDDDDNSVEQGRRLGESIM
CLNKQ
mcd1-Q266
NDDDDNSVEQGRRLGESIM
mcd1-m0
NFLFLFESEQGRRLGESIM
B.
Separated Sister Chromatids (% 2 Spots)
100
75
50
25
0
MCD1
mcd1-Q266
mcd1-m0
MCD1-AID
% Condensed rDNA Loops
75
50
25
0
MCD1
mcd-Q266
mcd1-m0
MCD1-AID
C.
MCD1/1-566
Human MCD1/1-631
Xenopus MCD1/1-631
Mouse MCD1/1-635
Dme MCD1/1-715
Elegans COH1/1-652
Pombe RAD21/1-628
REC8/1-680
Pombe REC8/1-561
D.
MCD1
mcd1-m0 MCD1-AID
S Phase
Separated Sister Chromatids (% 2 Spots)
100
75
50
25
0
30
60
90
120
150
Post G1 Release in Auxin (Minutes)

Supplemental Figure 1.

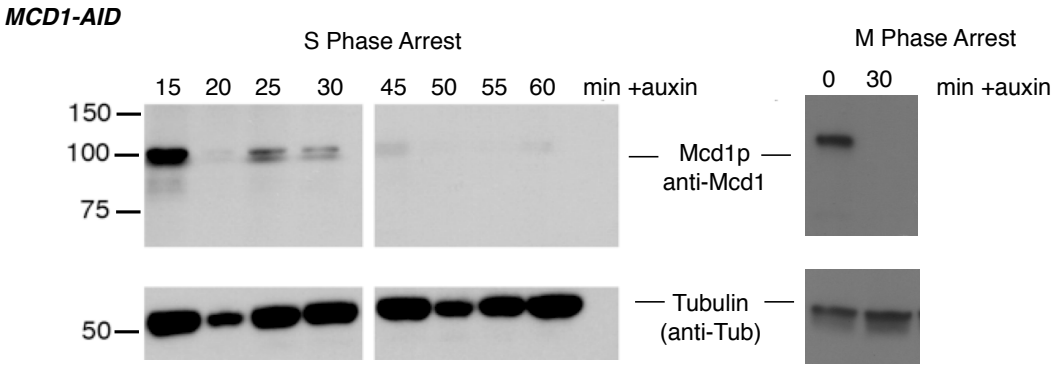

Supplemental Figure 2.

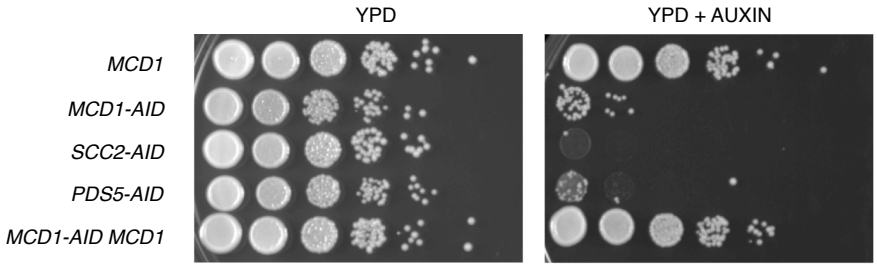

Supplemental Figure 3.

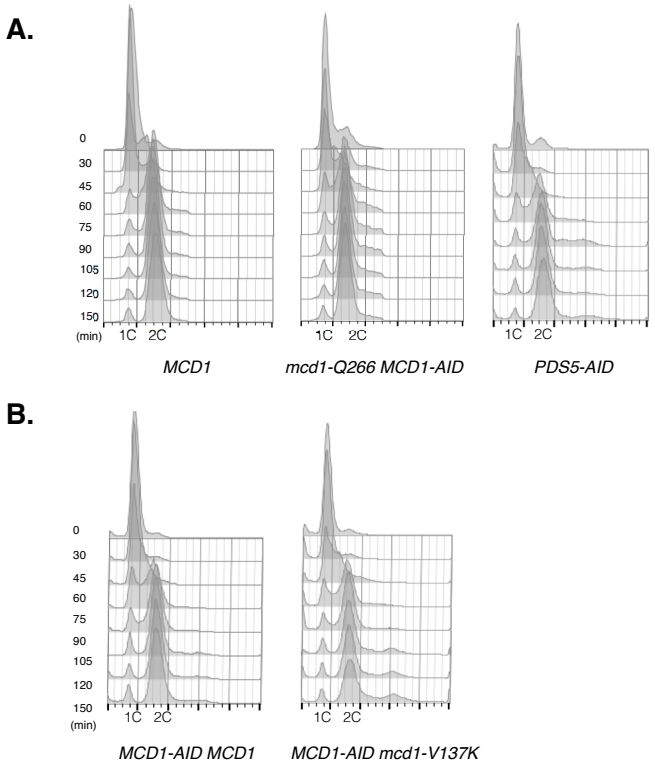

Supplemental Figure 4.

A.

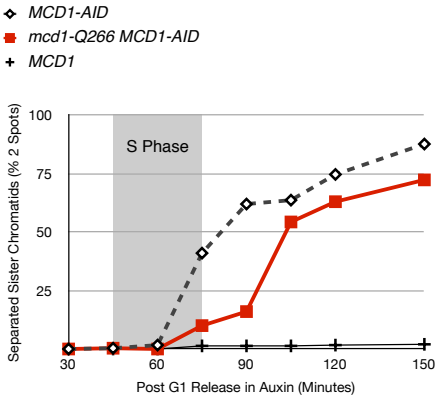

B.

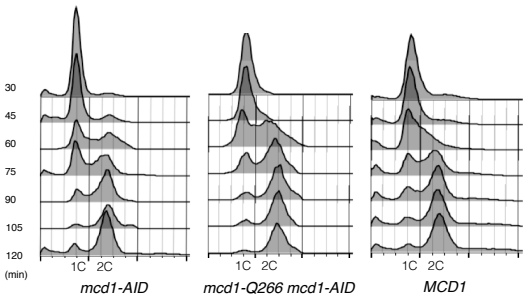

Supplemental Figure 5.

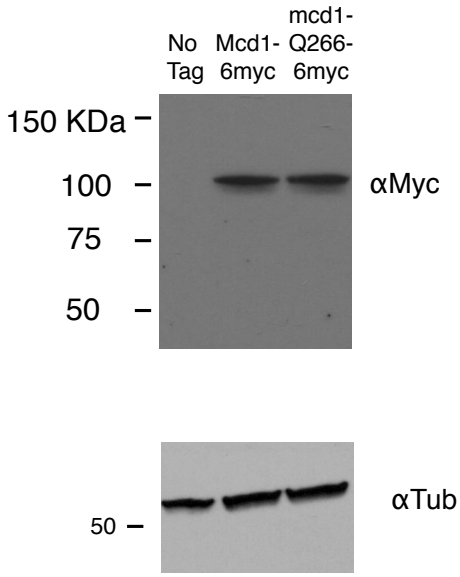

Supplemental Figure 6.

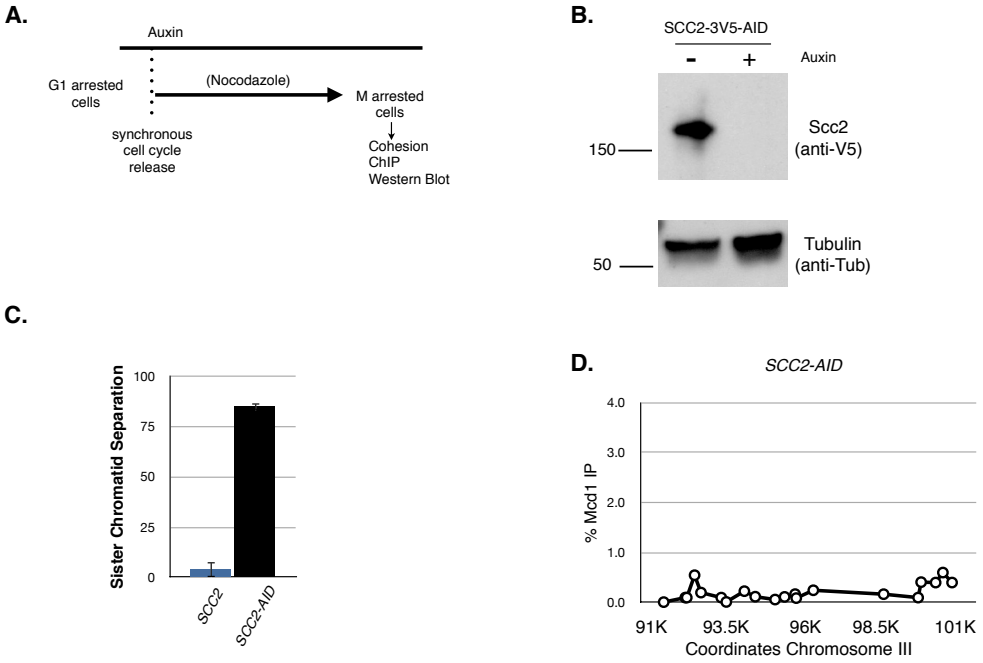

Supplemental Figure 7.

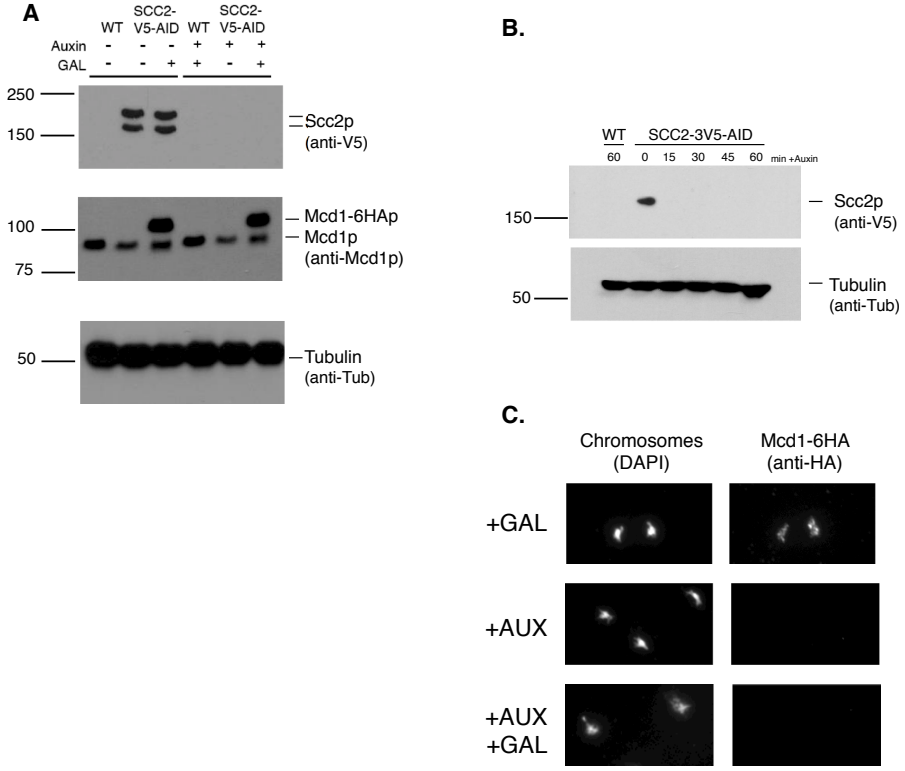

Supplemental Figure 8.

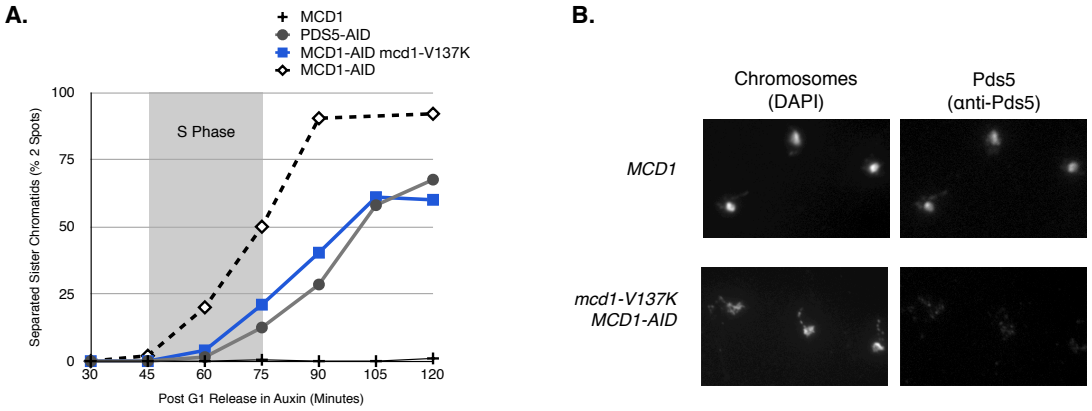

Supplemental Table 1

Position of Insertion	Sequence of Insertion	Strain Viability on GAL	
		23˚C	30˚C
L74	FKHEL	-	-
L75	LFKQL	- / +	-
Q76	VFKHQ	-	-
Q85	VFKQQA	-	-
L97	CLNTL	- / +	-
T133	VFKHTE	-	-
R135	VFKQRE	-	-
Q266	CLNKQ	-	- / +
R268	CLNRR	-	-
S525	CLNTS	- / +	-

CHAPTER 3: INTERALLELIC COMPLEMENTATION: FUNCTIONAL EVIDENCE FOR COHESIN-COHESIN INTERACTIONS ON DNA

Abstract

Cohesin has long been appreciated for its role in chromosome architecture, promoting sister chromatid cohesion, chromosome condensation, DNA repair, and transcriptional regulation. Despite its importance, the mechanism by which cohesin tethers the same (or different) DNA molecules remains unknown. In the absence of structural or biochemical information, the prevailing model for cohesin's tethering activity postulates that a single cohesin complex tethers DNA by the simple entrapment of both sister chromatids. Here, we report interallelic complementation for alleles of the Mcd1p or Smc3p subunit of the cohesin complex. On their own, these alleles in *mcd1* and *smc3* are unable to generate viability, sister chromatid cohesion or condensation. However, yeast cells carrying two alleles of either *mcd1* or *smc3* show robust restoration of growth, cohesion, and condensation. Interallelic complementation is a genetic signature which suggests that multiple cohesins can communicate to tether sister chromatids to mediate cohesion and condensation.

Introduction

The protein complex, cohesin, has long been appreciated for its essential role in mediating chromosome architecture (reviewed in Onn, 2008). Cohesin is composed of four core subunits: Smc1p, Smc3p, Mcd1p/Rad21p/Scc1p, and Scc3p (Losada *et al.*, 1998). This large protein complex physically links sister chromatids to generate cohesion (Guacci *et al.*, 1997; Michaelis *et al.*, 1997). This cohesion is critical for the migration of sister chromatids towards opposite poles, ensuring efficient and faithful chromosome segregation. Additional studies revealed this same complex also plays a role in generating chromosome condensation, regulation of gene expression, and DNA repair (Donze *et al.*, 1999; Rollins *et al.*, 1999; Sjögren and Nasmyth, 2001; Unal *et al.*, 2004; Yeh *et al.*, 2008; Stephens *et al.*, 2013). Despite its importance in chromosome architecture, the mechanism by which cohesin tethers regions of the same (or different) DNA molecules remains an enigma.

The simplest model for chromosome tethering by cohesin is the "embrace" model, which is based upon the ring-like structure of cohesin that can be visualized in electron micrographs as well as a number of biochemical and genetic analyses (Melby *et al.*, 1998; Huis In 't Veld *et al.*, 2014). A single cohesin ring would entrap two DNA molecules or two regions of the same molecules thereby tethering them together. For example, during DNA replication the entrapment of sister chromatids by a cohesin ring generates sister chromatid cohesion (Uhlmann and Nasmyth, 1998). .Alternative models suggest that a cohesin ring is insufficient for tethering. Rather, cohesin-cohesin interactions are required in order for cohesin to tether sister chromatids, for example the dimerization of two cohesins each independently bound to a DNA molecule. The definitive way to distinguish between these two models would be to visualize the

structure of cohesin as it tethers DNA, such as with high resolution electron microscopy. Unfortunately structural approaches have not yet been successful.

A simple biochemical assay to assess the interaction between two cohesins is the coimmunoprecipitation of differentially tagged copies of the same cohesin subunit, such as Smc1-HA and Smc1-MYC, when they are coexpressed in the same cell. While such an experiment has been attempted in budding yeast as well as other species, only one group has reported detecting such an interaction (Haering *et al.*, 2004; Zhang and Pati, 2009). These studies are based upon the analysis of solubilized cohesin in cell lysates but cohesin-cohesin interactions could be restricted to cohesin bound to DNA. While it is possible to solubilize chromatin by shearing, any coimmunoprecipitation of differentially marked cohesins in the presence of DNA is difficult to interpret. Coimmunoprecipitation could result from a direct interaction between cohesin subunits, or an indirect interaction from cohesin subunits bound independently to the same strand of DNA.

A classic genetic signature of protein-protein interaction is interallelic complementation, such as described for glutamate dehydrogenase, beta-galactosidase, ATP-PRTase/His1, or assembly of the Rad52 heptameric ring (PERRIN, 1963; CODDINGTON and FINCHAM, 1965; Korch and Snow, 1973; Boundy-Mills and Livingston, 1993). In these examples the products of two mutant alleles in the same gene are defective for function when expressed individually in cells. However when they are co-expressed in the same cell, they physically interact. The physical interaction restores function. In this report, we describe the existence interallelic complementation for alleles of the Mcd1p or Smc3p subunit of the cohesin complex. On their own, these alleles in *mcd1* and *smc3* are unable to generate viability, sister chromatid cohesion or condensation. However, yeast cells carrying two alleles of either *mcd1* or *smc3* show robust restoration of growth, cohesion, and condensation. These results suggest that cohesins communicate to perform their functions. Furthermore, in both cases, the presence of the product of one allele changes the physical properties of the product of the second allele, consistent with a mechanism of communication involving direct physical interaction.

Results

Identification of Interallelic Complementation Pairs in Recessive Cohesin Alleles

The *mcd1-Q266* allele of the cohesin's regulatory subunit, Mcd1p contains an in-frame, five amino acid insertion immediately following residue Q266 (described in Eng 2014). This allele does not support viability when present as the sole copy of this gene in yeast (Figure 1A and Eng et al. 2014). To study the impact of this lethal allele on cohesion and condensation, we previously introduced this allele into a strain harboring the *MCD1-*

AID allele. Proteins fused to AID (auxin induced degron) undergo ubiquitin dependent degradation in the presence of the plant hormone auxin. When *mcd1-Q266 MCD1-AID* strain was treated with auxin, the Mcd1-AIDp was degraded revealing the phenotype of cells harboring just mcd1-Q266p. These cells were inviable as expected and defective in the maintenance of cohesion and the establishment of condensation (Eng *et al.*, 2014).

An alternative and common strategy to study lethal alleles of cohesin subunits like *mcd1-Q266* has been to study them in the background of conditional temperature sensitive alleles. Indeed for *MCD1*, we and others have used *mcd1-1,* a well characterized temperature-sensitive allele of *MCD1,* which contains a serine to asparagine point mutation at residue 525 (termed *mcd1-1*) (Guacci *et al.*, 1997). Few if any cells in a *mcd1-1* culture grew at the non-permissive temperature (Figure 1A, Guacci et al 1997). To our surprise, the *mcd1-1 mcd1-Q266* double mutant, containing *mcd1-1* at the endogenous locus and *mcd1-Q266* on a centromere plasmid, was viable at the non-permissive temperature (Figure 1A). The fact that full viability was restored argued either for robust interallelic complementation between the *mcd1* alleles or conversion of one of the two alleles to wild type. We amplified the sequences of *mcd1* from the double mutant and confirmed the presence of both *mcd1-1* and *mcd1-Q266*. We had also built *mcd1-1 mcd1-Q266* strains where *mcd1-Q266* was integrated at the *URA3* locus, and again observed robust growth at the non-permissive temperature. This double mutant was treated with 5-FOA to select for cells that had lost *mcd1-Q266* integrated at the URA3 locus. The 5-FOA resistant cells were temperature sensitive, supporting the conclusion that the double mutant still had the *mcd1-1* allele, and establishing linkage of suppression of *mcd1-1* temperature sensitivity to the presence of *mcd1-Q266*. We also demonstrated allele specificity for this complementation having observed that the lethal alleles *mcd1-V137K* or *mcd1-R135* failed to grow in a *mcd1-1* background at the non-permissive temperature (Supplemental Figure 1A). Thus, the restoration of viability observed when cell contains both *mcd1-1 and mcd1-Q266* alleles in the *trans* configuration is due to interallelic complementation.

Two other examples of interallelic complementation came through our study of the lethal *smc3-K113R* allele. This allele alters a key residue in Smc3p whose acetylation is required for the establishment of cohesion (Rolef Ben-Shahar *et al.*, 2008; Unal *et al.*, 2008; Zhang *et al.*, 2008). To assess the effect of this allele on viability, we integrated it at the *LEU2* locus in a strain with the temperature sensitive *smc3-42* allele as had been done previously. However, we chose a lower non-permissive temperature of 34˚C. The *smc3-K113R smc3*-42 double mutant grew at 34˚C (Figure 1B) while neither the *smc3-K113R* or *smc3*-42 allele were able to support viability as sole source at 34˚C (Figure 1B). Through sequencing we demonstrated that both alleles were present in the double mutant indicating that neither allele had converted to wild-type. The complementation between *smc3-K113R* and *smc3-42* provided our second example of interallelic

complementation, and expanded this phenomenon to a second subunit of cohesin.

The interallelic complementation of *smc3-42* and *smc3-K113R* impeded our ability to assess any potential cohesion and condensation defects of smc3-K113Rp. To circumvent this technical difficulty, we integrated *smc3-K113R* at the *URA3* locus in the background of a different conditional allelle, *SMC3-AID^{608}* at the endogenous locus. As we previously described, *smc3-AID^{608}* encodes an Smc3 protein with an internal auxin degron cassette immediately following residue N607 (Guacci *et al.*, 2015). Strains expressing only Smc3-AID^{608}p were inviable in the presence of auxin at 23˚, 30˚ and 34˚C (Figure 1C, Supplemental Figure 2, and Guacci 2015). As expected, the *smc3-K113R SMC3-AID^{608}* strain failed to grow in the presence of auxin at 30˚C or 34˚C (Supplemental Figure 1 and data not shown). Thus at these two temperatures these two alleles did not complement each other. However to our surprise at 23˚C, this double mutant grew even in the presence of auxin almost as well as a wild-type *SMC3* strain (Figure 1C). Sequencing demonstrated the presence of both alleles in the double mutant. In addition, we treated the double mutant with 5-FOA to select for cells that had lost the *smc3-K113R* integrated at the URA3 locus. The 5-FOA resistant cells were auxin sensitive, confirming linkage of suppression of auxin sensitivity of *SMC3-AID^{608}* by *smc3-K113R.* Thus *smc3-K113R* complements the temperature-sensitivity of *smc3-42* and the auxin sensitivity of *SMC3-AID^{608}*. To demonstrate allelic specificity, we observed that the double acetyl-null allele smc3-K112/3-RR failed to complement *SMC3-AID^{608}* on auxin plates (Supplemental Figure 1B). Due to the interallelic complementation observed in *SMC3-AID^{608} smc3-K113R* strains, at, 23˚C, we lack the tools to determine whether Smc3-K113Rp is defective for cohesion or condensation at, 23˚C.

This final example of interallelic complementation was notable for two reasons. The amino acid changes encoded by *mcd1-1*, *mcd1-Q266, smc3-42* and *smc3-K113R* alleles all cluster near cohesin's head domain (Figure 1, diagram). The auxin cassette, by virtue of its position in Smc3p's coiled coil proximal to the hinge domain, is predicted to be very distal to the head domain (Figure 1, diagram). Thus interallelic complementation between *smc3-42* and *SMC3-AID^{608}* indicated that interallelic complementation could occur between alleles of *SMC3* that modulated different domains of cohesin.

Interallelic complementation likely occurs by providing distinct activities of cohesin

We could envision two mechanisms for interallelic complementation. One possibility was that the product of each mutant allele provided an activity that the other was missing. Alternatively one (or both) of the two mutant alleles allowed assembly of a complex that was functional, but its level of function was suboptimal, below a minimum needed for

viability. The presence of the second mutant allele would act by merely elevating the activity of the first allele, for example by providing more of that activity or titrating away an inhibitor.

If any of the alleles capable of interallelic complementation simply reduced cohesin activity below some critical level, then overexpression of the allele might restore cohesin function and viability. To test this possibility, we replaced the normal promoter of each mutant allele with the *GAL1* promoter. We then tested the ability of these mutant alleles when overexpressed to support viability as a sole source using the plasmid shuffle strategy. As expected, expression of *MCD1* or *SMC3* under the *GAL1* promoter was sufficient for viability as a sole source (Figure 2, top row of each panel). In contrast, *GAL1* mediated over-expression of *mcd1-1*, *mcd1-Q266*, *smc3-K113R*, or *smc3-42* was unable to support viability in the absence of wild-type at 34˚C or 37˚C, respectively (Figure 2, second and third rows of each panel). We confirmed that mcd1-1 protein levels increased as a result of galactose induced over expression (Supplemental Figure 3A). As there were no epitope tags on Smc3-K113Rp or smc3-42p, we indirectly measured over-expression by quantifying the amount of *SMC3, smc3-K113R*, and *smc3-42* mRNA before and after galactose induction (Supplemental Figure 3B). The average expression from three primer sets near the 5' end of *SMC3* was roughly 60 fold above pre-induction, consistent with activation of the *GAL1* promoter of the *GAL1-SMC3* construct. Our results strongly indicated that simply providing more of the product of any single allele (*smc3-42, smc3-K113R, mcd1-1,* or *mcd1-Q266)* and its associated activity were insufficient for viability. Furthermore we observed that the same *mcd1* alleles placed in the *cis* configuration, that is within the same gene, failed to support viability, even when over-expressed (Supplemental Figure 4). Thus the restoration of viability mediated by interallelic complementation likely occurred by each mutant allele providing a distinct function of Mcd1p that was missing in its partner.

The allele pairs of mcd1 and smc3 complement their defects in condensation

In budding yeast cohesin is critical for viability, sister chromatid cohesion and chromosome condensation. We asked whether the interallelic complementation we observed between pairs of alleles in *MCD1* or *SMC3* for viability reflected complementation of defects in cohesion, condensation or both. We recently showed that suppressors of lethal alleles of *SMC3* or *ECO1* (the cohesin acetyltransferase) restored condensation but little if any cohesion (Guacci and Koshland, 2012). This result indicates that condensation rather than cohesion is the major essential function of cohesin in budding yeast (Guacci and Koshland, 2012). This less stringent requirement for cohesion compared to other eukaryotes is made possible in budding yeast because of its unusual initiation of spindle assembly during S phase (Guacci and Koshland, 2012; Guacci *et al.*, 2015). This link between cohesin's condensation function and

viability led to two predictions. First, the inviability of each of the single alleles in this study likely reflected a defect in condensation. Second the viability of strains harboring pairs of lethal alleles in *MCD1* or *SMC3* likely reflected their ability to complement each other's defect in condensation.

To test directly these two predictions, we assayed condensation in cultures that had progressed from G1 to M, expressing only the product of each single allele or each pair of alleles. We generated these cultures by arresting them in G1 and then shifting them to conditions non-permissive for both single alleles. We then released the cultures from G1 arrest under these non-permissive conditions in the presence of nocodazole. These cultures proceeded through the cell cycle and then arrested in M phase. Chromosome spreads of these M-arrested cells were prepared to examine the morphology of the rDNA locus, a well-established metric for condensation in budding yeast (Guacci *et al.*, 1997; Lavoie *et al.*, 2004). Proper M phase condensation results in formation of rDNA loops (Figure 3A).

All mutant strains expressing only the single alleles showed a dramatic reduction in rDNA loops compared to wild-type. Thus, all single alleles caused a dramatic condensation defect as expected given their inviability (Figure 3B and 3C). In contrast all mutant strains that expressed a pair of alleles exhibiting interallelic complementation for viability, formed rDNA loops at levels indistinguishable from wild-type (Figure 3B and 3C). Thus as expected the viability of pairs of lethal alleles in *mcd1* or *smc3* reflected interallelic complementation of their shared condensation defect.

The allele pairs of mcd1 and smc3 complement their defects in cohesion establishment and maintenance respectively

We next asked whether the pairs of alleles that could complement their defects in viability and condensation could also complement their defects in cohesion. We used the same culturing conditions as described for assaying condensation. This regimen generated cells that had progressed from G1 to M, expressing only the product of each single allele or each pair of alleles. Cohesion in these M-arrested cells was assayed at a centromere-proximal locus (*TRP1*) as well as a chromosomal arm locus (*LYS4*) by the LacO / LacI-GFP system developed by Straight and Murray (Straight *et al.*, 1996). A severe cohesion defect was observed in cells expressing each of the single alleles. In contrast, mutants expressing each pair of alleles, the level of cohesion on the arm and near the centromere was very similar to wild type (Figure 4A and B). Thus, the pairs of lethal alleles in *mcd1* or *smc3* exhibited interallelic complementation for defects in cohesion as well as viability and condensation.

Knowledge of the cohesion defect in each of the single mutants provided additional insights into their interallelic complementation. Mutations in cohesin subunits or regulators can lead to defects in the establishment or maintenance of cohesion. The *mcd1-1* allele was known to cause a defect in cohesion establishment and maintenance while *mcd1-Q266* was known to be defective only in the maintenance of cohesion (Eng *et al.*, 2014). Thus the robust cohesion in the *mcd1-1 mcd1*-Q266 strain indicated that mcd1-1p and mcd1-Q266p minimally must have complemented their shared defect in cohesion maintenance. Our temporal analysis of cohesion in *smc3-42* and *smc3-K113R smc3-AID*^{608} strains at temperatures 30˚C and above revealed that they had defects in the establishment of cohesion (Supplemental Figure 5). Therefore the cohesion in the *smc3-42 smc3-K113R* strain indicated that smc3-42p and smc3-K113Rp must have complemented their defects in cohesion establishment. Thus interallelic complementation can lead to the restoration of cohesion establishment and maintenance as well as condensation and viability.

mcd1-1p is stabilized by the presence of its interallelic complementing partner, mcd1-Q266p

To address the molecular basis underlying these three examples of interallelic complementation, we asked whether the known molecular defects caused by each single allele was altered in cells that expressed both alleles. A molecular defect of the mcd1-1p at 37˚C is its degradation. We asked whether the stability of mcd1-1p changed in the presence of its complementing allelic partner, mcd1-Q266p. We treated cultures of *mcd1-1* and *mcd1-1 mcd1-Q266-6MYC* strains with nocodazole to arrest them in M phase. Each culture was then split in half, and one culture from each strain was incubated at 23˚C or 37˚C for an additional hour. We then harvested the cultures and assessed the amount of mcd1-1p by western blot analysis using a polyclonal antibody for Mcd1p. As expected, in an *mcd1-1* strain, mcd1-1p levels were reduced dramatically when grown at 37˚C compared to 23 C (Figure 5A). In the presence of mcd1-Q266-6MYCp, mcd1-1p levels remained high in cells grown at 37˚C (Figure 5A). To determine that the faster mobility species detected by our Mcd1p antibody was not a degradation product of mcd1-Q266-6MYC, we generated mcd1-1-3FLAGp, where three copies of the FLAG epitope were placed in the linker region of mcd1-1p. We could now discriminate between mcd1-1-3FLAGp and mcd1-Q266-6MYCp using antibodies specific for either epitope. Using the epitope specific antibody for mcd1-1-3FLAGp, we observed that mcd1-1-3FLAGp was degraded at 37˚C in *mcd1-1-3FLAG* strains, but mcd1-1-3FLAGp was stabilized at 37˚C in *mcd1-1-3FLAG mcd1-Q266-6MYC* strains (Figure 5B). Similar stabilization of mcd1-1p was observed in both S phase and M phase when cells were alternatively blocked with hydroxyurea instead of nocodazole (Figure 5B). The increased levels of mcd1-1p in the mcd1-1 mcd1Q266 strain likely was necessary to allow mcd1-1p and mcd1-266p to complement each others for their missing molecular function(s). However, this increase in the amount of mcd1-1p was not

likely sufficient to explain their ability to complement, as the elevated levels of mcd1-1p by its overexpression did not restore cohesin function as assayed by viability (Figure 2).

The chromosome binding defects of mcd1-1p and smc3-AIDp are suppressed by their interallelic complementing partners, mcd1-Q266p and smc3-K113Rp respectively.

Previous studies have shown that mcd1-1p and smc3-42p failed to bind chromosomes at the non-permissive temperature while their interallelic partners mcd1-Q266p and smc3-K113Rp bound to chromosomes and to CARs similar to wild-type. We asked whether the binding of these mutant cohesin subunits to chromosomes was restored by the presence of their interallelic complementing partners. For this purpose we generated four strains with the following four genotypes, *mcd1-1-3FLAG, mcd1-1-3FLAG mcd1-Q266-6MYC, smc3-42-6HA,* and *smc3-42-6HA smc3-K113R*. These strains were arrested in mitosis at the respective elevated temperature and then processed for chromosome spreads to assess global cohesin binding to chromosomes and chromatin immunoprecipitation to assess cohesin binding to four cohesin associated regions on chromosomes I, III, XII and XIV (Materials and methods, Eng et al 2014). As expected, no significant chromosome staining of mcd1-1 3FLAGp or smc3-42-6HAp was observed in *mcd1-1-3FLAG* or *smc3-42-6HA* cells (Supplemental Figure 6). Global chromosomal staining of mcd1-1-3FLAGp and smc3-42-6HAp was observed above background in the *mcd1-1-3FLAG mcd1-Q266-6MYC* and *smc3-42-6HA smc3-K113R* strains albeit this staining was weak in the latter case (Supplemental Figure 6). These results indicated that the presence of the interallelic partner partly complemented the global chromosomal binding defect of mcd1-1-3FLAGp and smc3-42-6HAp.

Our ChIP analysis of mcd1-1p and smc3-42p allowed us to examine this altered binding at higher resolution. Consistent with our observations by chromosome spreads, ChIP analysis of smc3-42-6HAp and mcd1-1-3FLAGp failed to show their enrichment at any of the four cohesin associated regions in *mcd1-1-3FLAG* or *smc3-42-3HA* stains (Figure 6). In the *mcd1-1-3FLAG mcd1-Q266-6MYC* strain, mcd1-1-3FLAGp as was mcd1-Q266-6MYCp were enriched significantly above background at all four regions (Figure 6 A and B, Supplemental Figure 7). Similarly, in the *smc3-42-6HA smc3-K113R* strain, smc3-42-6HAp was enriched significantly above background at all four regions (Figure 6 A and B). Thus, the chromosome binding defect of mcd1-1-3FLAGp and smc3-42-6HAp was dramatically improved by the presence of their interallelic complementing partner, mcd1-Q266p and smc3-K113Rp, respectively. The suppression of the binding defect by the interallelic complementing partners did not restore cohesin binding to wild-type levels (Figure 6). Notably the binding of smc3-42-6HAp was weaker in the presence of its partner than was observed for mcd1-1-3FLAGp with its partner. This weaker binding correlated with our observation that the cohesion in the *smc3-42 smc3-K113R* strain was less robust than the *mcd1-1 mcd1-Q266* strain (Figure 4 and Supplemental Figure

5A). Nonetheless the binding of mcd1-1-3FLAG promoted by the presence of the interallelic complementing partner was more robust at cohesin enriched regions detected by ChIP than globally detected by chromosome spreads.

Discussion.

In this report, we describe interallelic complementation between alleles of the Mcd1p or Smc3p subunit of cohesin. Strains expressing only individual alleles in mcd1 and smc3 are unable to generate viability, sister chromatid cohesion or condensation. However, yeast cells carrying pairs of either mcd1 or smc3 alleles show robust growth to near wild-type levels. In addition cohesin's two chromosome segregation functions, cohesion and condensation, are restored. This interallelic complementation is not a property of a small increase in activity of one of the two mutant allele products since overexpression of any of the individual mutant products did not restore cohesin function as assayed by viability. Furthermore, only certain pairs of alleles are capable of interallelic complementation. Together these two observations indicate that interallelic complementation occurs because the individual alleles cause defects in distinct molecular functions of the mutated subunit. We and others likely failed to observed interallelic complementation previously because most alleles have more a generic impact, abrogating all functions of the subunit. The notion that an individual subunit of cohesin could have multiple functions is not surprising given the known complex architecture in which each subunit interacts with multiple other subunits and the complex enzymatic functions of the SMC ATPases.

The molecular interpretation of our three examples of interallelic complementation is constrained significantly by the known stoichiometry of the cohesin complex. It is well established that each cohesin contains only one copy of each of the subunits (Losada *et al.*, 1998; Tóth *et al.*, 1999; Sumara *et al.*, 2000; Ding *et al.*, 2006; Holzmann *et al.*, 2011). Given this stoichiometry, the interallelic complementation we observe must result from interplay of two defective cohesin molecules, each harboring one of the mutant allele products.

This inter-complex complementation could occur by the two different mutant cohesins acting independently at distinct sites to provide a biological function missing by the other. For example one mutant cohesin could bind at chromosomal sites to promote cohesion but not condensation while the other mutant cohesin could bind at distinct sites to promote condensation but not cohesion; when expressed together they provide both activities. However, the alleles described here are defective for both cohesion and condensation. Thus the inter-complex complementation appears to reflect the restoration of a core cohesin activity needed for both of these biological functions. A second model for inter-complex complementation could be that one mutant complex

might indirectly activate the other complex by removing some barrier to cohesin function. For example, we show that the chromosome binding defect of cohesins with smc3-42p and mcd1-1p are suppressed by the presence of smc3-K113Rp and mcd1-Q266p respectively. Cohesins with smc3-K113Rp and mcd1-Q266p might titrate away Wpl1p, the inhibitor of cohesin binding to chromosomes. However, deletion of WPL1 does not phenocopy smc3-113Rp expression as it fails to suppress the inviability and cohesion defect of smc3-42 (this study and (Heidinger-Pauli *et al.*, 2008)). We also observe that the instability of smc3-42p and mcd1-1p are suppressed by the presence of smc3-K113Rp and mcd1-Q266 respectively. The smc3-K113Rp and mcd1-Q266p might titrate away some factor important for some cohesin specific degradation system. However the remarkable suppression of the artificially induced degradation of Smc3-AIDp by smc3-K113R makes this hypothesis also unlikely.

We prefer a model in which the inter-complex complementation is a manifestation of a direct interaction between cohesins on chromosomes that is important for their normal function in cohesion and condensation. We suggest that smc3-42p and mcd1-1p undergo transient non-productive binding to chromosomes because cohesins with these mutant subunits are unstable. In the case of mcd1-1p, the instability of the complex leads to mcd1-1p degradation. In cells expressing the interallelic complementing partner, the interaction between the smc3-42p and mcd1-1p cohesins with their chromosome bound partners stabilizes the t.s. proteins, thereby stabilizing their chromosomal binding. The stably bound mcd1-1 and smc3-42p cohesins can now help mediate cohesion and condensation. The suppression of the temperature sensitivity of ts proteins through their assembly into larger complexes has many precedents such as temperature sensitive virion proteins which became refractive to temperature inactivation after assembly into the virion (Gordon and King, 1994).

Proposing a model for the inter-cohesin interaction is constrained by our recently published observation that cohesin can remain stably bound to chromosomes without mediating cohesion. This separation of the chromosome binding and tethering activity of cohesin strongly suggests that cohesin's tethering activity must occur by two independent DNA binding activities, contributed by two cohesins (cohesin handcuff) or within one cohesin molecule (modified embrace) (Figure 7). With this constraint in mind, the inter-cohesin interaction could happen between cohesins each bound to different sister chromatids thereby forming the handcuff. In this case the interaction is essential for cohesin's tethering activity. Alternatively, the inter-cohesin interaction could occur between cohesins each with the capacity to tether sister chromatids, thus forming an oligomer akin to a slinky. In the slinky model, the interaction stabilizes the inherent tethered form of an individual cohesin.

The failure to observe any physical interaction between soluble cohesins is consistent with the idea that the physical interactions inferred from this study must happen on

chromosomes. Interestingly, when cohesin is subjected to a crosslinking reagent in vivo, a number of crosslinks between different regions of Smc3p or Smc1p were observed. While these crosslinks could represent intramolecular interactions within a subunit, they may, in light of our experiments, represent interactions between two Smc3ps or Smc1ps present in distinct but interacting cohesins. It would be interesting to compare the pattern of crosslinks observed with purified soluble cohesin monomers and cohesin bound to chromosomes.

While the exact molecular basis for cohesin-cohesin interactions revealed in this study remained to be elucidated, their discovery reflects a major molecular component of cohesin function that has escaped previous studies. Their study is likely to provide important new insights into cohesin molecular and biological functions. We strongly suspect that interactions between condensins or other Smc complexes are likely to be important for their function as well. It will be interesting to examine alleles of subunits in these other Smc complexes for their ability to exhibit interallelic complementation.

Methods.

Yeast strains, media, and reagents.

Yeast strains used in this study are the A346a background, and their genotypes are listed in the strain table. Synthetic dropout and YPD media were prepared as previously described (Guacci *et al.*, 1997). For experiments using the AID system, a 1M stock of 3-indoleacetic acid (Sigma-Aldrich, St. Louis, MO) was made in DMSO and added to plates or liquid cultures at a final concentration of 500µM, cooling agar used in plates to ~55˚C before adding auxin to each batch. The pH of our YEPA+DEX media is approximately 6.95.
Dilution Plating Assays.

Cells were grown to saturation in YPD media at 23°C (or 30°C when listed), diluted to OD_{660} 1.0 using YPD, and then plated in 10-fold serial dilutions. Cells were incubated on plates at relevant temperatures as described.

Shuffle strain construction.

Haploids containing plasmid pEU42 (*SMC3 URA3 CEN*) had their endogenous *SMC3* gene deleted and replaced by the HPH cassette (encodes resistance to Hygromycin B) using standard PCR mediated homology-based recombination. Alternatively, Haploids containing plasmid *pVG210* (*MCD1 URA3 CEN*) had their endogenous *MCD1* gene deleted and replaced by the *KanMx6* cassette. Constructs expressing *SMC3* or *MCD1* under the respective endogenous promoter (or if indicated in the figure legend, the

GAL1 promoter) were then transformed into strains either on centromere *TRP1* plasmids or integrated at the genomic *LEU2* locus. Clones were grown to saturation in YPD media at 23°C to allow loss of plasmid pEU42, then plated in 10- fold serial dilutions on media containing 5-fluoroorotic acid (5-FOA). 5-FOA selectively kills URA+ cells, thereby selecting for loss of pEU42 or pVG210, which allows assessment of test allele ability to support viability as the sole *SMC3* or *MCD1* in cells. As a control, cells were also plated on either YPD or URA- media.

Cohesion Assays.

To monitor cohesion from G1 to M, haploid yeast cells were initially grown to mid log phase at 23°C in YPD culture. Cells were staged to G1 by addition α factor (Sigma-Aldrich) to 10^{-8}M final conc. and incubation for 3hr. Cells were examined by light microscopy to confirm the presence of the schmoo morphology in 95% of the cells, at which point auxin was added (500μM final) to induced degradation of AID tagged proteins and cells incubated 1h more. Cells were released from G1 arrest by washing six times in YPD containing auxin and 0.1 mg/ml Pronase E (Sigma-Aldrich), then resuspended in fresh YPD containing auxin and nocodazole (Sigma-Aldrich) at 15 μg/ml final and incubated at 23˚C to allow cell-cycle progression until arrest in mid-M phase. To monitor cohesion and cell cycle progression and cohesion, cell aliquots were fixed every 15 minutes for DNA content by FACS and for cohesion via the LacI-GFP cohesion assay.
To monitor cohesion in M phase arrested cells, haploid yeast cells were grown at 23˚C to mid-log phase, and then nocodazole (15μg/ml) was added and cells incubate 3h at 23°C to arrest at mid-M phase. Arrests were confirmed by light microscopy for the classical large budded cellular phenotype (~95% of the population). Auxin (500μM final) was added to cultures and cells were incubated at 23°C. Aliquots were fixed and processed at timepoints indicated after auxin addition to assess cohesion via the GFP-LacI system.
Microscopy

Images were acquired with an Axioplan2 microscope (100× objective, numerical aperture 1.40; Zeiss Thornwood, NY) equipped with a Quantix charge-coupled device camera (Photometrics, Tucson, AZ).

Chromosome spreads and microscopy

Chromosome spreads were performed as previously described (Wahba *et al.*, 2013). Slides were incubated with a mouse anti-FLAG monoclonal (Sigma) at 1:2,000, mouse anti-V5 (Life Technologies) at 1:2,000, or polyclonal rabbit anti-Mcd1 at 1:2,000 dilutions. The primary antibody was diluted in blocking buffer (5% BSA, 0.2% milk, 1× PBS, 0.2% Triton X-100). The secondary Cy3-conjugated goat anti-mouse antibody (No.

115-165-003) was obtained from Jackson ImmunoResearch (West Grove, PA) and diluted 1:2000 in blocking buffer. Indirect immunofluorescence (IF) was observed using an Olympus IX-70 microscope with a 100×/NA 1.4 objective, and Orca II camera (Hamamatsu, Bridgewater, NJ).

Chromatin immunoprecipitation (ChIP)

Cells used for ChIP experiments were processed in the same manner as cells examined for cohesion assays as described in (Wahba *et al.*, 2013). Briefly, after synchronous release from G1 into mitotic arrest, $5x10^8$ large-budded cells were fixed for two hours with 1% formaldehyde. After cell lysis, chromatin was sheared 20 times for 45 s each (settings at duty cycle: 20%, intensity: 10, cycles/burst: 200; 30s of rest between cycles) using a Covaris S2. Immunoprecipitation of epitope tagged proteins were isolated using anti-FLAG (Sigma, St. Louis, MO), anti-HA (12CA5, Roche Life Sciences, USA), or anti-MYC (9E10, Roche Life Sciences, USA) monoclonal antibodies. Mcd1p was alternatively immunoprecipitated with a polyclonal rabbit anti-Mcd1 antibody (Covance Biosciences, NY). A no primary antibody control was also run to ensure specificity. Appropriate dilutions of input and immunoprecipitated DNA samples were used for PCR analysis to ensure linearity of the PCR signal. PCR and data analysis was carried out as described previously (Wahba *et al.*, 2013). All experiments were done at least twice and a representative data set is shown. ChIP primers are available upon request.

Flow Cytometry

Flow cytometry was conducted as described previously (Eng 2014, Guacci 2015).

References.

Boundy-Mills, K. L., and Livingston, D. M. (1993). A Saccharomyces cerevisiae RAD52 allele expressing a C-terminal truncation protein: activities and intragenic complementation of missense mutations. Genetics *133*, 39–49.

CODDINGTON, A., and FINCHAM, J. R. (1965). PROOF OF HYBRID ENZYME FORMATION IN A CASE OF INTER-ALLELIC COMPLEMENTATION IN NEUROSPORA CRASSA. J. Mol. Biol. *12*, 152–161.

Ding, D.-Q., Sakurai, N., Katou, Y., Itoh, T., Shirahige, K., Haraguchi, T., and Hiraoka, Y. (2006). Meiotic cohesins modulate chromosome compaction during meiotic prophase in fission yeast. The Journal of Cell Biology *174*, 499–508.

Donze, D., Adams, C. R., Rine, J., and Kamakaka, R. T. (1999). The boundaries of the silenced HMR domain in Saccharomyces cerevisiae. *13*, 698–708.

Eng, T., Guacci, V., and Koshland, D. (2014). ROCC, a conserved region in cohesin's Mcd1 subunit, is essential for the proper regulation of the maintenance of cohesion and establishment of condensation. Mol Biol Cell *25*, 2351–2364.

Gordon, C. L., and King, J. (1994). Genetic properties of temperature-sensitive folding mutants of the coat protein of phage P22. Genetics *136*, 427–438.

Guacci, V., and Koshland, D. (2012). Cohesin-independent segregation of sister chromatids in budding yeast. Mol Biol Cell *23*, 729–739.

Guacci, V., Koshland, D., and Strunnikov, A. (1997). A direct link between sister chromatid cohesion and chromosome condensation revealed through the analysis of MCD1 in S. cerevisiae. Cell *91*, 47–57.

Guacci, V., Stricklin, J., Bloom, M. S., Guō, X., Bhatter, M., and Koshland, D. (2015). A novel mechanism for the establishment of sister chromatid cohesion by the ECO1 acetyltransferase. Mol Biol Cell *26*, 117–133.

Haering, C. H., Schoffnegger, D., Nishino, T., Helmhart, W., Nasmyth, K., and Löwe, J. (2004). Structure and stability of cohesin's Smc1-kleisin interaction. Mol Cell *15*, 951–964.

Heidinger-Pauli, J. M., Unal, E., Guacci, V., and Koshland, D. (2008). The kleisin subunit of cohesin dictates damage-induced cohesion. Mol Cell *31*, 47–56.

Holzmann, J., Fuchs, J., Pichler, P., Peters, J.-M., and Mechtler, K. (2011). Lesson from the stoichiometry determination of the cohesin complex: a short protease mediated

elution increases the recovery from cross-linked antibody-conjugated beads. J. Proteome Res. *10*, 780–789.

Huis In 't Veld, P. J., Herzog, F., Ladurner, R., Davidson, I. F., Piric, S., Kreidl, E., Bhaskara, V., Aebersold, R., and Peters, J.-M. (2014). Characterization of a DNA exit gate in the human cohesin ring. Science *346*, 968–972.

Korch, C. T., and Snow, R. (1973). Allelic Complementation in the First Gene for Histidine Biosynthesis in SACCHAROMYCES CEREVISIAE. I. Characteristics of Mutants and Genetic Mapping of Alleles. Genetics *74*, 287–305.

Lavoie, B. D., Hogan, E., and Koshland, D. (2004). In vivo requirements for rDNA chromosome condensation reveal two cell-cycle-regulated pathways for mitotic chromosome folding. *18*, 76–87.

Losada, A., Hirano, M., and Hirano, T. (1998). Identification of Xenopus SMC protein complexes required for sister chromatid cohesion. Genes Dev. *12*, 1986–1997.

Melby, T. E., Ciampaglio, C. N., Briscoe, G., and Erickson, H. P. (1998). The symmetrical structure of structural maintenance of chromosomes (SMC) and MukB proteins: long, antiparallel coiled coils, folded at a flexible hinge. The Journal of Cell Biology *142*, 1595–1604.

Michaelis, C., Ciosk, R., and Nasmyth, K. (1997). Cohesins: chromosomal proteins that prevent premature separation of sister chromatids. Cell *91*, 35–45.

PERRIN, D. (1963). Immunological studies with genetically altered beta-galactosidases. Ann. N. Y. Acad. Sci. *103*, 1058–1066.

Rolef Ben-Shahar, T., Heeger, S., Lehane, C., East, P., Flynn, H., Skehel, M., and Uhlmann, F. (2008). Eco1-dependent cohesin acetylation during establishment of sister chromatid cohesion. Science *321*, 563–566.

Rollins, R. A., Morcillo, P., and Dorsett, D. (1999). Nipped-B, a Drosophila homologue of chromosomal adherins, participates in activation by remote enhancers in the cut and Ultrabithorax genes. Genetics *152*, 577–593.

Sjögren, C., and Nasmyth, K. (2001). Sister chromatid cohesion is required for postreplicative double-strand break repair in Saccharomyces cerevisiae. Curr Biol *11*, 991–995.

Stephens, A. D., Quammen, C. W., Chang, B., Haase, J., Taylor, R. M., and Bloom, K. (2013). The spatial segregation of pericentric cohesin and condensin in the mitotic spindle. Mol Biol Cell *24*, 3909–3919.

Straight, A. F., Belmont, A. S., Robinett, C. C., and Murray, A. W. (1996). GFP tagging of budding yeast chromosomes reveals that protein-protein interactions can mediate sister chromatid cohesion. Curr Biol *6*, 1599–1608.

Sumara, I., Vorlaufer, E., Gieffers, C., Peters, B. H., and Peters, J. M. (2000). Characterization of vertebrate cohesin complexes and their regulation in prophase. The Journal of Cell Biology *151*, 749–762.

Tóth, A., Ciosk, R., Uhlmann, F., Galova, M., Schleiffer, A., and Nasmyth, K. (1999). Yeast cohesin complex requires a conserved protein, Eco1p(Ctf7), to establish cohesion between sister chromatids during DNA replication. *13*, 320–333.

Uhlmann, F., and Nasmyth, K. (1998). Cohesion between sister chromatids must be established during DNA replication. Curr Biol *8*, 1095–1101.

Unal, E., Arbel-Eden, A., Sattler, U., Shroff, R., Lichten, M., Haber, J. E., and Koshland, D. (2004). DNA Damage Response Pathway Uses Histone Modification to Assemble a Double-Strand Break-Specific Cohesin Domain. Mol Cell *16*, 991–1002.

Unal, E., Heidinger-Pauli, J. M., Kim, W., Guacci, V., Onn, I., Gygi, S. P., and Koshland, D. E. (2008). A molecular determinant for the establishment of sister chromatid cohesion. Science *321*, 566–569.

Wahba, L., Gore, S. K., and Koshland, D. (2013). The homologous recombination machinery modulates the formation of RNA-DNA hybrids and associated chromosome instability. Elife *2*, e00505.

Yeh, E., Haase, J., Paliulis, L. V., Joglekar, A., Bond, L., Bouck, D., Salmon, E. D., and Bloom, K. S. (2008). Pericentric chromatin is organized into an intramolecular loop in mitosis. Curr Biol *18*, 81–90.

Zhang, J. *et al.* (2008). Acetylation of Smc3 by Eco1 is required for S phase sister chromatid cohesion in both human and yeast. Mol Cell *31*, 143–151.

Zhang, N., and Pati, D. (2009). Handcuff for sisters: a new model for sister chromatid cohesion. Cell Cycle *8*, 399–402.

Figure Legends.

Figure 1. Analysis of Single and Double Mutant Alleles of *mcd1* and *smc3.*
(A) Haploid yeast strains containing centromere plasmid pVG201 *{MCD1 URA3}* and a second centromere plasmid carrying *MCD1* (yTE474), *mcd1-Q266* (yTE478), no additional plasmid (yTE43), or mcd1-Q266 (yTE491). yTE474 and yTE478 carry a genomic deletion of the *mcd1* locus. yTE43 and yTE491 contain *mcd1-1* at the *MCD1* locus. The relevant *MCD1* genotype is indicated to the left of the panel. Liquid cultures were grown to saturation overnight at 23˚C and then plated in 10-fold serial dilutions on solid media containing dextrose (YPD) or 5-FOA to counterselect against cells carrying the *MCD1* centromere plasmid. The failure to grow on 5-FOA indicates that pVG201 (wild-type MCD1) must be retained. The mutant domain in mcd1-Q266p and mcd1-1p cohesin complexes are highlighted in red and marked with (❋).

(B) Haploid yeast strains containing centromere plasmid pEU42 *{SMC3 URA3}* and a second copy of *SMC3* (yVG3486-00), *smc3-K113R* (yVG3486-K113R); an *smc3-42* strain (yTE532), and a strain carrying both *smc3-42* and *smc3-42 smc3-K113R* (yTE534). The relevant *SMC3* genotype is indicated to the left side of the panel. Liquid cultures were grown to saturation overnight at 23˚C and then plates in 10-fold serial dilutions on solid media containing dextrose (YPD) or 5-FOA to counterselect against cells carrying the *SMC3 URA3* plasmid. The failure to grow on 5-FOA indicates that pEU42 (wild-type SMC3) must be retained. The mutant domain in smc3-K113Rp and smc3-42p cohesin complexes are highlighted in red and marked with (❋).

(C) Haploid yeast strains containing a single copy, in-frame auxin degron following amino acid N607 in Smc3 (*SMC3-AID*^{608} strains) carrying a second integrated copy of *SMC3* (yMB81-1A), no additional copy (yVG3651-3D), or *smc3-K113R* (yTE440) were grown to saturation overnight at 23˚C and then plated in 10-fold serial dilutions on solid media containing dextrose (YPD) or dextrose and auxin (YPD AUX). The relevant *SMC3* genotype is indicated to the left side of the panel. Photomicrographs were taken after 2 days growth at 23˚C. The auxin degron near the Smc3 hinge and smc3-K113R cohesin complexes are highlighted to the right in red and marked with (❋).

Figure 2. GAL1 Induced Over-Expression of *MCD1* and *SMC3* Alleles.
(A) Haploid yeast strains containing centromere plasmid pVG201 {*MCD1 URA*} and a second plasmid carrying a galactose inducible *MCD1* (yTE480), *mcd1-1* (yTE502), *mcd1-Q266* (yTE482); and a strain containing both *mcd1-1* and *mcd1-Q266* (TE491) were grown to saturation at 23˚C in rich media containing galactose. The relevant *MCD1* genotype is indicated to the left side of the panel. Cells were then plated in 10-fold serial dilutions on solid media containing dextrose (YPD) or 5-FOA and galactose (5-FOA GAL) to counterselect against cells containing the centromeric *MCD1* plasmid. The failure to grow on 5-FOA indicates that pVG201 (wild-type MCD1) must be retained.

(B) Haploid yeast strains containing centromere plasmid pEU42 *{SMC3 URA3}* and a second allele integrated at *LEU2* containing a galactose inducible *SMC3* (yTE424), *smc3-K113R* (yTE449), *smc3-42* (yTE420); and a strain containing both *smc3-42* and *smc3-K113R* (yTE505) were grown to saturation at 23˚C in rich media containing galactose. The relevant *SMC3* genotype is indicated to the left side of the panel. Cells were then plated in 10-fold serial dilutions on solid media containing dextrose (YPD) or 5-FOA and galactose (5-FOA GAL) to counterselect against cells containing the *CEN URA SMC3* plasmid. The failure to grow on 5-FOA indicates that pEU42 (wild-type SMC3) must be retained.

Figure 3. Analysis of Chromosome Condensation in *MCD1* and *SMC3* mutant allele strains.
(A) Identification of rDNA morphology by chromosome spreads. Yeast spheroplasts were prepared and chromosomes were spread on glass slides (see Materials and Methods). Prepared slides were visualized by DAPI staining in mounting media. Chromosome masses were scored for their morphology at the rDNA locus. The rDNA region is indicated with an arrow.

(B) Wild-type (yVG3349-1B) and strains harboring each single allele *mcd1-1* (yVG3312-7A), *mcd1-Q266 MCD1-AID* (yTE149), or both alleles *mcd1-Q266-6MYC mcd1-1* (yTE42) were cultured such that all strains passed from G1 to M phase arrest at 37˚C and in the presence of auxin. Cells were then harvested and processed for chromosome spreads. At least two hundred DAPI stained masses were scored for each genotype, and at least two biological replicates were completed for each genotype.

(C) Wild-type (yTE45) and strains harboring each single allele *smc3-42* (yVG3358-3B), *smc3-K113R smc3-AID*^{608} (yTE440), or both alleles *smc3-42 smc3-K113R* (yVG3473-1C) were cultured such that all strains passed from G1 to M phase arrest at 34˚C and in the presence of auxin. Cells were then harvested and processed for chromosome spreads. At least two hundred DAPI stained masses were scored for each genotype, and at least two biological replicates were completed for each genotype.

Figure 4. Analysis of Sister Chromatid Cohesion at CEN proximal (*TRP1*) and CEN distal (*LYS4*) loci in *MCD1* and *SMC3* allele strains.
(A) Wild-type (TRP1-LacO: yVG3460-2A. LYS4-LacO: yTE45.) or strains harboring *mcd1-1* (TRP1-LacO: yTE453. LYS4-LacO: yVG3312-7A.), *mcd1-Q266 MCD1-AID* (TRP1-LacO: yTE285. LYS4-LacO: yTE149.), or both alleles *mcd1-Q266 mcd1-1* (TRP1-LacO: yTE456. LYS4-LacO: yTE42.) The experimental regimen was identical to that described in Figure 3B. Cells were processed, fixed, and scored for cohesion at either the CEN proximal locus (*TRP1*) or the CEN distal locus (*LYS4*). At least two

hundred cells were scored for each genotype, and the experiment was repeated at two times.

(B) Wild-type (TRP1-LacO: yVG3460-2A. LYS4-LacO: yTE48.) or strains harboring *smc3-42* (TRP1-LacO: yTE494. LYS4-LacO: yVG3358-3B.), *smc3-K113R smc3-AID*^{608} (TRP1-LacO: yTE471. LYS4-LacO: yTE440.), or both alleles *smc3-K113R smc3-42* (TRP1-LacO: yTE500. LYS4-LacO: yVG3473-1C.) The experimental regimen was identical to that described in Figure 4A.

Figure 5. Analysis of Mcd1 Protein Levels in *MCD1* Allele Strains.
(A.) Early log phase cultures of haploid strains *mcd1-1* (yVG3312-7A) and *mcd1-1 mcd1-Q266-6MYC* (yTE42) were arrested in M phase with nocodazole for 2.5 hours. After all cultures had arrested with 95% large budded cells, cultures were incubated for an additional hour at either 23˚C or 37˚C. Cells were then harvested, lysed and prepared for protein analysis by SDS PAGE and western blotting. Tubulin was used as a loading control.

(B) Early log phase cultures of haploid strains *mcd1-1-3FLAG* (yTE103) and *mcd1-1-3FLAG mcd1-Q266-6MYC* (yTE181) were arrested arrested in S Phase (Hydroxyurea) or M phase (Nocodazole) for 2.5 hours. Following arrest, cultures were split in half and incubated for an additional hour at either 23˚C or 37˚C. Afterwards, all cultures were harvested, lysed, and prepared for SDS-PAGE and western blot analysis using mouse anti-FLAG or mouse anti-MYC antibodies to discriminate between both alleles of Mcd1p present. A nonspecific band with a faster mobility than Mcd1-3FLAGp was detected in cells lacking an epitope fusion protein. Tubulin was used as a loading control.

Figure 6. Restoration of mcd1-1-3FLAG and smc3-42-6HA Binding to Chromosomes in Interallelic Complementation Pairs.

(A) Early-log-phase cells containing internal 3FLAG epitope fusion proteins in Mcd1p of *MCD1-3FLAG MCD1-AID* (yTE171), *mcd1-1-3FLAG* (yTE103), or both *mcd1-1-3FLAG* and *mcd1-Q266-6MYC* (yTE181) were grown and arrested in M phase at 37˚C essentially as described in Figure 3B, except that auxin was not added to yTE103 or yTE181. Cells were fixed and prepared for chromatin immunoprecipitation using a mouse anti-FLAG antibody *(Materials & Methods)*. Following immunoprecipitation, cohesin associated regions (left to right: *CARL1, CARC1,* and centromeres I and XIV) were examined by quantitative PCR (qPCR). The genotype of interest is indicated above each set of graphs. The average of two biological replicates and the standard deviation between each is shown.

(B) Early-log-phase cells containing internal 6HA epitope fusion protein in Smc3p of wild-type (yGC1-8A), smc3-42-6HA (yVG3523-1A), or both smc3-42-6HAp and smc3-

K113Rp (yVG3527-1A) were grown and arrested in M phase at 34˚C essentially as described in Figure 3C, except without using auxin. Cells were fixed and processed for chIP-qPCR as described above in 6A. The same cohesin associated regions (left to right: *CARL1, CARC1,* and centromeres I and XIV) were examined. The genotype of interest is indicated above each set of graphs. The average of two biological replicates and the standard deviation between each is shown.

Figure 7. Model for How Cohesin Tethers DNA.
(Top Flow Chart.) Activation of the Smc1 ATPase head allows cohesin deposition onto chromosomes. A separate cohesin complex activates the Smc3 ATPase, but not the Smc1 ATPase. The interaction of cohesins already tethering a single chromatid generates cohesion and condensation. (Bottom Flow Chart) In the same cohesin complex, both the Smc3p ATPase and Smc1 ATPase are fired in sequence, trapping one sister in the ring formed by Mcd1 and the head domains of Smc1p and Smc3p, and the other sister in the "large ring" comprised of the coiled coils of Smc1 and Smc3. This establishes sister chromatid cohesion. Lateral interactions between cohesin complexes in turn allows for chromosome condensation.

Supplemental Figure 1. Allele specificity of complementation pairs.
(A) Allelic specificity of complementation pairs in *MCD1*. Haploid yeast strains mcd1-1 (yVG3312-7A), MCD1 mcd1-1 (yTE396), mcd1-V137K mcd1-1 (yTE388), or *mcd1-R135 mcd1-1* (yTE392) were grown to saturation overnight at 23˚C.Cells were then plated by serial dilution onto solid agar media (YPD) and incubated at either 23˚C or 37˚C. All dilutions shown were from the same YPD plate. Neither *mcd1-V137K mcd1-1* nor *mcd1-R135 mcd1-1* showed significant growth at 37˚C strains, but grew well at 23˚C.
(B) Auxin resistance of smc3-AID^{608} is not observed in smc3-K112/3-RR smc3-AID^{608} (y MB79-1A) strains. Wild-type (yMB84-1A) and smc3-K112/3-RR (yMB79-1A) were grown to saturation overnight and plated in 10-fold serial dilutions on solid agar rich media with dextrose (YPD) or supplemented with auxin (YPD AUX). Plates were incubated at 23˚C for 2 days. Compare growth to smc3-K113R smc3-AID^{608} serial dilutions in Figure 1C.

Supplemental Figure 2. smc3-K113R smc3-AID^{608} Show Temperature Dependence For Auxin Sensitivity. *Smc3-AID^{608}* strains (yVG3651-3D) carrying a second integrated copy of *SMC3* (yMB81-1A), or *smc3-K113R* (yTE440) were grown to saturation overnight at 34˚C and then back diluted to allow growth for six additional hours. Cells were plated in 10-fold serial dilutions onto solid agar rich media containing dextrose (YPD) or dextrose and auxin (YPD AUX). Note that auxin mediated degradation is more penetrant at 23˚C compared to 30˚C (see Nishimura and Kanemaki, 2009).

Supplemental Figure 3. Analysis of GAL expression in *MCD1* or *SMC3* over-expression strains.

(A) Analysis of Mcd1 protein levels in galactose inducible *mcd1-1* strains. Haploid *mcd1-1* (yVG3312-7A) and *pGAL-mcd1-1 mcd1-1* cells (yTE95) were grown in lactic-acid-glycerol rich media to early-log-phase at 30˚C. The culture was split into thirds. One sample was incubated for an additional hour with no additional changes. Galactose was added to the second culture (2% final) and incubated for an additional hour at 30˚C. The third culture was both upshifted to incubate at 37˚C and induced with galactose for one additional hour.Afterwards, five ODs of each treated sample was harvested and processed for SDS-PAGE and western blot analysis using antibodies against Mcd1 and Tubulin.
(B) RNA expression analysis in galactose inducible *smc3* strains. Strains from Figure 2B were grown in lactic acid glycerol-containing media to early log phase at 30˚C. Galactose was added (2% final) to induce *GAL1* expression for 1 hour. Twenty-five ODs of cells were collected from the pre and post galactose treated cells, and were subsequently prepared for RNA expression analysis following nucleic acid extraction with Trizol and lithium acetate precipitation. Expression of *SMC3* was analyzed by RT-qPCR using primers at the 5' end of *SMC3* in triplicate comparing fold expression over each pre-induction sample and normalized against tubulin.

Supplemental Figure 4. *mcd1-Q266* and *mcd1-1* Alleles in the *cis* Configuration Fail to Restore Viability.

(A) Schematic of mutants in Mcd1p. Wild-type Mcd1p is indicated on the left. The insertion mutation in Mcd1-Q266p lies in the linker domain of Mcd1, compared to mcd1-1p, which lies in the Mcd1's C terminal. mcd1-1,Q266 contains both mutations. The location of each mutation is marked with (❋) in red.

(B) Haploid *MCD1-AID* strains carrying an additional copy of *MCD1-6MYC* (yTE428), *pGAL-MCD1-6MYC* (yTE75), *pGAL-mcd1-1,Q266-6MYC* (yTE484), or *mcd1-1,Q266-6MYC* (yTE531) in addition to a haploid yeast strain carrying both *mcd1-1* and *mcd1-Q266-6MYC* (yTE42). Cells were grown to saturation overnight at 23˚C and spotted in 10-fold serial dilutions onto solid agar media containing dextrose (YPD), dextrose and auxin (YPD AUX), or galactose and auxin (YPGAL AUX). Plates were photographed after 2 days of growth.

(C) Haploid *mcd1-1* (yVG3312-7A) strains carrying an additional copy of *MCD1* (yTE396), *pGAL-mcd1-1-6MYC* (yTE523), *mcd1-1,Q266-6MYC* (yTE521), or pGAL-mcd1-1,Q266 (yTE519) were grown to saturation overnight at 23˚C in rich media. Cells were then spotted in 10-fold serial dilutions onto solid agar media containing dextrose (YPD), galactose (YPGAL). Plates were incubated at either 23˚C or 37˚C as indicated below each micrograph.

Supplemental Figure 5. Analysis of Cohesion Establishment of *smc3-K113R* in *smc3-*

42 or *smc3-AID*^{608} strain backgrounds.

(A) Haploid *smc3-42* strains (yTE494) carrying either *SMC3* (yTE496) or *smc3-K113R* (yTE500) integrated at URA3 was processed for cohesion analysis essentially as described in Figure 4B. Samples were harvested and fixed at regular intervals to assess cohesion kinetics during cell cycle progression. Bottom panel, flow cytometry analysis. All cells entered S phase by 30 minutes and no further replication was observed around 60 minutes. The shape of the peaks are different because cells were prepared by 4% PFA fixative instead of 70% Ethanol.

(B) Endpoint analysis of sister chromatid cohesion. The same strains assayed above in Supplemental 5A were examined for sister chromatid cohesion using the same regiment, but at 23˚C, 30˚C, and 34˚C. The data from 180 minute time point from the graph above is replotted for comparison.

(C) Haploid smc3-AID^{608} strains (yVG3651-3D) carrying either *SMC3* (yMB81-1A) or *smc3-K113R* (yTE440) were arrested in processed for cohesion analysis at 30˚C (in auxin supplemented media) essentially as described in 4B, and timepoints were taken at regular intervals to assess kinetics of cohesion loss. Bottom panel, flow cytometry analysis. All cells entered S phase by 30 minutes and no further replication was observed around 60 minutes.

(D) Endpoint analysis of sister chromatid cohesion. The same strains assayed above in Supplemental 5C were examined for sister chromatid cohesion using the same regiment, but at 23˚C, 30˚C, and 34˚C. The data from 180 minute time point from the graph above is replotted for comparison.

Supplemental Figure 6. Global binding of Mcd1p or Smc3p in Interallelic Complementation Pairs.
(A) Haploid yeast strains either *MCD1-3FLAG* (yTE171), *mcd1-1-3FLAG* (yTE103), or both *mcd1-1-3FLAG* at the endogenous locus and *mcd1-Q266-6MYC* integrated at *URA3* (yTE181) were grown to mid-log-phase. Cells were prepared for chromosome spreads as in Figure 3. The FLAG epitope in Mcd1-3FLAGp and mcd1-1-3FLAGp were visualized using a mouse anti-FLAG antibody by indirect immunofluorescence to discriminate against any other copies of Mcd1p present in each spread chromosome *(Materials and Methods).*
(B) Haploid yeast strains carrying a tandem repeated 6HA epitope fusion protein internally placed in *SMC3* (yGC1-8A) or in *smc3-42* (yVG3523-1A), or both *smc3-42-6HA* and *smc3-K113R* integrated at *LEU2* (yVG3527-1A). Cells were prepared as above in Supplemental Figure 6A. Smc3-6HAp and smc3-42-6HAp were visualized on spread chromosomes using a mouse anti-HA antibody as described above.

Supplemental Figure 7. Analysis of Mcd1-Q266-6MYCp Binding by chIP in *mcd1-1-3FLAG mcd1-Q266-6MYC* strains.

Chromosome binding at cohesin associated regions was assessed by chIP using the same experimental regiment described in 6A in strain TE181 with the mouse anti-FLAG antibody used for visualization of mcd1-Q266-6MYC by chromosome spreads.

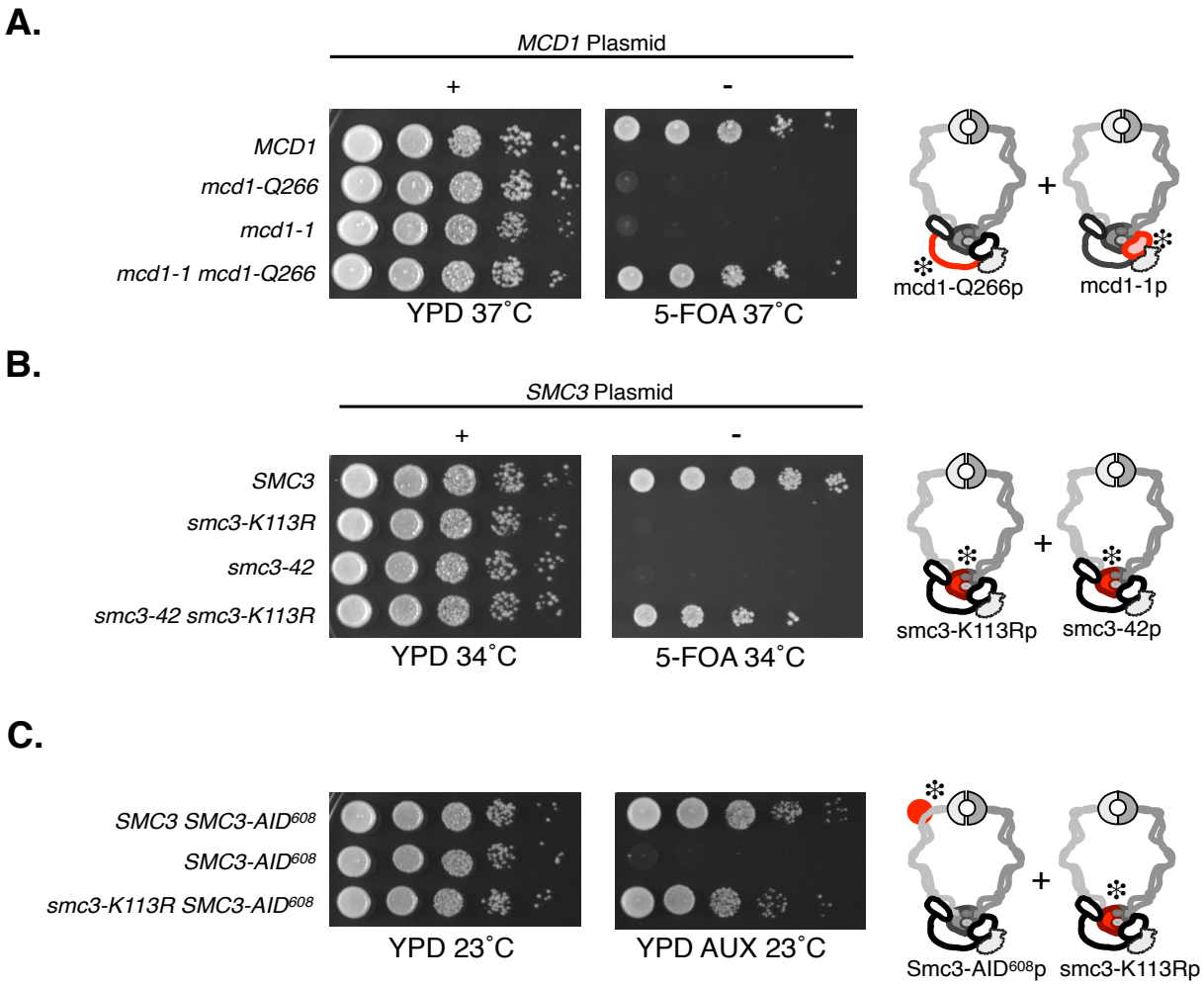
A.
MCD1 Plasmid
+
-
MCD1
mcd1-Q266
mcd1-1
mcd1-1 mcd1-Q266
YPD 37˚C
5-FOA 37˚C
mcd1-Q266p
+
mcd1-1p
B.
SMC3 Plasmid
+
-
SMC3
smc3-K113R
smc3-42
smc3-42 smc3-K113R
YPD 34˚C
5-FOA 34˚C
smc3-K113Rp
+
smc3-42p
C.
SMC3 SMC3-AID608
SMC3-AID608
smc3-K113R SMC3-AID608
YPD 23˚C
YPD AUX 23˚C
Smc3-AID608p
+
smc3-K113Rp

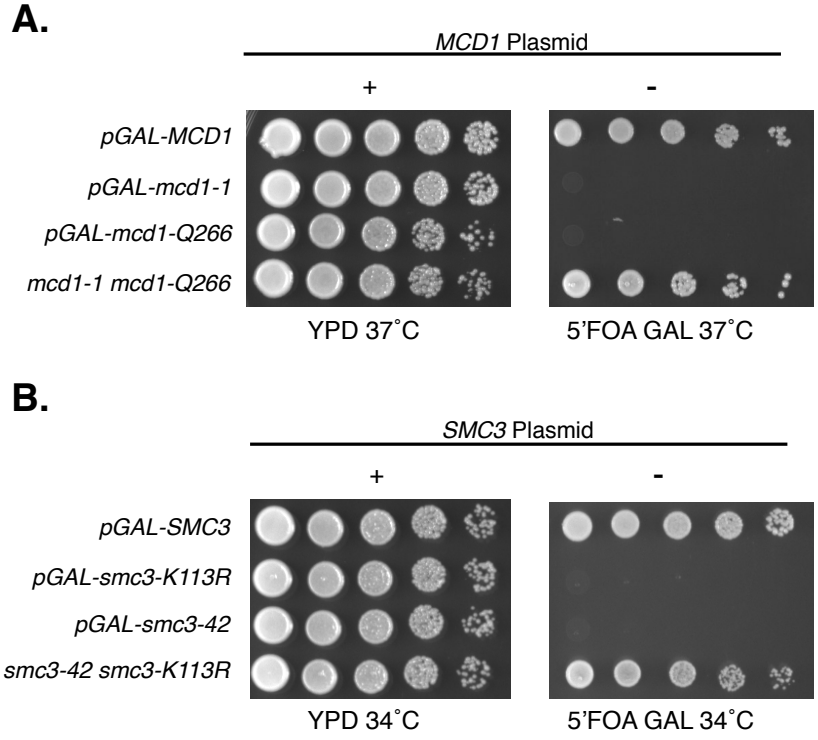
A.
MCD1 Plasmid
+
-
pGAL-MCD1
pGAL-mcd1-1
pGAL-mcd1-Q266
mcd1-1 mcd1-Q266
YPD 37˚C
5'FOA GAL 37˚C
B.
SMC3 Plasmid
+
-
pGAL-SMC3
pGAL-smc3-K113R
pGAL-smc3-42
smc3-42 smc3-K113R
YPD 34˚C
5'FOA GAL 34˚C

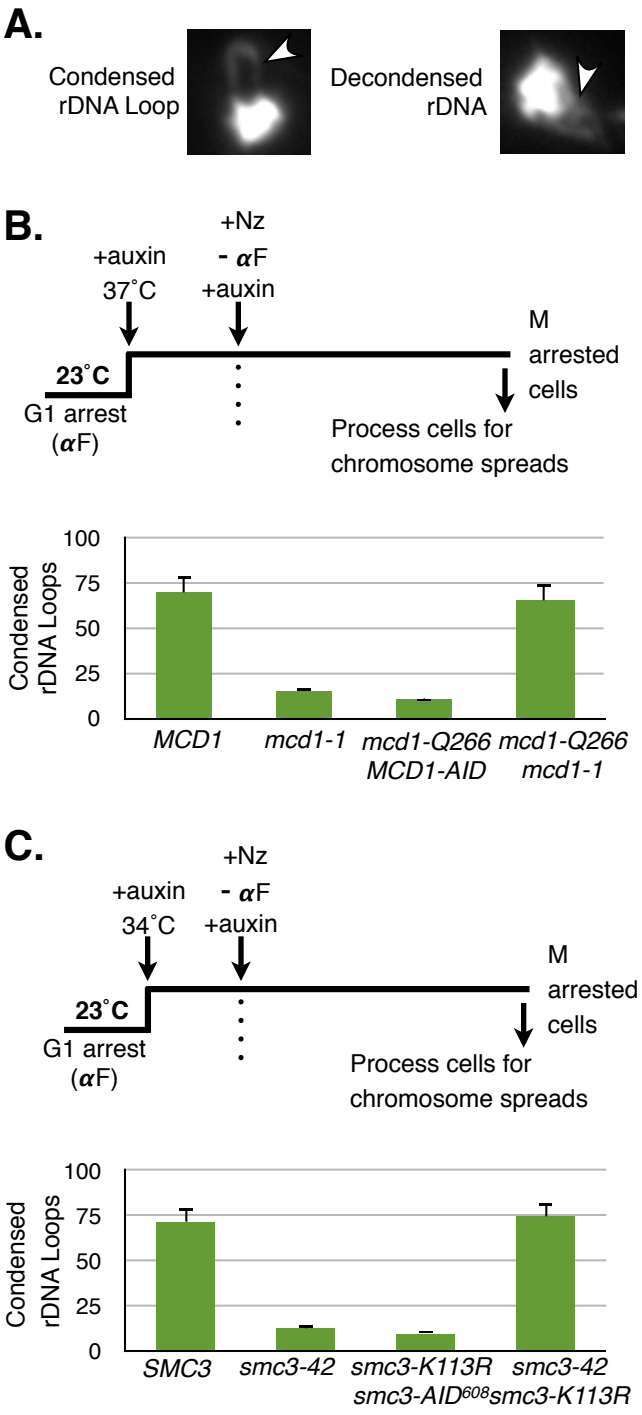
A.
Condensed rDNA Loop
Decondensed rDNA
B.
+Nz
- αF
+auxin
+auxin
37˚C
23˚C
G1 arrest (αF)
M arrested cells
Process cells for chromosome spreads
Condensed rDNA Loops
100
75
50
25
0
MCD1
mcd1-1
mcd1-Q266 MCD1-AID
mcd1-Q266 mcd1-1
C.
+Nz
- αF
+auxin
+auxin
34˚C
23˚C
G1 arrest (αF)
M arrested cells
Process cells for chromosome spreads
Condensed rDNA Loops
100
75
50
25
0
SMC3
smc3-42
smc3-K113R smc3-AID608smc3-K113R
smc3-42

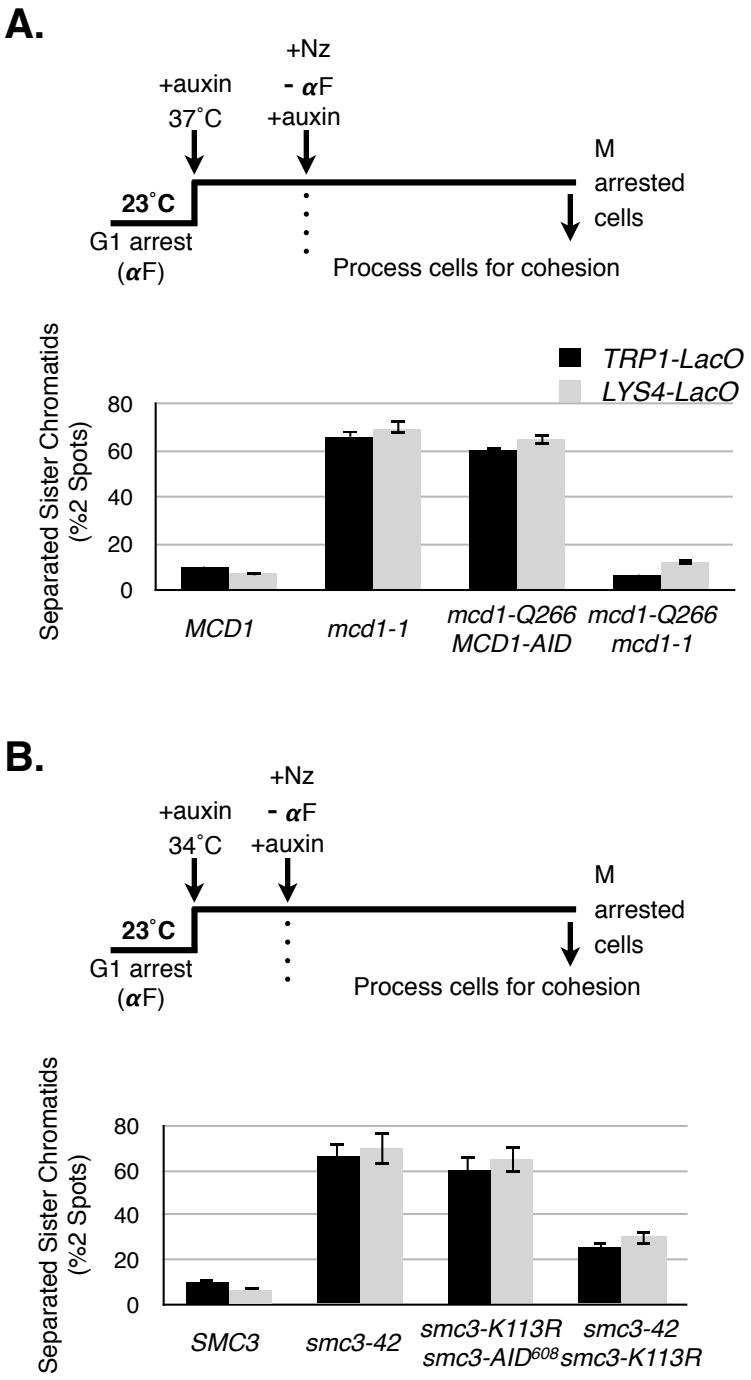
A.
+Nz
+auxin
- αF
37˚C
+auxin
M
arrested
cells
23˚C
G1 arrest
(αF)
Process cells for cohesion
TRP1-LacO
LYS4-LacO
Separated Sister Chromatids
(%2 Spots)
80
60
40
20
0
MCD1
mcd1-1
mcd1-Q266
MCD1-AID
mcd1-Q266
mcd1-1
B.
+Nz
+auxin
- αF
34˚C
+auxin
M
arrested
cells
23˚C
G1 arrest
(αF)
Process cells for cohesion
Separated Sister Chromatids
(%2 Spots)
80
60
40
20
0
SMC3
smc3-42
smc3-K113R
smc3-AID608
smc3-42
smc3-K113R

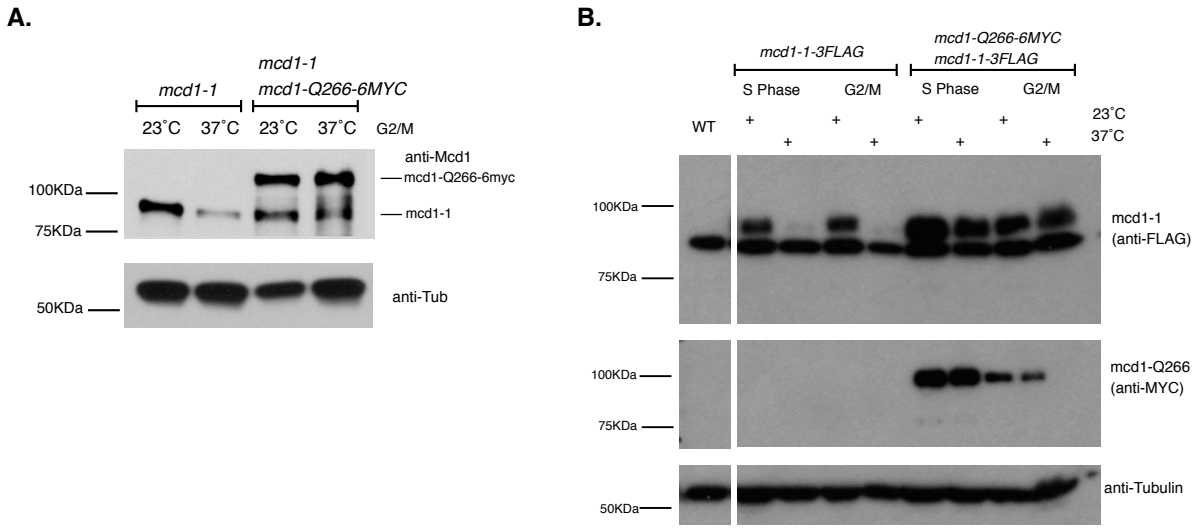
A.
mcd1-1
mcd1-1
mcd1-Q266-6MYC
23˚C
37˚C
23˚C
37˚C
G2/M
anti-Mcd1
mcd1-Q266-6myc
mcd1-1
100KDa
75KDa
50KDa
anti-Tub
B.
mcd1-1-3FLAG
mcd1-Q266-6MYC
mcd1-1-3FLAG
S Phase
G2/M
S Phase
G2/M
WT
23˚C
37˚C
100KDa
75KDa
mcd1-1
(anti-FLAG)
100KDa
75KDa
mcd1-Q266
(anti-MYC)
50KDa
anti-Tubulin

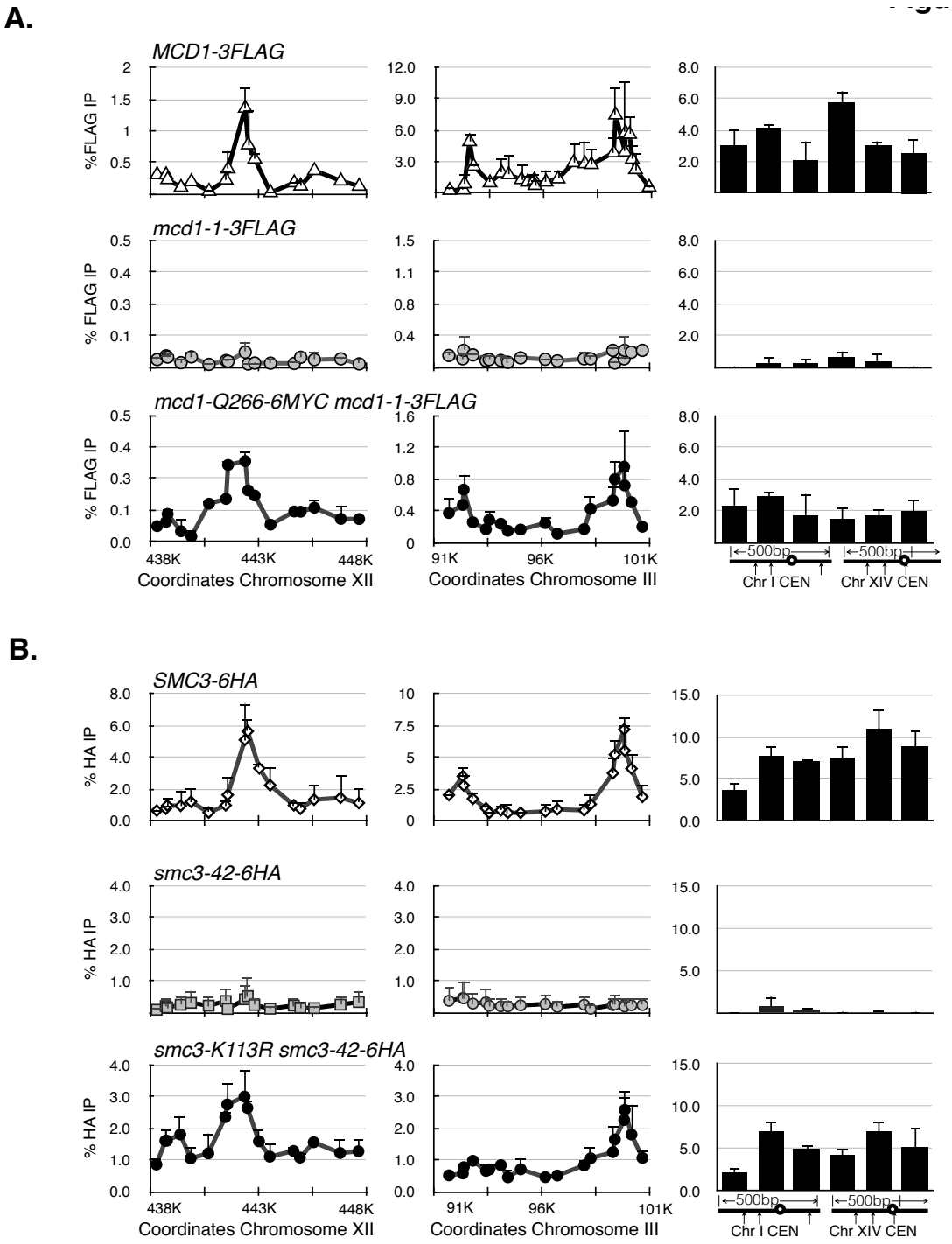
A.
MCD1-3FLAG
%FLAG IP
mcd1-1-3FLAG
% FLAG IP
mcd1-Q266-6MYC mcd1-1-3FLAG
% FLAG IP
438K
443K
448K
Coordinates Chromosome XII
91K
96K
101K
Coordinates Chromosome III
500bp
500bp
Chr I CEN
Chr XIV CEN
B.
SMC3-6HA
% HA IP
smc3-42-6HA
% HA IP
smc3-K113R smc3-42-6HA
% HA IP
438K
443K
448K
Coordinates Chromosome XII
91K
96K
101K
Coordinates Chromosome III
500bp
500bp
Chr I CEN
Chr XIV CEN

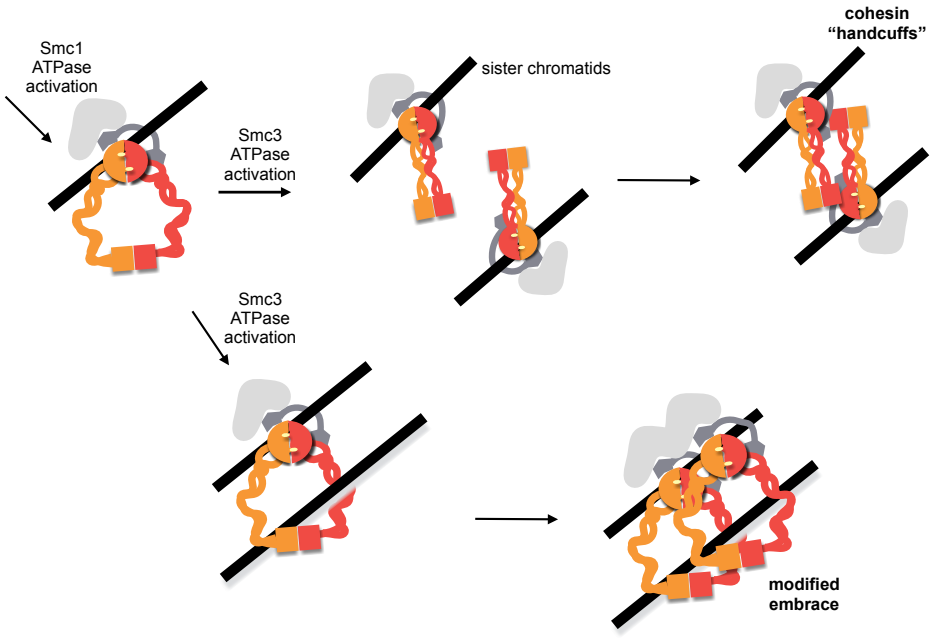
Smc1
ATPase
activation
Smc3
ATPase
activation
sister chromatids
cohesin
“handcuffs”
Smc3
ATPase
activation
modified
embrace

A.

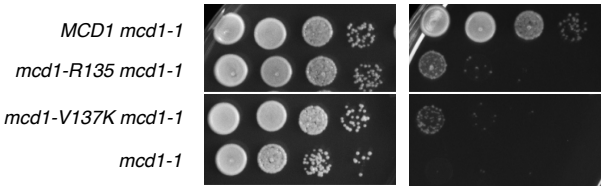
MCD1 mcd1-1
mcd1-R135 mcd1-1
mcd1-V137K mcd1-1
mcd1-1
YPD 23˚C
YPD 37˚C

B.

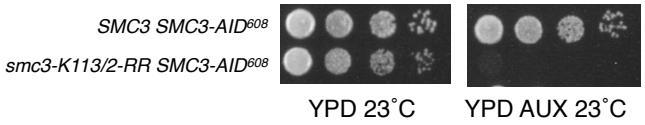
SMC3 SMC3-AID608
smc3-K113/2-RR SMC3-AID608
YPD 23˚C
YPD AUX 23˚C

A.

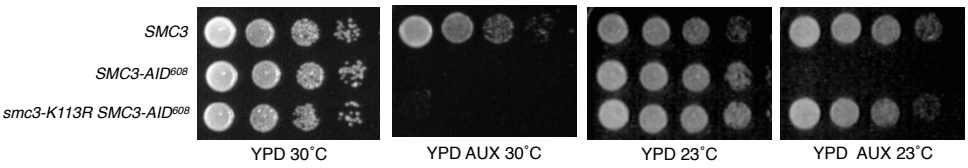
SMC3
SMC3-AID608
smc3-K113R SMC3-AID608
YPD 30˚C
YPD AUX 30˚C
YPD 23˚C
YPD AUX 23˚C

A.

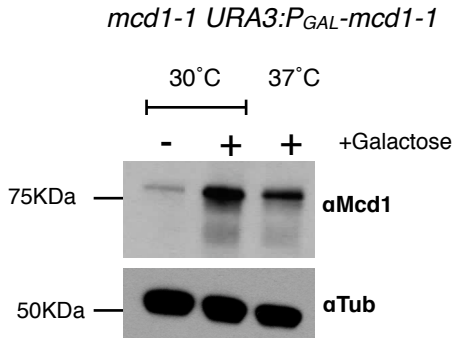
mcd1-1 URA3:PGAL-mcd1-1
30˚C
37˚C
-
+
+
+Galactose
75KDa
αMcd1
50KDa
αTub

B.

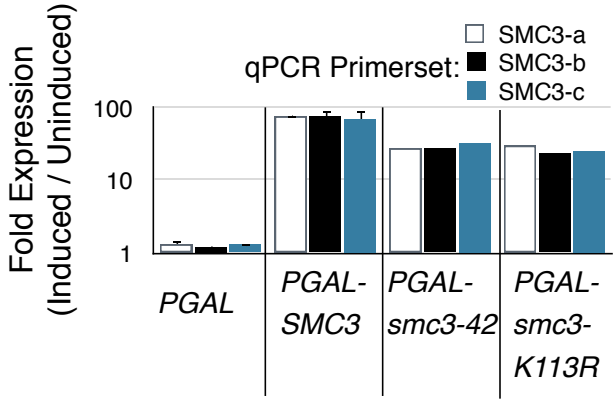
Fold Expression
(Induced / Uninduced)
qPCR Primerset:
SMC3-a
SMC3-b
SMC3-c
100
10
1
PGAL
PGAL-SMC3
PGAL-smc3-42
PGAL-smc3-K113R

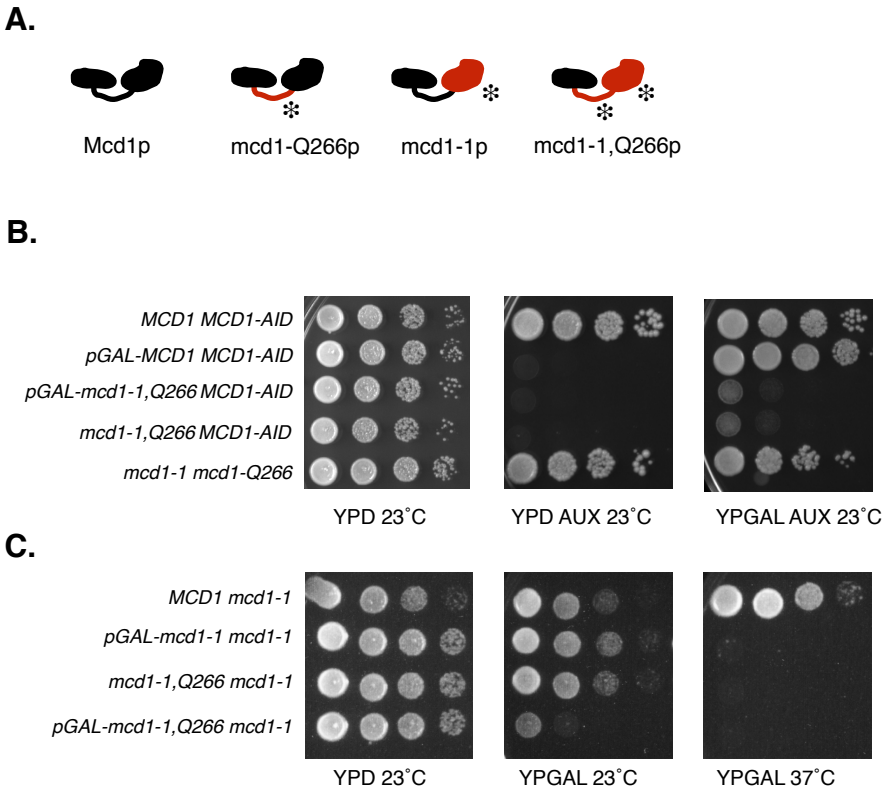
A.
Mcd1p
mcd1-Q266p
mcd1-1p
mcd1-1,Q266p
B.
MCD1 MCD1-AID
pGAL-MCD1 MCD1-AID
pGAL-mcd1-1,Q266 MCD1-AID
mcd1-1,Q266 MCD1-AID
mcd1-1 mcd1-Q266
YPD 23˚C
YPD AUX 23˚C
YPGAL AUX 23˚C
C.
MCD1 mcd1-1
pGAL-mcd1-1 mcd1-1
mcd1-1,Q266 mcd1-1
pGAL-mcd1-1,Q266 mcd1-1
YPD 23˚C
YPGAL 23˚C
YPGAL 37˚C

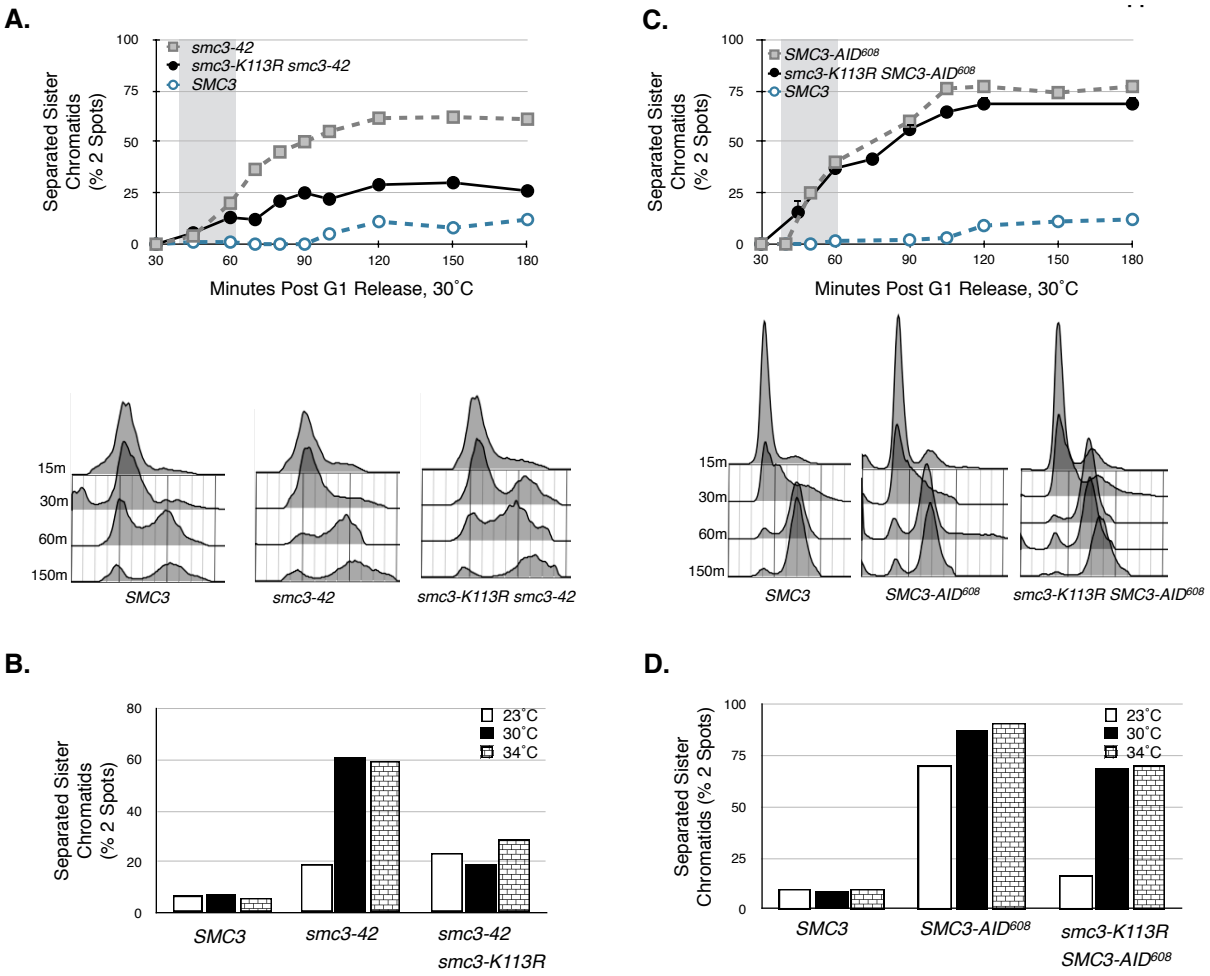
A.
smc3-42
smc3-K113R smc3-42
SMC3
Separated Sister Chromatids (% 2 Spots)
Minutes Post G1 Release, 30˚C
15m
30m
60m
150m
SMC3
smc3-42
smc3-K113R smc3-42
C.
SMC3-AID608
smc3-K113R SMC3-AID608
SMC3
Separated Sister Chromatids (% 2 Spots)
Minutes Post G1 Release, 30˚C
15m
30m
60m
150m
SMC3
SMC3-AID608
smc3-K113R SMC3-AID608
B.
23˚C
30˚C
34˚C
Separated Sister Chromatids (% 2 Spots)
SMC3
smc3-42
smc3-42 smc3-K113R
D.
23˚C
30˚C
34˚C
Separated Sister Chromatids (% 2 Spots)
SMC3
SMC3-AID608
smc3-K113R SMC3-AID608

A.

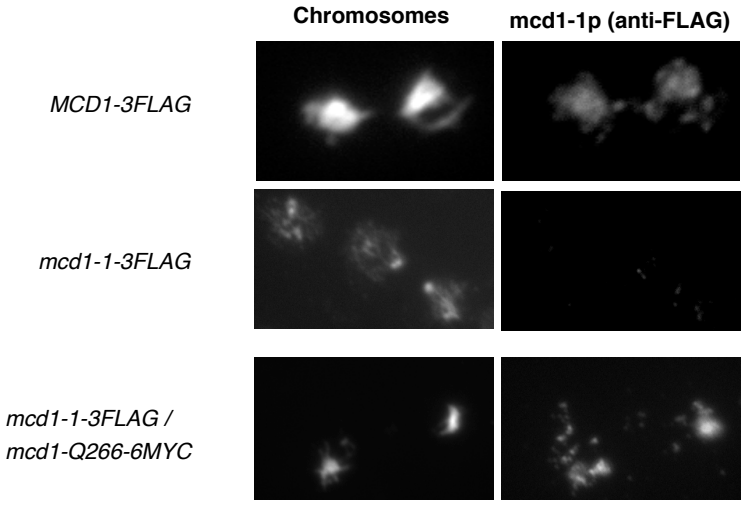
Chromosomes
mcd1-1p (anti-FLAG)
MCD1-3FLAG
mcd1-1-3FLAG
mcd1-1-3FLAG /
mcd1-Q266-6MYC

B.

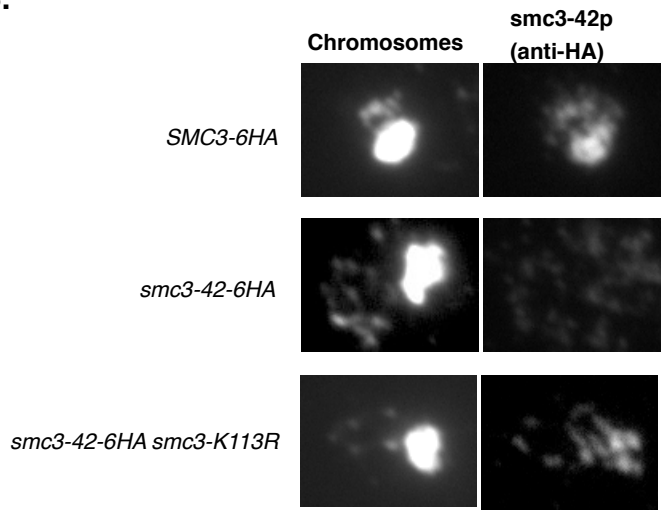
Chromosomes
smc3-42p
(anti-HA)
SMC3-6HA
smc3-42-6HA
smc3-42-6HA smc3-K113R

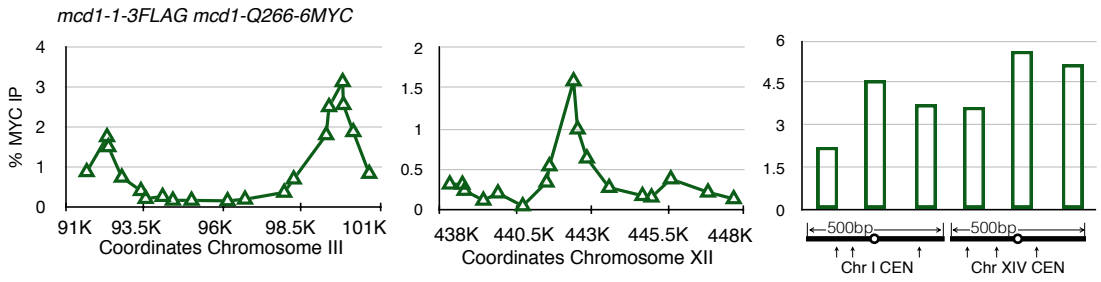
mcd1-1-3FLAG mcd1-Q266-6MYC
% MYC IP
0
1
2
3
4
91K
93.5K
96K
98.5K
101K
Coordinates Chromosome III
0
0.5
1
1.5
2
438K
440.5K
443K
445.5K
448K
Coordinates Chromosome XII
0
1.5
3
4.5
6
500bp
500bp
Chr I CEN
Chr XIV CEN

Strain Name	Genotype
yGC1-8A	SMC3-6HA in 3349-1B
yMB79-1A	MAT**a** smc3-K112/3-RR-LEU2:leu2-3,112 SMC3-3V5-AID^{608} TIR1-CaTRP1 LacO-NAT::lys4 pHIS3-GFP-LacI-HIS3:his3-11,15 ura3-52 bar1 GAL+
yMB81-1A	MAT**a** SMC3-LEU2:leu2-3,112 SMC3-3V5-AID^{608} TIR1-CaTRP1 LacO-NAT::lys4 pHIS3-GFP-LacI-HIS3:his3-11,15 ura3-52 bar1 GAL+
yMB84-1A	MAT**a** SMC3-LEU2:leu2-3,112 SMC3-3V5-AID^{608} TIR1-CaTRP1 LacO-NAT::trp1-1 pHIS3-GFP-LacI-HIS3:his3-11,15 ura3-52 bar1
yTE103	MAT**a** mcd1-1-[3FLAG-352]::HpHmx6 LacO(DK)-NAT::lys4 pHIS3-GFP-LacI-HIS3::his3-11,15 trp1-1 ura3-52 leu2-3,112 bar1 GAL+
yTE149	**MATa** mcd1-Q266-6MYC-URA3:ura3,52 MCD1-AID1::KanMx6 LacO-NAT::lys4 OsTIR1-CaLEU2:leu2-3,112 in yVG3349-1B
yTE171	**MATa** MCD1-3FLAG-URA3::ura3-52 MCD1-AID1::KanMx6 OsTIR1-CaLEU2:leu2-3,112 in yVG3349-1B
yTE181	**MATa** mcd1-Q266-6MYC-URA3:ura3,52 mcd1-1-[3FLAG-352]::HpHMx6 LacO(DK)-NAT::lys4 pHIS3-GFP-LacI-HIS3::his3-11,15 trp1-1 leu2-3,112 bar1 GAL+
yTE285	**MATa** mcd1-Q266-6MYC-URA3:ura3,52 MCD1-AID::KanMx6 LacO-NAT::trp1 OsTIR1-CaLEU2:leu2-3,112 in yVG3349-1B
yTE388	**MATa** mcd1-V137K-TRP1::trp1-1 mcd1-1 in yVG3312-7A
yTE392	**MATa** mcd1-RID-R135-TRP1::trp1-1 mcd1-1 in yVG3312-7A
yTE396	**MATa** MCD1-TRP1::trp1 mcd1-1 in yVG3312-7A
yTE42	**MATa** mcd1-Q266-6MYC-URA3::ura3-52 mcd1-1 in yVG3312-7A
yTE420	**MATa** smc3Δ {pEU42 CEN/ARS URA3 SMC3} pGAL-smc3-42-[S182L]-LEU2::leu2-3,112
yTE424	**MATa** smc3Δ {pEU42 CEN/ARS URA3 SMC3} pGAL-SMC3-LEU2::leu2-3,112
yTE428	**MATa** MCD1-6MYC-URA3::ura3-52 MCD1-3V5-AID2::KanMx6 TIR1-CaLEU2::leu2-3,112 pHIS3-LacI-GFP LacO-(DK)-NAT:lys4

yTE43	**MATa** mcd1-1 {pVG201 CEN/ARS URA3 MCD1}
yTE440	**MATa** smc3-K113R-URA3::ura3-52 SMC3-3V5-AID^{608} TIR1-CaTRP1::trp1-1 LacO-NAT::lys4 pHIS3-GFP-LacI-HIS3:his3-11,15 ura3-52 bar1
yTE449	**MATa** smc3Δ {pEU42 CEN/ARS URA3 SMC3} pGAL-smc3-K113R-LEU2::leu2-3,112
yTE45	**MATa** TIR1-URA3::ura3-52 in yVG3349-1B
yTE453	**MATa** mcd1-1-3V5-307:HpHmx6 LacO-NAT::trp1 pHIS3-GFP-LacI-HIS3:his3-11,15 ura3-52 bar1
yTE456	**MATa** mcd1-1-3V5-307:HpHmx6 mcd1-Q266-6MYC-URA3::ura3-52 LacO-NAT::trp1 pHIS3-GFP-LacI-HIS3:his3-11,15 bar1
yTE471	**MATa** smc3-K113R-URA3::ura3-52 SMC3-3V5-AID^{608} TIR1-CaTRP1::trp1-1 LacO-NAT::trp1 pHIS3-GFP-LacI-HIS3:his3-11,15
yTE474	**MATa** {CEN TRP1 MCD1} {pVG201 CEN/ARS URA3 MCD1} mcd1Δ::KanMx6 in yVG3349-1B
yTE478	**MATa** {CEN TRP1 mcd1-Q266} {pVG201 CEN/ARS URA3 MCD1} mcd1Δ::KanMx6 in yVG3349-1B
yTE48	**MATa** TIR1-CaLEU2 in yVG3349-1B
yTE480	**MATa** {CEN TRP1 pGAL1-MCD1} {pVG201 CEN/ARS URA3 MCD1} mcd1Δ::KanMx6 in yVG3349-1B
yTE482	**MATa** {CEN TRP1 pGAL1-mcd1-Q266} {pVG201 CEN/ARS URA3 MCD1} mcd1Δ::KanMx6 in yVG3349-1B
yTE484	**MATa** pGAL-mcd1-1,Q266-6MYC-URA3::ura3,52 MCD1-3V5-AID2 TIR1-CaLEU2::leu2-3,112 in yVG3349-1B
yTE491	**MATa** {CEN TRP1 mcd1-Q266} {pVG201 CEN/ARS URA3 MCD1} mcd1-1 in yVG3312-7A
yTE494	**MATa** smc3-42 LacO-NAT::trp1 pHIS3-GFP-LacI-HIS3:his3-11,15 leu2-3,112 bar1 trp1-1 GAL+
yTE496	**MATa** SMC3-URA3 smc3-42 LacO-NAT::trp1 pHIS3-GFP-LacI-HIS3:his3-11,15 leu2-3,112 bar1 trp1-1 GAL+
yTE500	**MATa** smc3-K113R-URA3 smc3-42 LacO-NAT::trp1 pHIS3-GFP-LacI-HIS3:his3-11,15 leu2-3,112 bar1 trp1-1 GAL+
yTE502	**MATa** mcd1Δ::KanMx6 {CEN/ARS URA3 MCD1} {CEN/ARS TRP1 pGAL-mcd1-1}
yTE505	**MATa** smc3-K113R-LEU2::leu2-3,112 smc3-42 LacO-NAT::lys4 pHIS3-GFP-LacI-HIS3:his3-11,15 leu2-3,112 bar1 trp1-1 GAL+
yTE519	**MATa** pGAL-mcd1-1,Q266-6MYC-URA3::ura3-52 in yVG3312-

	7A
yTE521	**MATa** mcd1-1,Q266-6MYC-URA3::ura3-52 in yVG3312-7A
yTE523	**MATa** mcd1-1-6MYC-URA3::ura3-52 in yVG3312-7A
yTE531	**MATa** mcd1-1,Q266-6MYC-URA3::ura3-52 MCD1-AID::KanMx6 pGPD1-OsTIR1-CaLEU2:leu2-3,112 in yVG3349-1B
yTE75	**MATa** pGAL-MCD1-6MYC-URA3::ura3-52 MCD1-AID::KanMx6 pGPD1-OsTIR1-CaLEU2:leu2-3,112 in yVG3349-1B
yTE95	**MATa** mcd1-1-6MYC-URA3::ura3-52 in yVG3312-7A
yVG3312-7A	**MATa** mcd1-1 LacO-NAT:lys4 trp1-1 bar1 pHIS3-GFP-LacIHIS3:his3-11,15 ura3-52 GAL+
yVG3349-1B	**MATa** LacO-NAT:lys4 trp1-1 bar1 pHIS3-GFP-LacIHIS3:his3-11,15 leu2-3,112 ura3-52 GAL+
yVG3358-3B	**MATa** smc3-42 LacO-NAT::lys4 pHIS3-GFP-LacI-HIS3:his3-11,15 leu2-3,112 bar1 trp1-1 GAL+
yVG3460-2A	**MATa** LacO-NAT:trp1 trp1-1 bar1 pHIS3-GFP-LacIHIS3:his3-11,15 leu2-3,112 ura3-52 GAL+
yVG3473-1C	**MATa** smc3-K113R-URA3 smc3-42 LacO-NAT::lys4 pHIS3-GFP-LacI-HIS3:his3-11,15 leu2-3,112 bar1 trp1-1 GAL+
yVG3486-00	**MATa** smc3Δ {pEU42 CEN/ARS URA3 SMC3} {CEN/ARS LEU2 SMC3}
yVG3486-K113R	**MATa** smc3Δ {pEU42 CEN/ARS URA3 SMC3} {CEN/ARS LEU2 smc3-K113R}
yVG3523-1A	**MATa** smc3-42-6HA-HIS3::his3-11,15 smc3Δ::HpHMx6 LacO(DK)-NAT::lys4 pHIS3-LacI-GFP-TRP-HIS trp1-1 leu2-3,112 ura3-52 GAL+ bar1
yVG3527-1A	**MATa** smc3-K113R-LEU2::leu2-3,112 smc3-42-6HA-HIS3::his3-11,15 smc3Δ::HpHMx6 LacO(DK)-NAT::lys4 pHIS3-LacI-GFP-TRP-HIS trp1-1 leu2-3,112 ura3-52 GAL+ bar1
yVG3651-3D	**MATa** SMC3-3V5-AID^{608} TIR1-TRP1 LacO-NAT::lys4 pHIS3-GFP-LacI-HIS3:his3-11,15 ura3-52 bar1 GAL+
yTE532	**MATa** smc3-42 {pEU42 CEN/ARS URA3 SMC3} LacO-NAT::lys4 pHIS3-GFP-LacI-HIS3:his3-11,15 leu2-3,112 bar1 trp1-1 GAL+
yTE534	**MATa** smc3-42 smc3-K113R-LEU2::leu2-3,112 {pEU42 CEN/ARS URA3 SMC3} LacO-NAT::lys4 pHIS3-GFP-LacI-HIS3:his3-11,15 leu2-3,112 bar1 trp1-1 GAL+

CHAPTER 4: DISCUSSION: How Does Cohesin Tether DNA?

Cohesin Architecture in Budding Yeast: Reconciling Disparate Reports

This dissertation details two key findings regarding the molecular mechanism underlying how the protein complex, cohesin, is able to tether DNA. First, we demonstrate that cohesin is able to stably bind chromosomes in a configuration that is unable to tether sister chromatids (Chapter 2, and Eng 2014). Second, we demonstrate the first report of interallelic complementation, which implies the existence of cohesin-cohesin interactions which can be used to restore cohesins's essential functions on chromosomes, namely sister chromatid cohesion and condensation (Chapter 3). Both of these findings are important because they lead to insights regarding how cohesin might be able to interact with its substrate in order to tether DNA. As we discussed in the introduction, both of these observations are in conflict with the simple "embrace" model, by which cohesin tethers sister chromatids by stably entrapping them its ring-like structure. Cohesin's stable entrapment of DNA in this ring would be both necessary and sufficient for tethering. A simplistic model such as this cannot account for our observations where we demonstrate that cohesin's binding to DNA does not dictate its ability to tether, and additionally, cohesin can act in concert with other cohesin complexes in order to generate function. For this reason we favor cohesin handcuff or cohesin slinky models, by which cohesin interacts with other cohesin complexes. These models are able to reconcile our data as well as other other reports from the literature (Chang *et al.*, 2005; Eng *et al.*, 2014; Guacci *et al.*, 2015).

A previous report from Haering and colleagues is the report most in conflict with the data and analyses presented in this report (Haering *et al.*, 2008). Haering and colleagues chemically cross-linked cohesin into a ring-like topology. They demonstrate that this ring-structure can change the mobility of replicated plasmids, albeit a small percentage of the total.

As we alluded to in chapter 2, there are a number of approaches to consider when considering the evidence. First, the authors rely on a plasmid sedimentation assay to isolate slower migrating forms of a centromere plasmid from crude yeast extracts. The authors show that the *in vivo* cross-linking efficiency of these *de novo* cysteines is near saturation. Taking cells exposed to this cross-linking reagent, the authors demonstrate that upon crosslinking, a percentage of the plasmid moves with noticeably slower mobility through an agarose gel, consistent with entrapment by cohesin. The plasmid mobility shift is abolished if cohesin is cleaved by TEV protease, confirming that the change in migration pattern is due to induced cysteine crosslinking of cohesin, entrapping the plasmid.

With this evidence in hand, can the authors conclude that cohesin is both necessary and sufficient to generate sister chromatid cohesion? Not readily. By crosslinking cohesin after it binds DNA, Haering and colleagues have established that cohesin topologically entraps DNA, as opposed to interacting with DNA outside of the ring. Cohesin that interacts with DNA in any other manner cannot be detected, such as for cohesin involved in the formation of the barrel at the centromere (Yeh 2006). Such an interaction was detected slightly above background by this assay, and only upon subsequent analysis by 2D agarose gel electrophoresis.

Secondly, the *de novo* crosslinks generated by this engineered cohesin complex readily generates covalent bonds at adjacent thiol groups up to 8Å apart. This short bond distance ensures that only the intended crosslinks between Smc1p and Smc3p, and alternatively, Smc1p and Mcd1p, are generated. The disadvantage to this technique is that the existence of a cohesin-cohesin dimer would only be protected if cohesin dimers were formed through the topological entrapment of cohesin by another cohesin, much like cohesin entraps DNA. If cohesin-cohesin interactions were mediated by any other site more than 8Å distal from these cysteines, they would not be crosslinked. Intra-cohesin interactions have been recently reported, using solvent accessible lysines preexisting in cohesin subunits which are then crosslinked (Huis In 't Veld *et al.*, 2014). These other sites of interaction are quite numerous (>100), but show clustering in distinct regions in the coiled-coils of Smc1 and Smc3 (which are more than 8Å distal from either region crosslinked).

A curious detail in Haering's report is that only a small fraction of centromeric plasmid is ever detected in the slowest migrating form (the cohesed form). How can only a small fraction of plasmids show a physical change in mobility, if the majority of cohesin has been crosslinked, and all plasmids should be replicated? One possible explanation is that the high speed, fifteen hour centrifugation necessary to separate fractions may not preserve the bulk of cohesin interactions. Indeed, the bulk of plasmids harvested from nocodazole arrested samples show very similar migration pattern as those from asynchronous cells (Ivanov and Nasmyth, 2007).

With these caveats in mind, it becomes apparent how one can reconcile evidence for communication between cohesin complexes (Chapter 3) and evidence for cohesin's topology from Haering et al (2008). Cohesin-cohesin interactions could still be occurring at sites distal from the head and hinge domains. We now know which domains in the coiled-coils of Smc1 and Smc3 show intra-molecular interactions (J Huis In 't Veld 2014, Chapter 3, and our unpublished results). By introducing *de novo* sites for crosslinking into these domains, we should be able to capture cohesins which are interacting with other

cohesin complexes. Since cohesin interactions can be used for sister chromatid cohesion, we would then expect a much higher percentage of plasmids to show the slower migration consistent with cohesion between sisters.

Both the handcuff model and the embrace model make opposing predictions regarding the behavior of plasmids in the sedimentation assay. To reiterate, the embrace model predicts that cohesin's stable binding to chromosomes is necessary and sufficient to tether sisters. The handcuff model, in contrast, predicts that cohesin can stably bind chromosomes, but a second step is necessary to tether sisters. The embrace model predicts that cohesin will only be detected on the slower migrating plasmid, and not in the earlier fractions, as plasmids from those fractions are not tethered. In contrast, the handcuff model predicts that cohesin will be detected in all fractions from the sedimentation assay, as cohesin would be competent to bind the plasmid but unable to tether. It would be easiest to perform chromatin immunoprecipitation from the isolated sedimentation fragments, rather than trying to optimize conditions to reproducibly transfer proteins from an agarose gel or the subsequent western blotting.

The plasmid mobility assay, however, still needs to be used with extreme caution. To reiterate, this assay is not an appropriate substitute as a direct measure for sister chromatid cohesion, compared to the LacO arrays or DNA FISH. It is unclear if the change in plasmid mobility is a direct consequence of cohesin tethering, or indirect, as through remodeling of nucleosomes. Many proteins could impact the migration of circular DNA through an agarose gel, and a high speed, fifteen-hour centrifugation necessary to separate fractions may not preserve the bulk of cohesin interactions. To detect such a physical interaction, it will be important to develop tools needed to visualize cohesin on DNA by high-resolution microscopy. Such an orthogonal approach will be important to validate our genetic observations.

Is the *ROCC* Box Required for Meiotic Cohesin to Tether Sister Chromatids?

In chapter 2, we discussed evidence that a specific region (termed *ROCC)* in *MCD1* is required to both maintain sister chromatid cohesion and establish chromosome condensation. In meiosis, Mcd1p cohesin complexes are largely replaced with a meiotic specific homolog, Rec8p (Klein *et al.*, 1999). Interestingly, mcd1-1 / mcd1-1 diploids show a decrease in efficiency in meiotic progression, suggesting that Mcd1p is not completely dispensable in this alternative cell cycle (Klein *et al.*, 1999). The poly aspartic-acid patch of the ROCC domain is largely absent in Rec8p (Figure 1). First, we could assess if *mcd1-rocc* diploids were competent for meiosis. As *mcd1-rocc* mutants are lethal, we could place *MCD1*

under a conditional promoter such as the *CUP1* or *GAL1* promoter. Diploids could be grown in copper-supplemented or galactose-containing media to express wild-type *MCD1*, and upon sporulation, block transcription of *MCD1.* Fission yeast cells expressing only Rad21p/Mcd1p during meiosis undergo equational division rather than reductional division (Yokobayashi *et al.*, 2003). It would be interesting to determine if mcd1-rocc mutants are lethal, and if they fail to maintain cohesion or condensation in the meiosis I.

It is unclear if the *ROCC* domain is mitotic specific or also found in Rec8p. It would be simple to introduce a similar mutation at the same position in *REC8* as *mcd1-Q266*, and screen if the mutation in *REC8* causes cellular inviability. Another RID mutagenesis screen in REC8 might be required to exhaustively determine if *ROCC* is present, but undetectable at the primary protein sequence level.

On Cohesin Accessory Factors: How Conserved is Wpl1p in Eukaryotes?

The identification of Rad61p/Wpl1p as the metazoan homolog of Wapl lead to a period of renewed interest, where many groups studied this cohesin accessory factor in both budding yeast and mammalian cell lines (Gandhi *et al.*, 2006; Kueng *et al.*, 2006). However, is yeast Wpl1p truly the budding yeast homolog of Wapl? Wpl1p shows 14% sequence conservation with human Wapl, primarily in a single carboxyl terminal domain (Kueng *et al.*, 2006). Alarmingly, while metazoan Wapl is an essential protein and required for sister chromatid cohesion, *wpl1Δ* yeast strains are viable with only a modest cohesion defect (Game *et al.*, 2003; Warren *et al.*, 2004) .

In appendix 1, I detail a report where we show that *WPL1* in budding yeast is essential under specific conditions, reconciling the phenotype reported in budding yeast from metazoans. Using *WPL1-AID* strains, I show that auxin treated stationary *WPL1-AID* are inviable after ~9 days of auxin treatment. This is consistent with a role for Wapl in either entry to, or exit from stationary phase, as reported in serum starved (G0) mammalian cell cultures (Tedeschi *et al.*, 2013). *wpl1Δ* strains and wild-type cells do not show any decrease in viability after treatment with auxin for the same duration. Intriguingly, *WPL1-AID* cultures turn bright red, consistent with scavenging adenine intermediates for inappropriate replication. Consistent with this physical observation, genomic DNA extracted from *WPL1-AID* cells after this extended auxin treatment cannot be resolved by pulse field gel electrophoresis, suggesting the formation of extremely large chromosomes or alternatively, the formation of replication bubbles that impede migration through an agarose gel.

Much work remains to elucidate the mechanism of Wpl1p activity, and to determine if Wpl1p is truly the homolog of Wapl. My analysis suggests that Wpl1p is essential in yeast cells, but only when depleted in stationary phase cultures. Does a *wpl1Δ* strain carry a tightly linked suppressor? Or, do *wpl1Δ* cells show an adaptive response when entering stationary phase? We can determine if wpl1Δ strains carry a tightly linked suppressor by deep sequencing *wpl1Δ* strains and determining if they contain any additional genetic mutations near the *WPL1* locus. Determining if *wpl1Δ* strains show an adaptive response upon entering G0 will be more difficult; we will have to examine the transcriptional profile by RNA-seq from wild-type and *wpl1Δ* cells over the same nine day auxin treatment timeframe. Before we attempt any such transcriptional analysis, we will have to determine where *WPL1-AID* strains are lethal (entry to G0, G0 arrest, or exit to S phase), perhaps by determining the appearance kinetics of high molecular weight chromosomes.

Additionally, it should be trivial to determine the chromosome structure of auxin treated *WPL1-AID* strains. If *WPL1-AID* strains are undergoing inappropriate replication and forming replication bubbles, we should be able to destroy these replication bubbles by treating cells with exonuclease I, which will destroy the single strand regions near active replication forks. Flow cytometry of stationary cultures from *WPL1-AID* strains would also show an increase in cells with intermediate DNA content, as compared to wild-type stationary cultures. Alternatively, if chromosomes are undergoing fusion to generate extremely large chromosomes, they should be resolvable by pulsed field electrophoresis under modified conditions. Fused telomeres should be also detectable by Southern blotting (van Steensel *et al.*, 1998; Pobiega and Marcand, 2010).

To address if Wpl1p is truly the budding yeast homolog of metazoan Wapl, Judith Kassis (NIH) has kindly gifted me with a plasmid containing the Drosophila cDNA of the long isoform of Wapl. If Wapl and Wpl1p are performing similar functions in both yeast and metazoans, the expression (or over-expression) or Wapl in yeast should phenocopy Wpl1. For example, *eco1Δ wpl1Δ* strains are viable (Sutani *et al.*, 2009; Guacci and Koshland, 2012). Induced expression of *WAPL* in *eco1Δ wpl1Δ* should lead to cellular inviability and a condensation defect, if the strain now behaves as an *eco1Δ WPL1+* strain. Wapl should also physically interact with yeast Pds5p and Scc3p by coimmunoprecipitation. Finally, both *smc3-K112/3-RR wpl1Δ* and *mcd1-Q266 wpl1Δ* strains are viable and have wild-type chromosome condensation (Eng *et al.*, 2014; Guacci *et al.*, 2015). Expression of *WAPL* in either of these strains should cause lethality and result in condensation defects. These experiments in sum would show a functional complementation of Drosophila *WAPL* with *wpl1Δ* budding yeast cells. It is formally possible that no complementation would exist, and that lethality will not be restored in any case, as the protein sequences are simply too divergent. However, it has been

previously shown that human RAD21 can complement budding yeast MCD1 (Heidinger-Pauli *et al.*, 2009).

Elucidating Cohesion Generation in the Absence of Wpl1

Deletion of the *wpl1* locus restores viability and condensation in both smc3-K112/3-RR SMC3-AID and mcd1-Q266 MCD1-AID strains. However, the cohesion defect in both of these viable strains is exacerbated. Both of these strains exhibit exquisite sensitivity to DNA damage and microtubule depolymerizing agents, as cohesin function is still compromised under those conditions. We can exploit a previous paradigm for identification of spontaneous suppressor mutants with these strains, as we had previously for *eco1Δ wpl1Δ* strains (Guacci *et al.*, 2015). By plating *mcd1-Q266 MCD1-AID wpl1Δ* strains on drug plates, we can screen for spontaneous suppressors that are now resistant to either of these genetic insults. Many of these spontaneous suppressors will inevitably result from gene conversion events by which mcd1-Q266 is restored to wild-type. These false positives can be eliminated by PCR amplification of *MCD1* and a PmeI digest to confirm the presence or absence of the PmeI insertion in the *mcd1-Q266* allele. Mutants that are drug resistant, auxin resistant, and still harbor *mcd1-Q266* will then be scored for sister chromatid cohesion. The best candidates will restore cohesion (in the presence of auxin) to wild-type levels, as opposed to *wpl1Δ* cell levels. We can then identify these suppressor mutants by deep sequencing or candidate sequencing of known cohesin genes. Mutants identified as suppressors of *wpl1Δ mcd1-Q266 MCD1-AID* will then be transformed into *wpl1Δ smc3-K112/3-RR SMC3-AID* strains and tested for cross-suppression in that genetic background.

On Cohesin Accessory Factors:
The Role of Cdc5/Polo Kinase on Sister Chromatid Cohesion

Another disparity exists between the molecular mechanisms of cohesin function between yeast cohesin and mammalian cohesin. It has been established that yeast cohesin is phosphorylated by Cdc5p, but the GAL1 mediated repression of *CDC5* does not result in a cohesion defect (Alexandru *et al.*, 2001). However, a similar strategy by which *CDC5* is repressed by a mitotic-specific promoter during meiosis results in a cohesion maintenance defect and arrest in metaphase I (Clyne *et al.*, 2003; Lee and Amon, 2003). In higher eukaryotes, Cdc5 is required during chromosome resolution as well as sister chromatid cohesion at the centromere (Losada *et al.*, 2002; Clarke *et al.*, 2005). These observations imply that the failure to observe a cohesion defect in mitotic budding yeast cells is the exception to the rule, and not the norm.

In Appendix 2, I describe some preliminary evidence in which CDC5-AID strains show a cohesion maintenance defect upon auxin treatment. This resolves the inconsistency in field, suggesting that Cdc5's function in maintaining sister chromatid cohesion is conserved throughout eukaryotes. We also used phosTAG gels to ask if mcd1-Q266p in *mcd1-Q266-6MYC MCD1-AID* strains showed an change in phosphorylation, but did not detect any difference compared to wild-type. These two observations suggested that the *rocc* domain was impacting Cdc5p enrichment at CARC1, but not necessarily to change the phosphorylated state of mcd1-Q266. Was it possible that Cdc5p had a role outside of its kinase activity? It remains to be determined if a kinase dead Cdc5p also binds to CARC1 (or chromosomes) with the same high enrichment as wild-type Cdc5p.

Is Interallelic Complementation a Property of SMC Complexes in General?

In this report we detail two examples of interallelic complementation in recessive paired alleles, with one example in *mcd1* and a second in *smc3.* This demonstrates that interallelic complementation is not restricted to a single subunit of the cohesin complex, but is a general property of cohesin complexes. However, it is intriguing to speculate if other SMC family proteins also show communication, as through interallelic complementation. A recent report from the D'amien Damours laboratory suggested that interallelic complementation occurred between recessive allles of Smc4 (Robellet *et al.*, 2015). The authors did not interpret their result as interallelic complementation, partly because Robellet and colleagues did not explicitly test the two single alleles (*smc4-1* and *smc4-82*) for condensation and viability (Robellet *et al.*, 2015). The observation however, can be easily tested with the right set of strains.

While interallelic complementation has not been observed in higher eukaryotes, the same experimental limitations in budding yeast still apply to higher eukaryotes. Smc1p, Smc3p, and Mcd1p exist as single copy genes in mammals (reviewed in Peters *et al.*, 2008). Tang and colleagues observed weak complementation between recessive alleles of MEI-S332A, but these recessive alleles of mei-s332a did not restore wild-type function (Tang *et al.*, 1998). Synthetic sick interactions between recessive mutants of ORD (a Mcd1 homolog) have also been reported (Bickel *et al.*, 1996). It would be interesting to introduce both the smc3-42 (smc3-S182L) and smc3-K113R mutations into the same mammalian cell to assess cohesion and viability, as both of these residues are highly conserved.

References.

Alexandru, G., Uhlmann, F., Mechtler, K., Poupart, M. A., and Nasmyth, K. (2001). Phosphorylation of the cohesin subunit Scc1 by Polo/Cdc5 kinase regulates sister chromatid separation in yeast. Cell *105*, 459–472.

Bickel, S. E., Wyman, D. W., Miyazaki, W. Y., Moore, D. P., and Orr-Weaver, T. L. (1996). Identification of ORD, a Drosophila protein essential for sister chromatid cohesion. Embo J *15*, 1451–1459.

Chang, C.-R., Wu, C.-S., Hom, Y., and Gartenberg, M. R. (2005). Targeting of cohesin by transcriptionally silent chromatin. *19*, 3031–3042.

Clarke, A. S., Tang, T. T.-L., Ooi, D. L.-Y., and Orr-Weaver, T. L. (2005). POLO kinase regulates the Drosophila centromere cohesion protein MEI-S332. Dev Cell *8*, 53–64.

Clyne, R. K., Katis, V. L., Jessop, L., Benjamin, K. R., Herskowitz, I., Lichten, M., and Nasmyth, K. (2003). Polo-like kinase Cdc5 promotes chiasmata formation and cosegregation of sister centromeres at meiosis I. Nat Cell Biol *5*, 480–485.

Eng, T., Guacci, V., and Koshland, D. (2014). ROCC, a conserved region in cohesin's Mcd1 subunit, is essential for the proper regulation of the maintenance of cohesion and establishment of condensation. Mol Biol Cell *25*, 2351–2364.

Game, J. C., Birrell, G. W., Brown, J. A., Shibata, T., Baccari, C., Chu, A. M., Williamson, M. S., and Brown, J. M. (2003). Use of a genome-wide approach to identify new genes that control resistance of Saccharomyces cerevisiae to ionizing radiation. Radiat. Res. *160*, 14–24.

Gandhi, R., Gillespie, P. J., and Hirano, T. (2006). Human Wapl is a cohesin-binding protein that promotes sister-chromatid resolution in mitotic prophase. Curr Biol *16*, 2406–2417.

Guacci, V., and Koshland, D. (2012). Cohesin-independent segregation of sister chromatids in budding yeast. Mol Biol Cell *23*, 729–739.

Guacci, V., Stricklin, J., Bloom, M. S., Guō, X., Bhatter, M., and Koshland, D. (2015). A novel mechanism for the establishment of sister chromatid cohesion by the ECO1 acetyltransferase. Mol Biol Cell *26*, 117–133.

Haering, C. H., Farcas, A.-M., Arumugam, P., Metson, J., and Nasmyth, K. (2008). The cohesin ring concatenates sister DNA molecules. Nature *454*, 297–301.

Heidinger-Pauli, J. M., Unal, E., and Koshland, D. (2009). Distinct targets of the Eco1 acetyltransferase modulate cohesion in S phase and in response to DNA damage. Mol Cell *34*, 311–321.

Huis In 't Veld, P. J., Herzog, F., Ladurner, R., Davidson, I. F., Piric, S., Kreidl, E., Bhaskara, V., Aebersold, R., and Peters, J.-M. (2014). Characterization of a DNA exit gate in the human cohesin ring. Science *346*, 968–972.

Ivanov, D., and Nasmyth, K. (2007). A physical assay for sister chromatid cohesion in vitro. Mol Cell *27*, 300–310.

Klein, F., Mahr, P., Galova, M., Buonomo, S. B., Michaelis, C., Nairz, K., and Nasmyth, K. (1999). A central role for cohesins in sister chromatid cohesion, formation of axial elements, and recombination during yeast meiosis. Cell *98*, 91–103.

Kueng, S., Hegemann, B., Peters, B. H., Lipp, J. J., Schleiffer, A., Mechtler, K., and Peters, J.-M. (2006). Wapl Controls the Dynamic Association of Cohesin with Chromatin. Cell *127*, 955–967.

Lee, B. H., and Amon, A. (2003). Role of Polo-like kinase CDC5 in programming meiosis I chromosome segregation. Science *300*, 482–486.

Losada, A., Hirano, M., and Hirano, T. (2002). Cohesin release is required for sister chromatid resolution, but not for condensin-mediated compaction, at the onset of mitosis. Genes Dev. *16*, 3004–3016.

Peters, J.-M., Tedeschi, A., and Schmitz, J. (2008). The cohesin complex and its roles in chromosome biology. Genes Dev. *22*, 3089–3114.

Pobiega, S., and Marcand, S. (2010). Dicentric breakage at telomere fusions. Genes Dev. *24*, 720–733.

Robellet, X., Thattikota, Y., Wang, F., Wee, T.-L., Pascariu, M., Shankar, S., Bonneil, É., Brown, C. M., and D'Amours, D. (2015). A high-sensitivity phospho-switch triggered by Cdk1 governs chromosome morphogenesis during cell division. Genes Dev. *29*, 426–439.

Sutani, T., Kawaguchi, T., Kanno, R., Itoh, T., and Shirahige, K. (2009). Budding yeast Wpl1(Rad61)-Pds5 complex counteracts sister chromatid cohesion-establishing reaction. Curr Biol *19*, 492–497.

Tang, T. T., Bickel, S. E., Young, L. M., and Orr-Weaver, T. L. (1998). Maintenance of sister-chromatid cohesion at the centromere by the Drosophila

MEI-S332 protein. Genes Dev. *12*, 3843–3856.

Tedeschi, A. *et al.* (2013). Wapl is an essential regulator of chromatin structure and chromosome segregation. Nature *501*, 564–568.

van Steensel, B., Smogorzewska, A., and de Lange, T. (1998). TRF2 protects human telomeres from end-to-end fusions. Cell *92*, 401–413.

Warren, C. D., Eckley, D. M., Lee, M. S., Hanna, J. S., Hughes, A., Peyser, B., Jie, C., Irizarry, R., and Spencer, F. A. (2004). S-phase checkpoint genes safeguard high-fidelity sister chromatid cohesion. Mol Biol Cell *15*, 1724–1735.

Yokobayashi, S., Yamamoto, M., and Watanabe, Y. (2003). Cohesins determine the attachment manner of kinetochores to spindle microtubules at meiosis I in fission yeast. Mol Cell Biol *23*, 3965–3973.

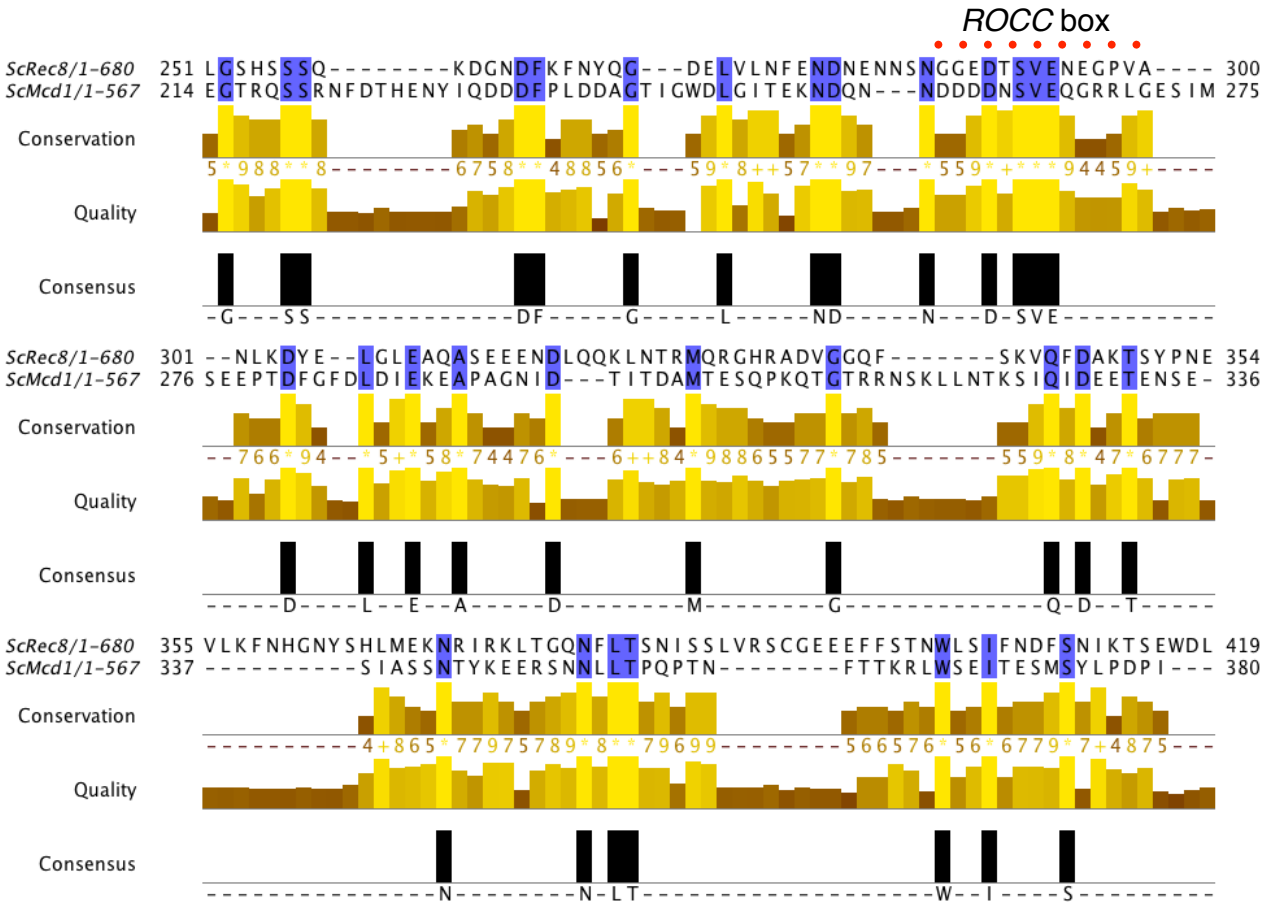

Figure 1. Protein Alignment of Mcd1p and Rec8p. Protein sequences from budding yeast Recap and Mcd1p were aligned using Clustal Omega to identify regions of conservation. The *ROCC* box is indicated with a dashed line. The coiled coil of Mcd1 and Rec8 show limited sequence conservation.

Analysis of Loss of Protein Allele of Wpl1p, the Yeast Homolog of Wapl

The cohesin accessory factor Wpl1 (Wapl in metazoans) was first identified in budding yeast as a radiation sensitive gene in budding yeast (Game *et al.*, 2003). However, standard molecular cloning techniques have demonstrated that it is dispensable for viability either by deleting its sequence in a haploid or sporulating *WPL1/wpl1Δ* diploids and recovering four viable tetrads (Warren *et al.*, 2004; Sutani *et al.*, 2009; Lopez-Serra *et al.*, 2013). In contrast, the metazoan homolog of Wpl1 is essential (Vernì *et al.*, 2000; Gandhi *et al.*, 2006; Kueng *et al.*, 2006; Cunningham *et al.*, 2012). A recent report from the Jan Michael Peters laboratory provided strong evidence that Wapl was involved in mediating chromatin structure in quiescent, serum starved mammalian cell culture, and its depletion caused gross chromosomal abnormalities ("vermicelli chromosomes") (Tedeschi *et al.*, 2013). As no investigator had been described a role for Wpl1 in stationary cultures of budding yeast, it was possible that Wpl1's role in quiescent cells would be conserved, even if it was still dispensable for mitotic division.

To specifically deplete Wpl1 from stationary cells, we exploited the use of the auxin degron to generate carboxyl-terminal Wpl1-AID in-frame fusion proteins (a kind gift of Vincent Guacci). *WPL1-AID* cells were grown to saturation for two days at 23˚C. Afterwards, the growth media was pH'ed to 6.3 using a potassium phosphate buffer and auxin was added to a final concentration of 500uM. Since yeast cells divide roughly every 90 minutes, and human cell culture doubles every 24 hours, I speculated that it might be possible to see a gross defect in chromosome morphology by chromosome spreads after eight to twelve hours, and potentially a decrease in viability when plating to single colony forming units. Unfortunately, chromosome spreads and viability (%CFUs) of *WPL1-AID* strains looked nearly identical to the wild-type control. Chromosome spreads from stationary cultures show very small (but well formed) R-loops. A few red colonies were appeared on the YPD plates where I plated *WPL1-AID* cells to count CFUs, which I dismissed as contamination. As there was no phenotype, I moved on to other projects, but left the auxin treated cultures on my bench over the weekend.

Interestingly, five days post auxin treatment (it took roughly 3 days post plating to count CFUs) I noticed that the WPL1-AID culture treated with auxin had started to turn a different, reddish color compared to the wild-type control. It is important to note that both *WPL1-AID* and its isogenic wild-type parent are ADE+. At this point I serially diluted both the wild-type and the *WPL1-AID* strains on solid agar plates, and surprisingly, only the wild-type strain grew on the YPD plate. To eliminate the possibility that *WPL1-AID* cells are unable to stably exit stationary phase even when auxin is not added, I aged a saturated WPL1-AID culture by letting it incubate on my bench for two weeks. Without the addition of auxin, aged

WPL1-AID cultures were able to grow on solid agar plates upon serial dilution and plating.

I next repeated the experiment to compare the behavior of *WPL1-AID* to *wpl1Δ* strains. *WPL1-AID*, *wpl1Δ,* and wild-type cultures were grown to saturation for 2 days at 23˚C as before, buffered to pH 6.3, and treated with auxin for eight days. The *WPL1-AID* culture once again turned red (Figure A1-A). Neither wpl1Δ nor wild-type cells turned red upon auxin treatment, nor showed any decrease in viability (Figure A1-A and A1-B).

Why was the stationary phase depletion of Wpl1p a lethal event? If Wpl1p was required for chromatin structure during in quiescent cells, we might be able to see cytological changes if we visualized chromosomes by chromosome spreads. I was unable to prepare spheroblasts for chromatin spreads from any of the stationary cultures, perhaps due to a more rigid cell wall from stationary phase cells. However, I was able to extract yeast chromosomes from and resolve their structure by pulse field and simple agarose gel electrophoresis (Figure A1-C). Surprisingly, while both wild-type and *wpl1Δ* chromosomes looked normal, but chromosomes from *WPL1-AID* strains could not be detected. Instead only staining was observed in the agarose plug (Figure A1-C). To rule out the possibility that chromosomes from *WPL1-AID* strains were shattered and migrating much faster than intact yeast chromosomes, I resolved chromosomes from *WPL1-AID* cells on a 1% agarose gel. No fragments between 100bp-5kb were detected. It is likely that *WPL1-AID* yeast chromosomes from this regiment were unable to enter the pulsed field gel, rather than running off the dye front.

One possible interpretation of this result is that chromosomes from *WPL1-AID* cells are inappropriately entering replication. Replicating DNA is thought to remain trapped in the agarose plug and is resistant to pulsed field electrophoresis (Stamato and Denko, 1990; Dewey *et al.*, 1997). Alternatively, yeast chromosomes from *WPL1-AID* strains may have undergone non-homologous joining or telomeric fusion, resulting in extremely large chromosomes. As the agarose plug itself was noticeably pink in color, it is likely that *WPL1-AID* was scavenging adenine intermediates in the absence of nutrients, which could have been used for replication.

References.

Cunningham, M. D., Gause, M., Cheng, Y., Noyes, A., Dorsett, D., Kennison, J. A., and Kassis, J. A. (2012). Wapl antagonizes cohesin binding and promotes

Polycomb-group silencing in Drosophila. Development *139*, 4172–4179.

Dewey, W. C., Wong, R. S., and Albright, N. (1997). Pulsed-field gel electrophoretic migration of DNA broken by X irradiation during DNA synthesis: experimental results compared with Monte Carlo calculations. Radiat. Res. *148*, 413–420.

Game, J. C., Birrell, G. W., Brown, J. A., Shibata, T., Baccari, C., Chu, A. M., Williamson, M. S., and Brown, J. M. (2003). Use of a genome-wide approach to identify new genes that control resistance of Saccharomyces cerevisiae to ionizing radiation. Radiat. Res. *160*, 14–24.

Gandhi, R., Gillespie, P. J., and Hirano, T. (2006). Human Wapl is a cohesin-binding protein that promotes sister-chromatid resolution in mitotic prophase. Curr Biol *16*, 2406–2417.

Kueng, S., Hegemann, B., Peters, B. H., Lipp, J. J., Schleiffer, A., Mechtler, K., and Peters, J.-M. (2006). Wapl Controls the Dynamic Association of Cohesin with Chromatin. Cell *127*, 955–967.

Lopez-Serra, L., Lengronne, A., Borges, V., Kelly, G., and Uhlmann, F. (2013). Budding yeast Wapl controls sister chromatid cohesion maintenance and chromosome condensation. Curr Biol *23*, 64–69.

Stamato, T. D., and Denko, N. (1990). Asymmetric field inversion gel electrophoresis: a new method for detecting DNA double-strand breaks in mammalian cells. Radiat. Res. *121*, 196–205.

Sutani, T., Kawaguchi, T., Kanno, R., Itoh, T., and Shirahige, K. (2009). Budding yeast Wpl1(Rad61)-Pds5 complex counteracts sister chromatid cohesion-establishing reaction. Curr Biol *19*, 492–497.

Tedeschi, A. *et al.* (2013). Wapl is an essential regulator of chromatin structure and chromosome segregation. Nature *501*, 564–568.

Vernì, F., Gandhi, R., Goldberg, M. L., and Gatti, M. (2000). Genetic and molecular analysis of wings apart-like (wapl), a gene controlling heterochromatin organization in Drosophila melanogaster. Genetics *154*, 1693–1710.

Warren, C. D., Eckley, D. M., Lee, M. S., Hanna, J. S., Hughes, A., Peyser, B., Jie, C., Irizarry, R., and Spencer, F. A. (2004). S-phase checkpoint genes safeguard high-fidelity sister chromatid cohesion. Mol Biol Cell *15*, 1724–1735.

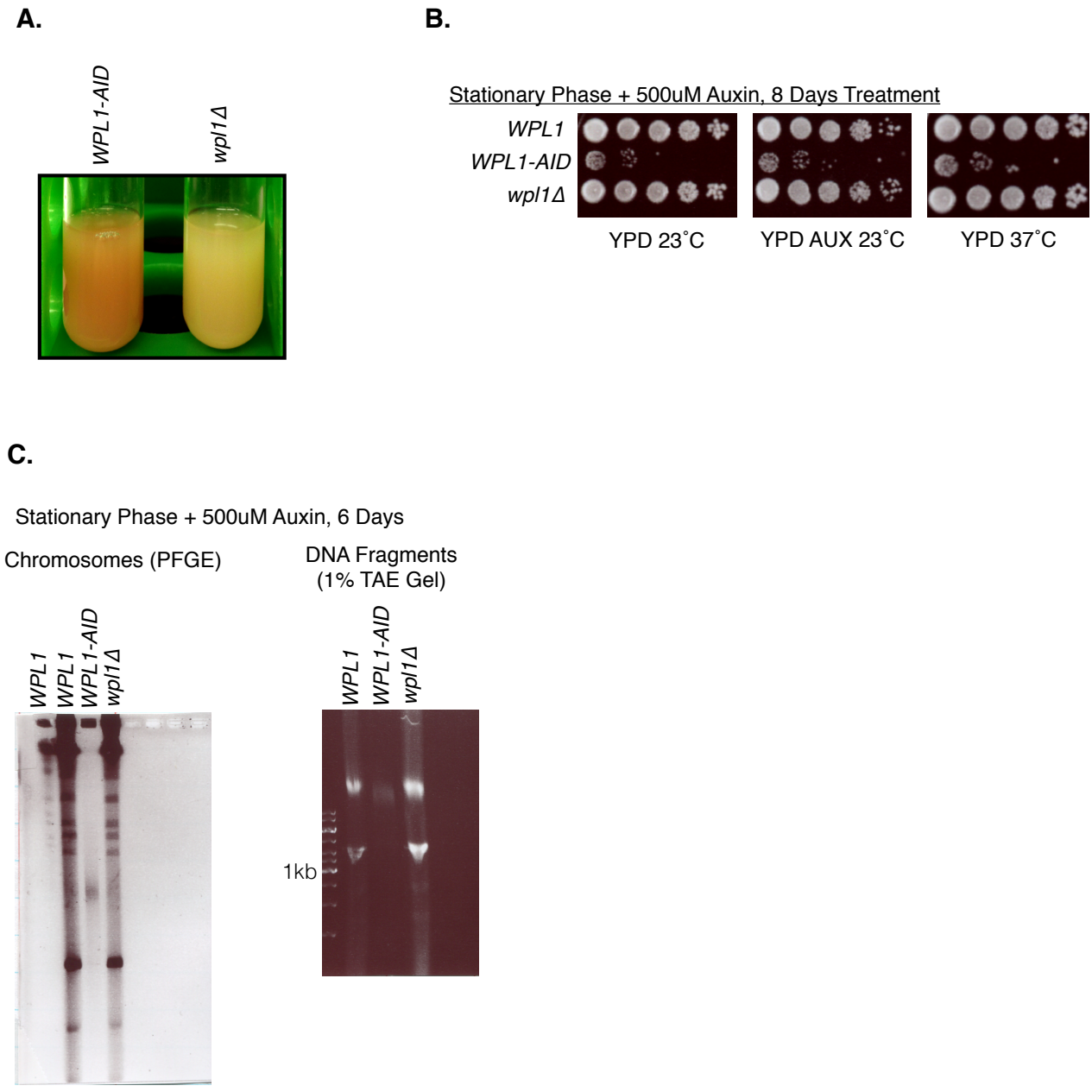

Figure A1-1. Analysis of Auxin Sensitive Allele of Wpl1. A. Haploid yeast strains (WT, WPL1-AID, or wpl1Δ) were grown to saturation at 23˚C for two days. Auxin (500uM final) was then added to each stationary culture, and incubated for an additional six days at room temperature. At time of auxin addition, culture medium was buffered with potassium phosphate to pH 7 (20mM final). Photomicrograph of auxin treated *WPL1-AID* and *wpl1Δ* cultures were photographed approximately eight days after auxin addition. Note the red coloration in the *WPL1-AID* culture, but not in the *wpl1Δ* culture. Wild-type cultures did not change color upon auxin addition for the same incubation time (data not shown). The liquid colorimetric assay was completed two times. **B.** Growth of wild-type, *WPL1-AID*, and *wpl1Δ* cultures after long term auxin treatment. Top. Haploid yeast strains (WT, WPL1-AID, wpl1Δ) were grown to saturation and plated onto solid agar media with or without auxin (YPD or YPD + AUX). Both WPL1-AID and wpl1Δ show robust growth on auxin plates without extended treatment with auxin in stationary. Bottom. Cells from regiment A were serial diluted and plated onto sold agar media eight days after auxin addition. **C.** Pulsed field gel analysis of chromosomes. Cells from genotypes and regiment from A were harvested and processed for pulsed field gel electrophoresis to resolve chromosomes. Chromosomes from WPL1-AID cells cannot be resolved by pulse field, and are not shattered, as no fragments are observed on a standard 1% TAE gel.

Appendix 2: Cdc5 Is Required for the Maintenance of Sister Chromatid Cohesion

How is cohesin's tethering activity regulated? It has been long known that cohesin is phosphorylated, and that the phosphorylated form is more amenable to cleavage by Esp1 during anaphase-onset (Alexandru *et al.*, 2001; Hornig and Uhlmann, 2004). However, temperature sensitive mutants in *CDC5* as well repressing *CDC5* expression using a GAL shutoff assay does not reveal cohesion defects but instead pleiotrophic phenotypes (Clyne *et al.*, 2003; Rossio *et al.*, 2010; Szakal and Branzei, 2013; Valerio-Santiago *et al.*, 2013; Zhang *et al.*, 2013; Botchkarev *et al.*, 2014; Walters *et al.*, 2014).

If Cdc5 was a direct regulator of cohesin's tethering activity, we needed to determine if it showed any temporal or spatial overlap with cohesin. The first hint was that Cdc5 was expressed starting at the G1/S transition, which was the time that *MCD1* is expressed. Second, a report identified that Cdc5 spatially mapped to cohesin associated regions (CARs), suggesting that this kinase was localized to the same regions cohesin bound DNA to tether sister chromatids (Rossio *et al.*, 2010).

Was cohesin required for Cdc5p to enrich at CARs? We first confirmed that Cdc5-3HAp and cohesin (by virtue of tracking Mcd1p) bound to both CARC1 and CARL1 by chIP-qPCR (Figure A2-1A). The patterns were fairly similar, but not exactly identical (Figure A2-1A). We repeated the ChIP experiment in an *MCD1-AID CDC5-3HA* strain such that we could conditionally inactivate Mcd1 in G1 and determine if Cdc5 enrichment in a cell cycle was cohesin dependent. Surprisingly, upon auxin-mediated depletion of Mcd1p, Cdc5p binding to CARC1 was reduced two fold, and the shape of the peak was flatter. This result suggests that Cdc5 enrichment at CARs is at least partially dependent on cohesin.

If Cdc5p enrichment at CARs was partially dependent on cohesin, why was Cdc5p dispensable for sister chromatid cohesion? Interestingly, Cdc5p is required for the maintenance of sister chromatid cohesion in yeast meiosis I (Clyne *et al.*, 2003; Lee and Amon, 2003). This suggested that previous experiments may have missed Cdc5's role in yeast mitosis, perhaps due to incomplete knockdown of Cdc5p. Other experiments in yeast mitosis had suggested that Cdc5p was required for maintenance by disturbing Pds5p localization, but relied on over-expression of *CDC5* (Baldwin *et al.*, 2009).

To resolve this discrepancy, we sought to use a mutant allele of *CDC5* which would behave as a true loss-of-protein allele, rather than the inactivation of a single domain, or rely on transcriptional repression. As such we generated *CDC5-AID2*, a strain harboring an in-frame AID cassette at the carboxyl terminus of *CDC5*. This allele contains a nine amino acid polylinker between the last residue of *CDC5* and the first residue of *AID2*. CDC5-AID strains are inviable on

auxin plates, but curiously, AID-CDC5 strainswere viable on auxin plates (Figure A2-2A). We scored CDC5-AID2 strains for sister chromatid cohesion, and consistent with the meiosis I data, observed that CDC5-AID strains could establish, but failed to maintain cohesion.

We noticed that the *ROCC* box of mcd1-Q266 contains a putative Cdc5 phosphorylation site (Snead *et al.*, 2007). Were mcd1-Q266 mutants defective for Cdc5 function? To address this possibility, we generated mcd1-Q266-6MYC MCD1-AID CDC5-3HA strains such that we could track Cdc5p in the crude extract as well as binding to chromatin by ChIP. Intriguingly, Cdc5-3HA protein levels were elevated in the crude extracts resolved by SDS-PAGE (Figure A2-3A). By ChIP, the amount of Cdc5-3HA bound to CARC1 was slightly elevated compared to a control sample, suggesting that Cdc5 was still competent to bind in the *rocc* mutant *mcd1-Q266* (Figure A2-3B).

References.

Alexandru, G., Uhlmann, F., Mechtler, K., Poupart, M. A., and Nasmyth, K. (2001). Phosphorylation of the cohesin subunit Scc1 by Polo/Cdc5 kinase regulates sister chromatid separation in yeast. Cell *105*, 459–472.

Baldwin, M. L., Julius, J. A., Tang, X., Wang, Y., and Bachant, J. (2009). The yeast SUMO isopeptidase Smt4/Ulp2 and the polo kinase Cdc5 act in an opposing fashion to regulate sumoylation in mitosis and cohesion at centromeres. Cell Cycle *8*, 3406–3419.

Botchkarev, V. V., Rossio, V., and Yoshida, S. (2014). The budding yeast Polo-like kinase Cdc5 is released from the nucleus during anaphase for timely mitotic exit. Cell Cycle *13*, 3260–3270.

Clyne, R. K., Katis, V. L., Jessop, L., Benjamin, K. R., Herskowitz, I., Lichten, M., and Nasmyth, K. (2003). Polo-like kinase Cdc5 promotes chiasmata formation and cosegregation of sister centromeres at meiosis I. Nat Cell Biol *5*, 480–485.

Hornig, N. C. D., and Uhlmann, F. (2004). Preferential cleavage of chromatin-bound cohesin after targeted phosphorylation by Polo-like kinase. Embo J *23*, 3144–3153.

Lee, B. H., and Amon, A. (2003). Role of Polo-like kinase CDC5 in programming meiosis I chromosome segregation. Science *300*, 482–486.

Rossio, V., Galati, E., Ferrari, M., Pellicioli, A., Sutani, T., Shirahige, K., Lucchini, G., and Piatti, S. (2010). The RSC chromatin-remodeling complex influences mitotic exit and adaptation to the spindle assembly checkpoint by controlling the

Cdc14 phosphatase. The Journal of Cell Biology *191*, 981–997.

Snead, J. L., Sullivan, M., Lowery, D. M., Cohen, M. S., Zhang, C., Randle, D. H., Taunton, J., Yaffe, M. B., Morgan, D. O., and Shokat, K. M. (2007). A coupled chemical-genetic and bioinformatic approach to Polo-like kinase pathway exploration. Chem. Biol. *14*, 1261–1272.

Szakal, B., and Branzei, D. (2013). Premature Cdk1/Cdc5/Mus81 pathway activation induces aberrant replication and deleterious crossover. Embo J *32*, 1155–1167.

Valerio-Santiago, M., de Los Santos-Velázquez, A. I., and Monje-Casas, F. (2013). Inhibition of the mitotic exit network in response to damaged telomeres. PLoS Genet *9*, e1003859.

Walters, A. D., May, C. K., Dauster, E. S., Cinquin, B. P., Smith, E. A., Robellet, X., D'Amours, D., Larabell, C. A., and Cohen-Fix, O. (2014). The yeast polo kinase Cdc5 regulates the shape of the mitotic nucleus. Curr Biol *24*, 2861–2867.

Zhang, S., Xie, M., Ren, G., and Yu, B. (2013). CDC5, a DNA binding protein, positively regulates posttranscriptional processing and/or transcription of primary microRNA transcripts. Proc Natl Acad Sci USA *110*, 17588–17593.

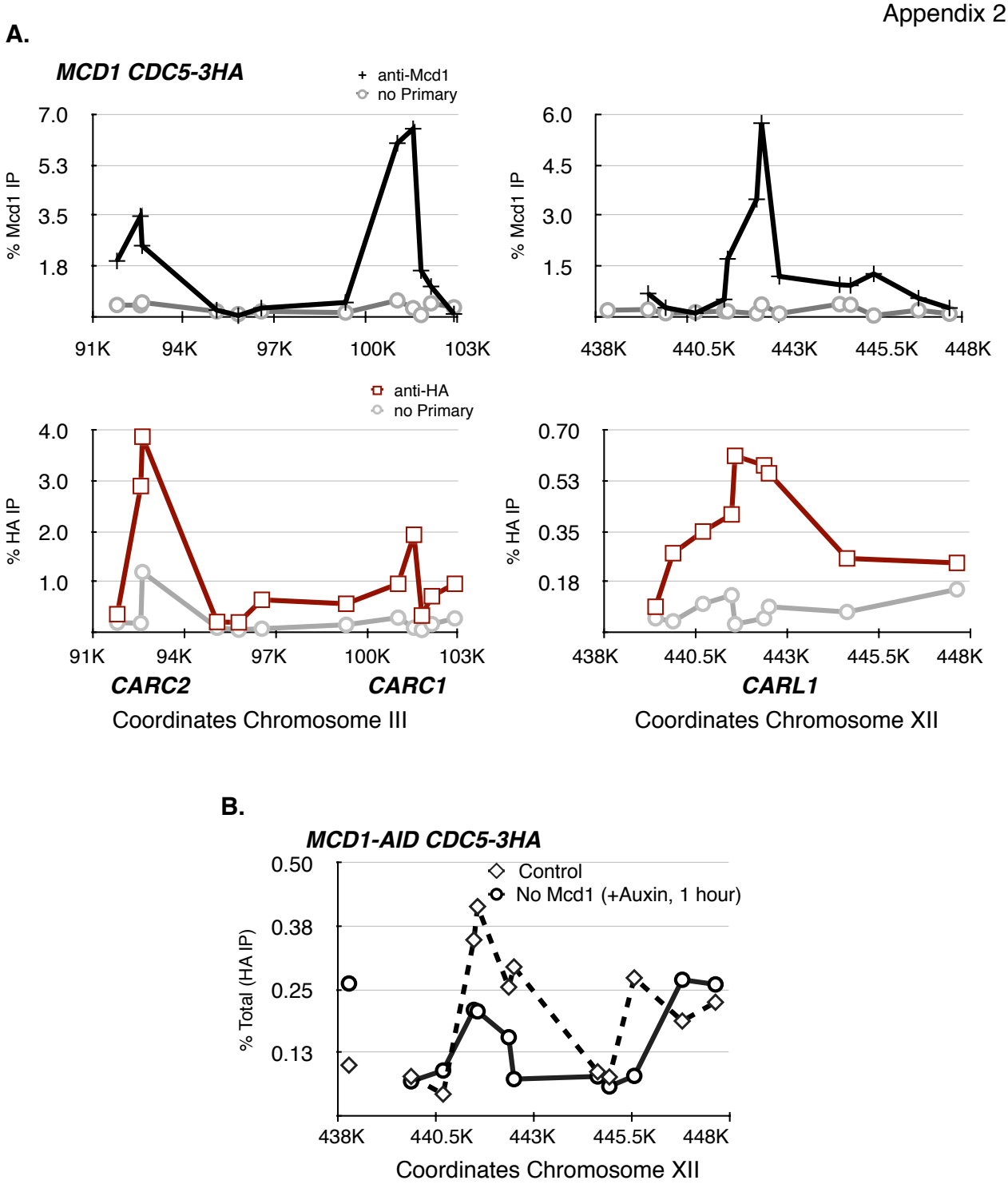

Figure A2-1. Analysis of Cdc5 Binding to CARs by chromatin immunoprecipitation (ChIP). A. Log phase haploid yeast strain TE248 *(CDC5-3HA-HIS3mX)* was arrested in M phase with nocodazole, fixed for 2 hours, and processed for chromatin immunoprecipitation by standard procedures. The HA epitope at the carboxyl-terminus of Cdc5p was immunoprecipitated with an anti-HA antibody. A rabbit polyclonal antibody against Mcd1 was similarly used for Mcd1p. The pattern of binding for Cdc5p confirms a global Cdc5p enrichment at CAR sites, as reported in Rossio, JBC, 2010 doi: 10.1083/jcb.201007025. **B.** Log phase haploid yeast strain TE316 *(MCD1-AID1 CDC5-3HA-His3mX)* was arrested in nocodazole for 3 hours. The culture was then split in half an incubated for an additional hour with or without the addition of auxin to the media. Cells were then harvested and processed for ChIP as in A. No global loss of Cdc5p was detected by western blot analysis upon auxin addition (data not shown).

A.

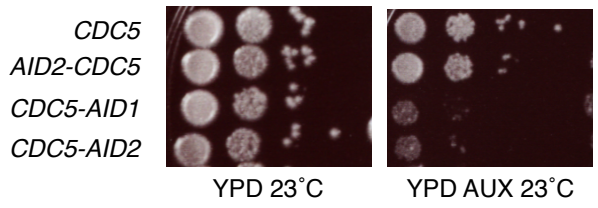

B.

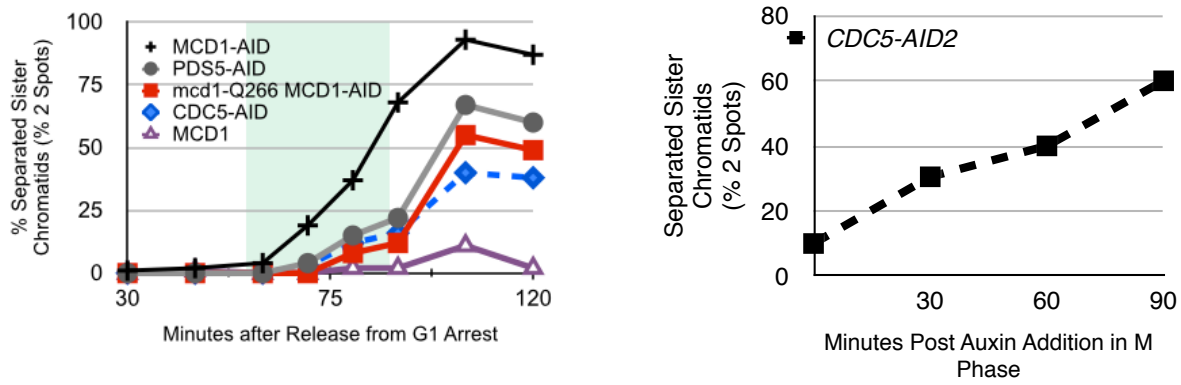

Figure A2-2. Analysis of cohesion in Cdc5-AID strains. A. Amino-terminus or carboxyl-terminus AID epitopes were introduced in-frame with the *CDC5* open reading frame and selected for with the KanMx6 drug selection cassette. WT CDC5: VG3349-1B. AID2-CDC5: TE303. CDC5-AID1: TE300. CDC5-AID2: TE353. Identified transformants were then grown to saturation overnight at 23˚C in rich media and plated in 10 fold serial dilutions onto solid media with or without auxin (YPD or YPD + AUX) and incubated for 2 days. Note that the amino terminal AID tagged CDC5 grows on auxin plates, but neither of the carboxyl CDC5-AID fusion proteins grow. **B.** Cohesion establishment assay. See Eng, Guacci, and Koshland 2014, Figure 2 or chapter 2, for detailed protocol. CDC5-AID strains are able to establish, but cannot maintain cohesion. Cdc5-AID strains are also unable to maintain cohesion in M phase upon loss of Cdc5.

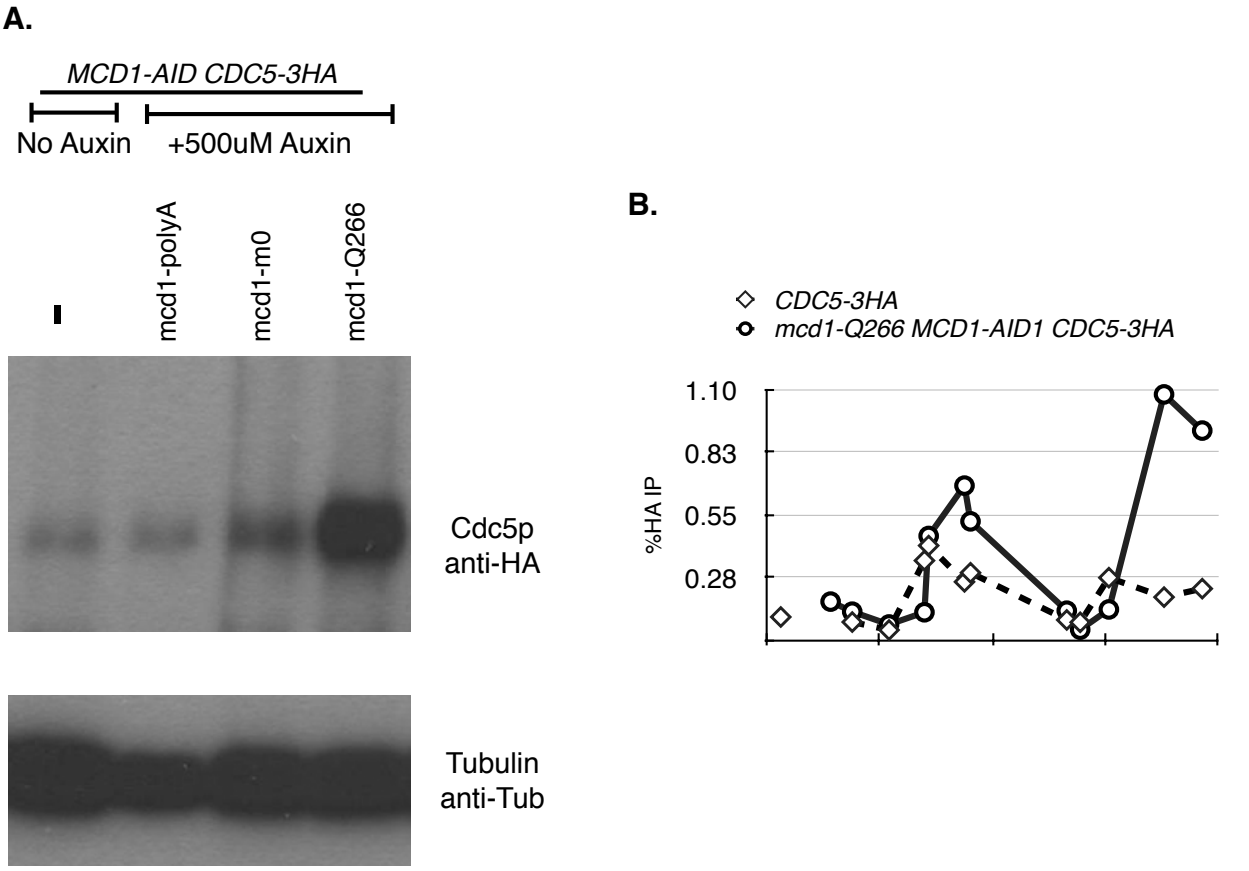

Figure A2-3. Analysis of Cdc5p Behavior in mcd1-Q266 MCD1-AID strains. *MCD1-AID CDC5-3HA* strains carrying a second additional copy of MCD1 (no additional copy: TE316. mcd1-polyA: TE326. mcd1-m0: TE330.) were arrested in G1 with alpha factor and treated with auxin for 1 hour. Cells were then washed and released in the presence of auxin and nocodazole to allow cell cycle progression for 150 minutes. **A.** Cells from each genotype were then harvested and processed for western blot analysis against Cdc5-3HAp using the HA epitope. More Cdc5-3HA was detected in mcd1-m0 and mcd1-Q266 strains compared to the parent. **B.** Cells from mcd1-Q266-6MYC MCD1-AID CDC5-3HA processed in A were fixed, harvested, and prepared for chromatin immunoprecipitation. A *MCD1-AID CDC5-3HA* strain was also prepared for ChIP analysis in the same manner but without the addition of auxin. mcd1-Q266-6MYC MCD1-AID CDC5-3HA strains show Cdc5p binding to CARL1 as good or slightly better than the parent MCD1-AID CDC5-3HA strain in the absence of auxin.

Appendix 3: Optimization of the Auxin Degron

AID Fusion Proteins as a Tool to Study Sister Chromatid Cohesion

The use of the auxin degron has, retrospectively, been very successful. To date, all genes previously characterized as essential components of the core cohesin complex and its accessory factors have been confirmed. Many of these genes were made as auxin-sensitive alleles using the carboxyl-terminus, one step tagging cassettes described by Nishimura and colleagues (Nishimura *et al.*, 2009).

Table A3-1: Characterization of AID Sensitive Cohesin Alleles.

AID Allele of Gene	Viability on Auxin Plates	Cohesion Defect	Notes	First Published In
MCD1	Inviable	90-95%		(Eng *et al.*, 2014)
SMC1	Inviable		Internal AID cassettes placed in many positions of coiled coil	Unpublished
SMC3	Inviable	70% at 23˚C 95% at 30˚C	SMC3-AID^{608} published; Internal AID cassettes placed in many positions of coiled coil	(Guacci *et al.*, 2015)
SCC3	Inviable	80%		(Orgil *et al.*, 2015)
PDS5	Inviable	60-70%		(Eng *et al.*, 2014)
WPL1	Viable	30%	rDNA Loops are compact and v. bright by DAPI stained chromosome spreads	(Guacci *et al.*, 2015)
CTF7	Inviable	70-80%	Also known as ECO1	(Guacci *et al.*, 2015)
SCC2	Inviable	70-80%		(Eng *et al.*, 2014)
SCC4	Inviable	Not Tested	SCC4-AID colonies are small and nibbled	Unpublished
CDC5	Inviable	45-50%		Unpublished
DRE2	Viable	None	See TE438 and TE439	Unpublished

We were interested in validating *DRE2* as a new cohesin accessory factor, as a report from the Philip Hieter laboratory reported that *DRE2* is an essential gene with a 44% cohesion defect (Ben-Aroya *et al.*, 2008). Unfortunately, *DRE2-AID2* strains are viable on auxin plates, and do not show a cohesion defect in nocodazole arrested cells. As the AID tag generally reduces basal protein level of the target gene even in the absence of auxin, it was curious to note that *DRE2-AID2* cells did not show any sensitivity to benomyl, camptothecin, or hydroxyurea, while all mutant cohesin alleles do. We conclude that Dre2p is not an essential protein, and is not involved in sister chromatid cohesion.

Generation of New TIR1 Integration Plasmids and Auxin Sensitive Cassettes

To expand the range of strains we could introduce auxin tags into, I collaborated with Vinny Guacci and Leon Chan to generate a new panel of TIR integration plasmids. These plasmids use selectable markers from *Candida albicans* to eliminate homology to the open reading frames in budding yeast and instead use homology to the 5' and 3' UTRs for integration. The plasmids are cut with PmeI, releasing a Pringle style linear integration fragment, which can be used in a yeast transformation reaction without further purification.

Table 2. TIR1 Integration Plasmids.

Vector Name	Promoter	Integration Locus
pTIR1	ADH1	HIS3
pTIR2	GPD1	HIS3
pTIR3	ADH1	LEU2
pTIR4	GPD1	LEU2
pTIR5	ADH1	TRP1
pTIR6	GPD1	TRP1

In sending out these plasmids to labs across the United States, we sometimes received reports that the AID system had variable penetrance on auxin plates. A large portion of the variability arose from different water sources and a range of YEP media being prepared at different pH's, sometimes with and without buffering agents. In order to systematically address these issues, I prepared new solid agar YEP plates supplemented with auxin, but setting the pH, dropwise, with HCl or NaOH (Figure A3-1). At pH 7, SCC2-AID1 strains are sick but viable on auxin plates. However, dropping the pH to 5.5 or 6.0 improved the auxin sensitivity such that very few colonies appeared, even after 6 days (Figure A3-1). Wild-type strains were inviable on auxin plates at pH 5.0 or 8.0, setting the upper and lower bounds for making auxin plates.

We also cloned and expressed two new versions of an AID tag, which we refer to as AID2. This AID was cloned from an Arabidopsis cDNA library and encodes *IAA7*. *IAA7* had been described as having a shorter half-life in Arabidopsis, compared to IAA17, which was used in the Nishimura and Kanemaki report (Gray *et al.*, 2001; Nishimura *et al.*, 2009).

The second version of AID2 we generated is called ScAID2. This was a kind gift from Sandy Silverman, from David Botstein's lab at Princeton. Sandy calculated which codons in AID2 could be optimized for expression in budding yeast, and printed the new open reading frame using DNA synthesis technology. We then subcloned his codon optimized gene into one of our integration cassettes, in frame with a 3V5 epitope tag and a KanMx6 selection marker.

Finally, we examined the published crystal structure of TIR1 (Tan *et al.*, 2007). A curious observation was the presence of inositol hexaphosphate as a cofactor found in the active site, in complex with the small molecule, auxin (Tan *et al.*, 2007). We added inositol hexaphosphate to the solid media additionally supplemented with auxin and observed a dosage dependence inviability (Figure A3-2). The choice of auxin did not matter, as we observed similar phenotypes using either indole acetic acid (IAA) or naphthalene acetic acid (NAA). However, the temperature at which the plates were incubated displayed exceedingly different phenotypes. Wild-type strains were inviable on auxin plates supplemented with IP6 when the plates were incubated at 37˚C. The same strains were viable on the same plates when incubated at 23˚C. Determining the optimal concentration of IP6 to add to plates appears to be something which should be determined empirically, for every AID tag of interest. It should also be something done as a last resort, after switching to AID2 and pH'ing the media has already been attempted.

References.

Ben-Aroya, S., Coombes, C., Kwok, T., O'Donnell, K. A., Boeke, J. D., and Hieter, P. (2008). Toward a comprehensive temperature-sensitive mutant repository of the essential genes of Saccharomyces cerevisiae. Mol Cell *30*, 248–258.

Eng, T., Guacci, V., and Koshland, D. (2014). ROCC, a conserved region in cohesin's Mcd1 subunit, is essential for the proper regulation of the maintenance of cohesion and establishment of condensation. Mol Biol Cell *25*, 2351–2364.

Gray, W. M., Kepinski, S., Rouse, D., Leyser, O., and Estelle, M. (2001). Auxin regulates SCF(TIR1)-dependent degradation of AUX/IAA proteins. Nature *414*,

271–276.

Guacci, V., Stricklin, J., Bloom, M. S., Guō, X., Bhatter, M., and Koshland, D. (2015). A novel mechanism for the establishment of sister chromatid cohesion by the ECO1 acetyltransferase. Mol Biol Cell *26*, 117–133.

Nishimura, K., Fukagawa, T., Takisawa, H., Kakimoto, T., and Kanemaki, M. (2009). An auxin-based degron system for the rapid depletion of proteins in nonplant cells. Nat. Methods *6*, 917–922.

Orgil, O., Matityahu, A., Eng, T., Guacci, V., Koshland, D., and Onn, I. (2015). A conserved domain in the scc3 subunit of cohesin mediates the interaction with both mcd1 and the cohesin loader complex. PLoS Genet *11*, e1005036.

Tan, X., Calderon-Villalobos, L. I. A., Sharon, M., Zheng, C., Robinson, C. V., Estelle, M., and Zheng, N. (2007). Mechanism of auxin perception by the TIR1 ubiquitin ligase. Nature *446*, 640–645.

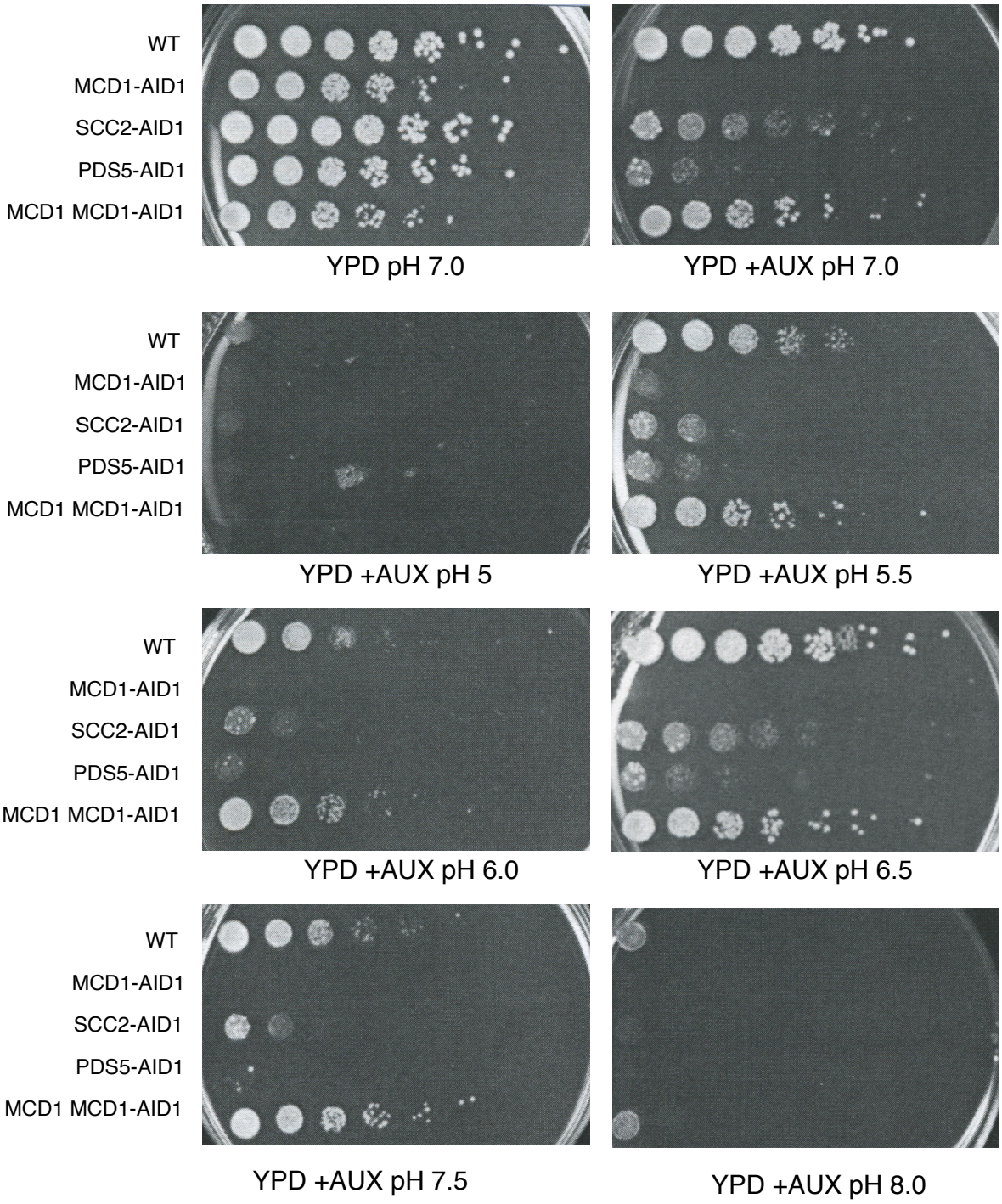

Figure A3-1. Analysis of Auxin Sensitivity and Environmental pH. WT (VG3349-1B), MCD1-AID1, SCC2-AID1, PDS5-AID1, and MCD1-URA3 MCD1-AID1 were grown to saturation overnight at 23˚C. Cells plated in ten fold serial dillutions onto solid agar media with or without auxin (500uM final) (YPD or YPD + AUX) which had been previously adjusted for pH with HCl or NaOH. Note that *SCC2-AID* and *PDS5-AID strains* are sick but viable on auxin plates at pH 7.0 but show a much better response around pH 6.0. Note that wild-type yeast strains are inviable on auxin plates at pH 8.0 or 5.0.

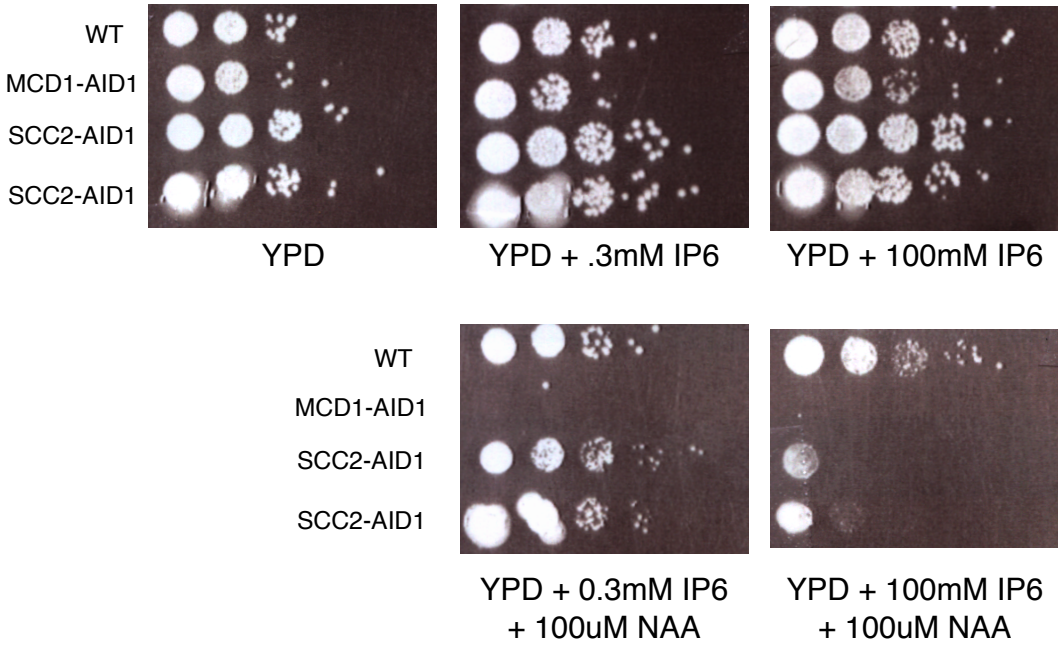

Figure A3-2. Analysis of Inositol Hexaphosphate (IP6) on Auxin Sensitivity. Strains of genotypes indicated to left of panel were spotted on solid agar plates supplemented with or without auxin (NAA) or inositol hexaphosphate (IP6) at the concentrations indicated. Note that 100mM IP6 shows a synthetic interaction in the presence of auxin, where auxin alone has only a modest penetrance. Only MCD1-AID is inviable on 100uM NAA plates, where SCC2-AID1 is viable. Identical results were observed with indole acetic acid (IAA) as the source of auxin.